



**US Army Corps  
of Engineers®**  
Engineer Research and  
Development Center

**ERDC**  
INNOVATIVE SOLUTIONS  
for a safer, better world

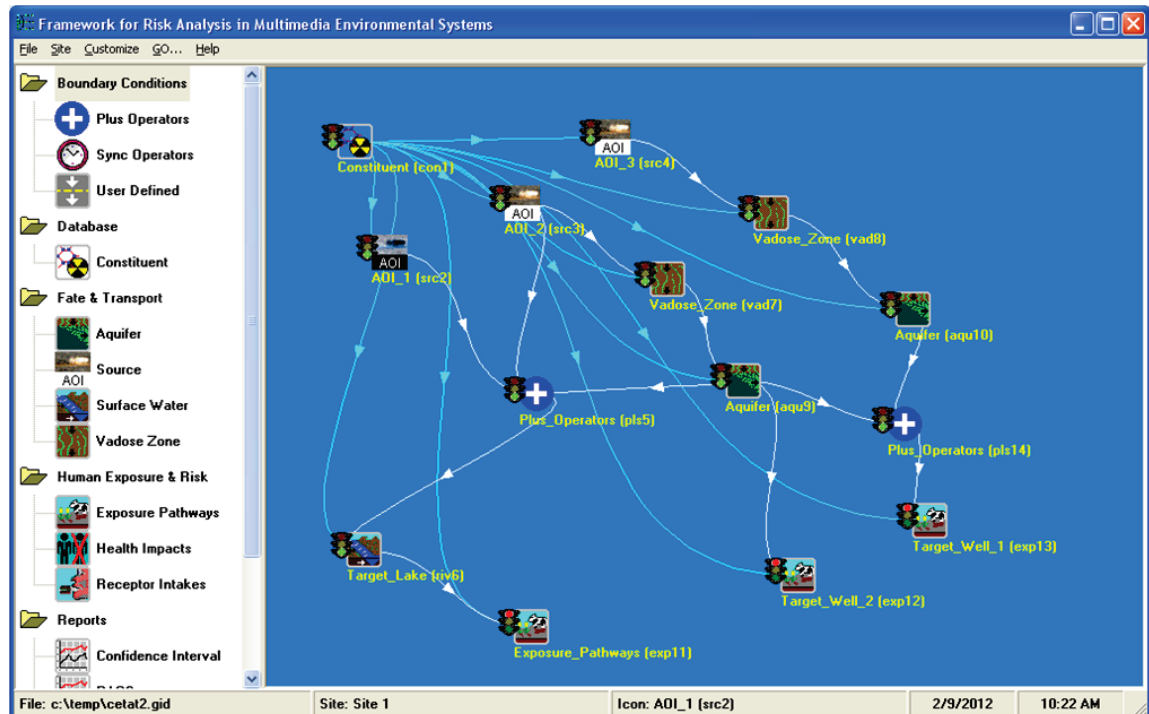
*Environmental Security Technology Certification Program*

# **Field Demonstration and Validation of TREECS™ and CTS for the Risk Assessment of Contaminants on Department of Defense (DoD) Ranges**

ESTCP Project Number ER-201435

Mark S. Dortch, Billy E. Johnson, and Eric J. Weber

April 2017



## REPORT DOCUMENTATION PAGE

*Form Approved  
OMB No. 0704-0188*

The public reporting burden for this collection of information is estimated to average 1 hour per response, including the time for reviewing instructions, searching existing data sources, gathering and maintaining the data needed, and completing and reviewing the collection of information. Send comments regarding this burden estimate or any other aspect of this collection of information, including suggestions for reducing the burden, to Department of Defense, Washington Headquarters Services, Directorate for Information Operations and Reports (0704-0188), 1215 Jefferson Davis Highway, Suite 1204, Arlington, VA 22202-4302. Respondents should be aware that notwithstanding any other provision of law, no person shall be subject to any penalty for failing to comply with a collection of information if it does not display a currently valid OMB control number.

**PLEASE DO NOT RETURN YOUR FORM TO THE ABOVE ADDRESS.**

1. REPORT DATE (DD-MM-YYYY)	2. REPORT TYPE	3. DATES COVERED (From - To)		
01/04/2017	Final Report	April 2014 - April 2017		
4. TITLE AND SUBTITLE		5a. CONTRACT NUMBER		
Field Demonstration and Validation of TREECS™ and CTS for the Risk Assessment of Contaminants on Department of Defense (DoD) Ranges		5b. GRANT NUMBER		
		5c. PROGRAM ELEMENT NUMBER		
		5d. PROJECT NUMBER		
6. AUTHOR(S) Mark S. Dortch, Billy E. Johnson, and Eric J. Weber		ER-201435		
		5e. TASK NUMBER		
		5f. WORK UNIT NUMBER		
7. PERFORMING ORGANIZATION NAME(S) AND ADDRESS(ES) ERDC-EL, 3909 Halls Ferry Road, Vicksburg, MS 39180 EPA, 960 College Station Road, Athens GA 30605 PNNL, 902 Battelle Blvd, Richland, WA 99354		8. PERFORMING ORGANIZATION REPORT NUMBER		
9. SPONSORING/MONITORING AGENCY NAME(S) AND ADDRESS(ES) Environmental Security Technology Certification Program Program Office 4800 Mark Center Drive Suite 17D03 Alexandria, VA 22350-3605		10. SPONSOR/MONITOR'S ACRONYM(S) ESTCP		
		11. SPONSOR/MONITOR'S REPORT NUMBER(S)		
12. DISTRIBUTION/AVAILABILITY STATEMENT Approved for public release; distribution is unlimited.				
13. SUPPLEMENTARY NOTES N/A				
14. ABSTRACT The objective of this project was to demonstrate and validate the integrated Training Range Environmental Evaluation and Characterization System (TREECS™) and Environmental Fate Simulator (EFS) modeling system to show that its performance is consistent, reliable, and cost effective and that TREECS™/EFS advances the ability to reliably quantify the potential of environmental risks from munitions constituents (MCs) on Department of Defense (DoD) training and testing ranges.				
15. SUBJECT TERMS Training Range Environmental Evaluation and Characterization System (TREECS™), Environmental Fate Simulator (EFS), modeling, munitions constituents (MCs), risk quantification.				
16. SECURITY CLASSIFICATION OF: a. REPORT		17. LIMITATION OF ABSTRACT UL	18. NUMBER OF PAGES 177	19a. NAME OF RESPONSIBLE PERSON Dr. Billy Johnson
b. ABSTRACT				19b. TELEPHONE NUMBER (Include area code) 601-634-3714
c. THIS PAGE Unclassified				

**The U.S. Army Engineer Research and Development Center (ERDC)** solves the nation's toughest engineering and environmental challenges. ERDC develops innovative solutions in civil and military engineering, geospatial sciences, water resources, and environmental sciences for the Army, the Department of Defense, civilian agencies, and our nation's public good. Find out more at [www.erdc.usace.army.mil](http://www.erdc.usace.army.mil).

To search for other technical reports published by ERDC, visit the ERDC online library at <http://acwc.sdp.sirsi.net/client/default>.

# **Field Demonstration and Validation of TREECS™ and CTS for the Risk Assessment of Contaminants on Department of Defense (DoD) Ranges**

ESTCP Project Number ER-201435

Billy E. Johnson

*Environmental Laboratory*  
*U.S. Army Engineer Research and Development Center*  
*3909 Halls Ferry Road*  
*Vicksburg, MS 39180*

Mark S. Dortch

*LimnoTech, Inc.*  
*501 Avis Drive*  
*Ann Arbor, MI 48108*

Eric J. Weber

*Exposure Methods and Measurements Division*  
*USEPA National Exposure Research Laboratory*  
*960 College Station Road*  
*Athens, GA 30605*

Final report

Approved for public release; distribution is unlimited.

Prepared for    Environmental Security Technology  
                    Certification Program (ESTCP)  
                    4800 Mark Center Dr., Suite 17D08  
                    Alexandria, VA 22350-3605

Under    Project ER-201435, “Field Demonstration and Validation of TREECS™ and CTS  
                    for the Risk Assessment of Contaminants on Department of Defense (DoD)  
                    Ranges”

## Abstract

The Training Range Environmental Evaluation and Characterization System (TREECSTM) was developed to forecast the fate of and risk from munitions constituents (MC), such as high explosives (HE) and metals, within and transported from firing/training ranges to surface water and ground-water. The Chemical Transformation Simulator (CTS) was developed by the U.S. Environmental Protection Agency to provide physicochemical properties of complex organic chemicals. TREECSTM requires such properties for predicting environmental fate of MC. This study validated the capability of TREECSTM and CTS to predict MC (HE RDX) concentrations in receiving waters down-gradient of training/firing ranges for three installations: Demolition Area 2 of Massachusetts Military Reservation, MA.; Artillery Impact Area of the U.S. Military Academy, West Point, NY.; and Zulu Impact Area of Marine Corps Base Camp Pendleton, CA. The study also demonstrated the utility of these modeling system for forecasting the fate of emerging HE NTO, DNAN, and NQ associated with new in-sensitive munitions and evaluating best management practices for reducing down-gradient receiving water concentrations. The overall benefit of this work is to help transition these tools to the user community for use towards ensuring range compliance and sustainability into the future.

**DISCLAIMER:** The contents of this report are not to be used for advertising, publication, or promotional purposes. Citation of trade names does not constitute an official endorsement or approval of the use of such commercial products. All product names and trademarks cited are the property of their respective owners. The findings of this report are not to be construed as an official Department of the Army position unless so designated by other authorized documents.

**DESTROY THIS REPORT WHEN NO LONGER NEEDED. DO NOT RETURN IT TO THE ORIGINATOR.**

# Contents

<b>Abstract.....</b>	<b>ii</b>
<b>Figures and Tables .....</b>	<b>vi</b>
<b>Preface .....</b>	<b>ix</b>
<b>Unit Conversion Factors.....</b>	<b>x</b>
<b>Executive Summary .....</b>	<b>xi</b>
<b>Acronyms and Abbreviations.....</b>	<b>xvii</b>
<b>1 Introduction .....</b>	<b>1</b>
1.1 Background.....	1
1.2 Objective of the demonstration .....	2
1.3 Regulatory drivers.....	3
<b>2 Technology .....</b>	<b>4</b>
2.1 Technology description and development.....	4
2.2 Advantages and limitations of the technology.....	15
<b>3 Performance Objectives .....</b>	<b>18</b>
3.1 Objective: TREECS™ accurately simulates long-term fate of MC on ranges .....	19
3.1.1 Data requirements.....	20
3.1.2 Success criteria.....	20
3.2 Objective: TREECS™-CTS can be used to assess uncertainty in inputs .....	21
3.2.1 Data requirements.....	22
3.2.2 Success criteria.....	22
3.3 Objective: TREECS™-CTS can be quickly set up and run with readily available data .....	22
3.3.1 Data requirements.....	22
3.3.2 Success criteria.....	22
3.4 Objective: training requirements are reasonable .....	22
3.4.1 Data requirements.....	23
3.4.2 Success criteria.....	23
3.5 Objective: TREECS™-CTS can be applied to evaluate range management and/or remediation strategies .....	23
3.5.1 Data requirements.....	23
3.5.2 Success criteria.....	24
3.6 Objective: TREECS™-CTS can be applied to evaluate the fate of emerging MC.....	24
3.6.1 Data requirements.....	24
3.6.2 Success criteria.....	24

<b>4 Site Description .....</b>	<b>25</b>
<b>5 Test Design .....</b>	<b>26</b>
5.1 Overall concept .....	26
5.2 Model validation .....	26
5.3 Baseline characterization .....	27
5.4 Field data .....	28
5.5 Uncertainty analysis .....	28
5.6 Fate of emerging MC (EC) associated with IM .....	29
5.7 BMP assessment.....	29
<b>6 Demo Area 2, MMR .....</b>	<b>30</b>
6.1 Site description .....	30
6.2 Model inputs for validation .....	32
6.3 Validation results .....	38
6.4 Uncertainty analysis .....	42
6.5 Fate of emerging MC (EC) associated with IM .....	47
6.5.1 <i>Initial inputs and results</i> .....	47
6.5.2 <i>Refined inputs and simulation results for DNAN and NTO</i> .....	51
6.6 BMP assessment.....	55
<b>7 Artillery Impact Area (AIA), USMA .....</b>	<b>58</b>
7.1 Site description .....	58
7.2 Model inputs for validation .....	59
7.2.1 <i>Soil model inputs</i> .....	60
7.2.2 <i>Stream model inputs</i> .....	66
7.2.3 <i>RDX residue mass loading rate</i> .....	69
7.3 Validation results .....	70
7.4 Uncertainty analysis .....	74
7.5 Fate of emerging MC (EC) associated with IM .....	76
7.5.1 <i>Initial inputs and results</i> .....	77
7.5.2 <i>Refined inputs and simulation results for DNAN and NTO</i> .....	81
7.6 BMP assessment.....	83
<b>8 Zulu Impact Area (ZIA), Marine Corp Base (MCB) Camp Pendleton, CA.....</b>	<b>87</b>
8.1 Site description .....	87
8.2 Model inputs for validation .....	93
8.2.1 <i>Soil model inputs</i> .....	95
8.2.2 <i>Stream model inputs</i> .....	101
8.2.3 <i>Groundwater modeling inputs</i> .....	104
8.3 Validation results .....	109
8.4 Uncertainty analysis .....	113
8.5 Fate of emerging MC (EC) associated with IM .....	116
8.5.1 <i>Initial inputs and results</i> .....	116
8.5.2 <i>Refined inputs and simulation results for DNAN and NTO</i> .....	122
8.6 BMP assessment.....	124

<b>9 Performance Assessment.....</b>	<b>128</b>
9.1 Validation accuracy .....	129
9.2 Uncertainty analysis .....	130
9.3 TREECS™-CTS set-up time .....	130
9.4 Training.....	131
9.5 BMP assessments.....	131
9.6 EC fate .....	131
<b>10 Cost Assessment.....</b>	<b>132</b>
10.1 Cost model.....	132
10.2 Cost drivers.....	133
10.3 Cost analysis.....	134
<b>11 Implementation Issues.....</b>	<b>135</b>
<b>References.....</b>	<b>136</b>
<b>Appendix A: Points of Contact .....</b>	<b>141</b>
<b>Appendix B: Predicting the Fate of Insensitive Munitions Explosive Components.....</b>	<b>142</b>
<b>Report Documentation Page</b>	

# Figures and Tables

## Figures

Figure 1. Conceptual Site Model and schematic of model linkages within TREECS™, Tier 2 (red denotes features in Tier 2 that are not in Tier 1).....	6
Figure 2. FRAMES CSM workspace within TREECS™ Advanced Tier 2 option. ....	6
Figure 3. The primary modules and work flow diagram for CTS. ....	11
Figure 4. Front page of CTS providing the user with options for the selection of the CTS workflows and descriptions of the CTS modules, physicochemical property calculators and reaction libraries. ....	12
Figure 5. CTS Chemical editor module. ....	13
Figure 6. CTS Reaction Pathway simulator module. ....	14
Figure 7. Example output from the CTS Physicochemical Properties calculator module. ....	15
Figure 8. Demo Area 2 of MMR, Cape Cod, MA (modified from AMEC Earth and Environmental, 2004). ....	31
Figure 9. RDX plume delineation and monitoring wells for Demo Area 2 with groundwater contours in feet National Geodetic Vertical Datum (NGVD) (modified from AMEC Earth and Environmental, 2004). ....	32
Figure 10. Computed and observed RDX soil concentrations at MMR Demo Area 2 .....	40
Figure 11. Computed and observed RDX aquifer concentrations at MW161 down-gradient of MMR Demo Area 2.....	40
Figure 12. Computed (with and without source removal) and observed (2001–2015) RDX aquifer concentrations at MW161 down-gradient of MMR Demo Area 2.....	42
Figure 13. Computed and measured groundwater concentrations of RDX at MW161 down-gradient of Demo Area 2 with upper (UCL) and lower (LCL) confidence limits for uncertainty on RDX half-life. ....	45
Figure 14. Computed and measured groundwater concentrations of RDX at MW161 down-gradient of Demo Area 2 with upper (UCL) and lower (LCL) confidence limits for uncertainty on RDX $K_d$ in soil and groundwater.....	46
Figure 15. Computed aquifer concentrations at MW161 down-gradient of Demo Area 2 for five ECs and RDX with half-life of 100 years for all MCs in all media.....	51
Figure 16. Computed aquifer concentrations of RDX at MW161 down-gradient of Demo Area 2 for four BMPs compared to base condition. ....	57
Figure 17. Site map of USMA (modified from ATC 2004a). ....	58
Figure 18. Map showing inconclusive range area, artillery duded impact area, and streams of the RTC (modified from EA 2011). ....	60
Figure 19. Delineation of AIA watershed and AOI in Google™ Earth. ....	61
Figure 20. Computed and measured concentration of RDX in Popolopen Brook down-gradient of the AIA, USMA. ....	71

Figure 21. Computed and measured concentration of RDX in Popolopen Brook down-gradient of the AIA, USMA, with upper (UCL) and lower (LCL) 95% confidence limits for uncertainty on RDX residue initial mean particle diameter and stream flow rate. ....	76
Figure 22. Computed water concentrations in Popolopen Brook down-gradient of AIA, USMA, for five ECs and RDX. ....	81
Figure 23. Computed water concentrations in Popolopen Brook down-gradient of AIA, USMA, for five ECs and RDX, with improved inputs for DNAN and NTO. ....	84
Figure 24. Computed water concentrations of RDX in Popolopen Brook down-gradient of the AIA, USMA, for three BMPs compared to base condition. ....	86
Figure 25. MCB Camp Pendleton stratigraphy (modified from AMP 2013). ....	89
Figure 26. Rough delineation of ZIA as viewed in Google Earth™. ....	90
Figure 27. WSS-generated AOI and soil map within the cratered area of the ZIA as viewed in WSS. ....	91
Figure 28. Las Flores watershed, stream network and ZIA (modified from AMP 2013). ....	91
Figure 29. Modeling CSM for ZIA and receiving waters, Camp Pendleton, CA. ....	94
Figure 30. CSM as modeled in TREECS™ with Advanced Tier 2 option. ....	95
Figure 31. Computed RDX mass flux in recharge into the Las Flores aquifer. ....	105
Figure 32. Computed and measured (via analytical estimation) concentration of RDX in Las Flores Creek down-gradient of the ZIA, Camp Pendleton, CA. ....	111
Figure 33. Computed and measured concentration of RDX at receptor well, Las Flores aquifer, Camp Pendleton, CA. ....	112
Figure 34. Computed and measured concentration of RDX in lower end of Las Flores Creek down-gradient of the ZIA, Camp Pendleton, with 95% UCL and LCL for uncertainty on initial mean particle diameter of RDX residue. ....	115
Figure 35. Computed and measured concentration of RDX at receptor well in Las Flores aquifer down-gradient of the ZIA, Camp Pendleton, with 95% UCL and LCL for uncertainty on recharge fluxes, flux plain width and Darcy velocity. ....	116
Figure 36. Computed water concentrations in Las Flores Creek down-gradient of ZIA, Camp Pendleton, for five EC and RDX. ....	121
Figure 37. Computed water concentrations at receptor well of Las Flores aquifer, Camp Pendleton, for five EC and RDX. ....	121
Figure 38. Computed water concentrations at receptor well of Las Flores aquifer, Camp Pendleton, for five EC and RDX, with improved inputs for DNAN and NTO. ....	124
Figure 39. Computed water concentrations of RDX in Las Flores Creek down-gradient of the ZIA, Camp Pendleton, for three BMPs compared to base condition. ....	126
Figure 40. Computed water concentrations of RDX in Las Flores aquifer down-gradient of the ZIA, Camp Pendleton, for three BMPs compared to base condition. ....	127

## Tables

Table 1. Demonstration performance objectives and success criteria. ....	18
--	----

Table 2. Available observed data for model comparison. ....	28
Table 3. Tier 2 soil model input values for Demo Area 2, MMR. ....	34
Table 4. MEPAS vadose model input values for Demo Area 2, MMR. ....	36
Table 5. MEPAS aquifer model input values for Demo Area 2, MMR. ....	37
Table 6. Additional soil model inputs for the five ECs for Demo Area 2 application. ....	47
Table 7. Additional MEPAS vadose and aquifer model inputs for five ECs at Demo Area 2. ....	50
Table 8. Soil characteristics, measured batch $K_d$ , and corresponding $K_{oc}$ values for DNAN and NTO for four soils similar to Demo Area 2 soils (Dontsova et al. 2014). ....	53
Table 9. Tier 2 soil model input values for AIA, USMA. ....	63
Table 10. CMS input values used for AIA, USMA. ....	67
Table 11. Munitions usage and detonation characteristics for the AIA, USMA. ....	70
Table 12. RDX concentration and precipitation on day of, and two days preceding sampling for RDX in Popolopen Brook <sup>1</sup> , USMA. ....	72
Table 13. Performance metrics of model accuracy for stream concentration of RDX down-gradient of the AIA, USMA. ....	73
Table 14. Additional soil model inputs of the five ECs for AIA application, USMA. ....	77
Table 15. Additional CMS inputs for the five EC for Popolopen Brook application, USMA. ....	79
Table 16. Soil characteristics and measured batch $K_d$ and corresponding $K_{oc}$ values for DNAN and NTO for four soils similar to AIA soils (Dontsova et al. 2014). ....	82
Table 17. Tier 2 soil model input values for Zulu impact area, Camp Pendleton, CA. ....	99
Table 18. CMS input values for Las Flores Creek, Camp Pendleton, CA. ....	103
Table 19. MEPAS vadose zone model inputs for Las Flores aquifer, Camp Pendleton, CA. ....	107
Table 20. MEPAS aquifer model inputs for Las Flores aquifer, Camp Pendleton, CA. ....	108
Table 21. Additional soil model inputs for the five EC for ZIA application, Camp Pendleton. ....	117
Table 22. Additional CMS inputs for the five EC for Las Flores Creek application, Camp Pendleton. ....	119
Table 23. EC $K_d$ values used in vadose and aquifer models for Las Flores basin. ....	120
Table 24. Soil characteristics and measured batch $K_d$ and corresponding $K_{oc}$ values for DNAN and NTO for two soils similar to ZIA soils (from Dontsova et al. 2014). ....	122
Table 25. Performance objectives success ratings for MMR Demo Area 2 application. ....	128
Table 26. Performance objectives success ratings for AIA application. ....	128
Table 27. Performance objectives success ratings for ZIA – Las Flores watershed application. ....	129

## Preface

This study was conducted for the Environmental Security Technology Certification Program (ESTCP) under the Environmental Restoration work topic area as ESTCP Project Number ER-201435. “Field Demonstration and Validation of TREECS™ and CTS for the Risk Assessment of Contaminants on Department of Defense (DoD) Ranges.” The technical monitor was Dr. Andrea Leeson, Deputy Director of ESTCP and the Environmental Restoration Program Manager.

The work was performed by the Water Quality and Contaminant Modeling Branch (WQCMB), Environmental Processes and Effects Division (EPED), U.S. Army Engineer Research and Development Center, Environmental Laboratory (ERDC-EL). At the time of publication, Dr. Dorothy Tillman was Chief, WQCMB; Warren Lorentz was Chief, EPED; and Dr. Beth Fleming was Director of ERDC-EL. Dr. Elizabeth Ferguson was Technical Director of military materials in the environment.

The authors would like to acknowledge the Exposure Methods and Measurements Division, National Exposure Research Laboratory, U.S. Environmental Protection Agency (EPA), for the Contaminant Transformation Simulator (CTS) that was developed by EPA and used as part of this project.

The Commander of ERDC was COL Bryan S. Green and the Director was Dr. David W. Pittman.

## Unit Conversion Factors

Multiply	By	To Obtain
acres	4,046.873	square meters
degrees Fahrenheit	(F-32)/1.8	degrees Celsius
feet	0.3048	meters
inches	0.0254	meters
microns	1.0 E-06	meters
miles (U.S. statute)	1,609.347	meters

## Executive Summary

The TREECS™-CTS modeling system was applied to three military training sites where the high explosive RDX has been detected in down-gradient receiving waters (i.e., groundwater or surface water). The three study sites were Demolition (Demo) Area 2 of the Massachusetts Military Reservation (MMR), MA. Artillery Impact Area (AIA) of the U.S. Military Academy (USMA), NY., and Zula Impact Area (ZIA) of Marine Corps Base (MCB) Camp Pendleton, CA. The model for each site was validated against observed RDX concentrations and an uncertainty analysis was conducted to evaluate the capability of the model to bracket observed data within the 95% confidence interval. The model was then applied for emerging constituent (EC) components of insensitive munitions (IM) at each study site to demonstrate the ability to evaluate EC fate relative to that of RDX. Then the model of each site was used to evaluate the effectiveness of three range management and/or remediation strategies (i.e., Best Management Practices, or BMPs) to reduce RDX concentrations to demonstrate the utility of TREECS™ for such purposes.

Almost all of the project objectives performance metrics were satisfied. The first quantitative metric on the ability of the model to accurately simulate the long-term fate of MC was graded as highly successful for all three study sites.

The quantitative metric on the capability to assess the uncertainty of model inputs was graded as moderately successful due to the fact that the confidence bands did not include two AIA surface water observations and one ZIA aquifer observation. The sensitivity and uncertainty analysis feature of TREECS™ is not flawed and operates as intended. The failure to capture the observations within the uncertainty bands at the AIA was attributed to widely varying stream flow rates at the AIA; whereas, average annual flows were used in the model. The use of daily varying flows in the model would provide closer agreement with observations, thus bolstering the uncertainty objective. Also, even with average annual hydrology, the use of broader uncertainty limits on stream flow would lead to satisfying the uncertainty objective for all data at the AIA study site. The lack of information on the exact location of the observation well down-gradient of the ZIA could contribute to the inability of the uncertainty bands to capture the observation. Also, broader uncertainty limits on inputs for the dimensions of the recharge zone, the recharge flow rate, and the Darcy flow

would lead to confidence bands that include the observation. Therefore, the moderate success of the uncertainty objective could have been upgraded to successful through the adjustment of uncertainty limits. The uncertainty limits were set based on site conditions and not observed data since observed data may not be available in many applications. However, there is still a need to bound predictions using best available information as done herein.

The first qualitative metric on the ability to set up a model with readily available data within 80 labor hours was successful for all three study sites. The second qualitative metric on reasonable training requirements has not been graded and is pending the execution of such training which is being planned for 2017. The third qualitative metric on the use of TREECS™-CTS to evaluate range management and/or remediation strategies (BMPs) was successful for all three study sites. The fourth qualitative metric on the use of TREECS™-CTS to evaluate the fate of emerging MC was successful.

An analysis of rainfall data and observed RDX measurements showed that the detection of RDX concentrations in streams is dependent on the occurrence of substantial rainfall just prior to, or during stream sampling. RDX concentrations were below detection in Popolopen Brook, USMA, and Las Flores Creek, Camp Pendleton, when there had not been substantial rainfall a day or two prior to sampling. Concentrations of RDX were above detection when there had been recent rainfall. Given the low sorption partitioning of RDX, its capacity to dissolve, and its slow degradation rate, RDX can move from range soils to streams only when it rains and it travels out of the stream system quickly dropping below detection after rainfall-runoff has ceased.

Model results for Popolopen Brook and Las Flores Creek showed a correspondence in ratios for rainfall and stream concentrations. Specifically, the ratio of the sampling date rainfall to the average annual rainfall per rainfall event was computed for each observation. The ratio of observed stream concentration to predicted stream concentration (using average annual hydrology) was also computed. A comparison of the two ratios showed remarkable agreement. This agreement supports the concept that TREECS™, applied with average annual hydrology, predicts stream concentrations associated with average annual rainfall per rainfall event. The

use of the daily hydrology option in TREECS™ should allow closer agreement or correspondence between model and observed stream concentrations. However, use of this option can result in much longer model execution times, which hinders making long-term (e.g., 100 years) simulations, especially when including Monte Carlo uncertainty analysis.

Predicting the fate of ECs associated with IM explosive formulations presents a unique challenge given that less is known regarding the physico-chemical properties of ECs than legacy explosive components. TREECS™-CTS was applied to previously reported laboratory studies (Dontsova et al. 2014) to assess the capability to predict the fate of ECs and to provide guidance for applications involving IM components. Two laboratory modeling assessments were conducted. One assessment involved modeling column breakthrough studies of IMX-101 components where a solid phase IMX-101 particle was placed at the top of the column. Thus, this experiment involved solid phase dissolution and subsequent transport with sorption partitioning. The second assessment involved modeling a laboratory column study of NTO transport where a continuous, constant flow of water with dissolved NTO was introduced at the top of the column.

The model accurately reproduced the experimental results of the IMX-101 column study without involving any model calibration (except for adjustment of initial solid phase particle size of the explosive). It was determined that the initial particle size should be set to the mass-weighted average particle size based on each formulation component particle size. The rationale for using the mass-weighted particle size is that the slower dissolving DNAN matrix of IMX-101 surrounds the smaller crystal-line NTO and NQ particles, thus limiting the crystalline surface area exposed to water and slowing the crystal dissolution rate. However, after dissolving some of the highly soluble crystals, the exposed DNAN surface area increases, which corresponds to a smaller DNAN particle that dissolves faster. This application provided important guidance for applying TREECS™ to IM formulations, such as IMX-101.

The model accurately reproduced the experimental results of the NTO column transport study. Experimentally determined  $K_d$  and half-life values for NTO were used in the model. Thus, this application simply confirmed the capability of the model to accurately model a site given reasonable input parameters for sorption and degradation.

The CTS was used to provide supplemental values for fate determining MC proper-ties. This information was especially useful for modeling the fate of ECs for high explosive formulations of IM. The ECs NTO, DNAN, NQ, AP, and CL-20 were modeled for each study site and compared with the RDX results. All of these EC, except CL-20, were found to be exported to down-gradient receiving waters faster (reaching peak concentrations quicker) than RDX due to their higher water solubility. CL-20 moves much more slowly due to a solubility that is lower than that of RDX. The speed of down-gradient migration (i.e., export) increases with the solubility of the EC. There was an exception to this for NQ and NTO, where NQ was ex-ported faster than NTO, although it has a lower solubility than NTO. This discrepancy was due to using a higher NTO soil  $K_d$  value than that of NQ, thus slowing the export of NTO from AOI soil.

Similar to RDX, explosive EC concentrations are highly transient in sur-face water, from non-detectable to values of concern, due to low  $K_d$  values and wide variations in rainfall and stream water flow rates. This transient feature can lessen environ-mental exposure and risk concerns. There is a much greater potential for environ-mental concern of ECs in groundwater where relatively high concentrations can be reached fairly quickly and per-sist for long periods due to high solubility, low  $K_d$  values, and slow degra-dation rates. The EC modeling results herein reinforce the need to keep a watch on ECs in groundwater resources.

One of the most sensitive and the most uncertain fate determining MC properties is the natural degradation rate (i.e., half-life) for various media. For Demo Area 2, MMR, degradation in the vadose zone was most im-portant due to the much longer transit time in that medium than in soil and aquifer. However, in most cases, degradation rates for aquifer waters will be the most important input, especially for ECs with high solubility which limits soil residence time. Degradation rates for MC in streams is much less important due to the transient nature discussed above and the short transit times. It is urgently important to develop improved estimates of natural degradation rates of ECs for the vadose zone and groundwater with a higher priori-ty on groundwater. Given the high solubility and rela-tively low  $K_d$  values of ECs (particularly NTO, NQ, and AP), ECs can reach relatively high groundwater concentrations relatively soon after range loading. Thus, knowing the potential for degradation is increasingly im-portant, requiring future research to gain a better understanding of natu-ral degradation rates of ECs.

A cost-benefit-analysis (CBA) was conducted for TREECS™-CTS. The CBA compared the cost to apply TREECS™-CTS to a study site against the cost to conduct field sampling and analysis for the site as part of an Operational Range Assessment Program (ORAP) Phase II analysis. The cost to apply TREECS™-CTS is about half of that required for ORAP Phase II sampling and analysis. Considering that ORAP Phase II must be conducted every five years (as a minimum) across multiple referred sites, these cost savings could expand to about \$3,000,000 Army wide every five years.

The benefits of using TREECS™-CTS go far beyond the cost savings associated with modeling versus monitoring. Modeling can be used to forecast not only if protective action limits (PALs) will be exceeded but when they will be exceeded. Additionally, the modeling system can be used to assess BMP strategies for avoiding future PAL exceedance and to evaluate the carrying capacity of existing and future ranges. Modeling can provide insight for improved sample design and monitoring. Modeling allows the assessment of “what if” scenarios without the risks and costs associated with trial-and-error field implementation. Moreover, TREECS™-CTS usage can and should be an integral part of the successful administration of ORAP and related range sustainment programs which can avoid many millions, if not billions, of dollars being lost if operational ranges are closed due to compliance failure.

There are really no major implementation issues associated with applying TREECS™-CTS. Training is helpful and should be conducted for successful use. Installation of TREECS™ on DoD and Army-owned computers requires the System Administrator since it is client based, and there are many military security constraints, such as requiring a Certificate of Worthiness (CON) for installed software. TREECS™ has an Army CON. Installation on contractor-owned computers entails much fewer hurdles; CTS is a web-based tool running behind EPA’s firewall on a server. As a result, potential users must request and establish a log-in account for the EPA server. The CTS will be made fully available to the public in early 2017.

Presently, there are no DoD or Army directives that require the use of TREECS™, and as a result, TREECS™ has not experienced the use that was originally envisioned during its developmental funding. Thus, the benefits of having a powerful forecast modeling tool such as TREECS™ are

not being realized. TREECS™ is a mature, validated modeling tool that is fairly easy to apply relatively quickly. Qualified contract environmental personnel could be readily trained for applying TREECS™-CTS to provide the most expedient and cheapest route to range applications. TREECS™ will not be fully utilized without a requirement for implementation and application. An Army or DoD directive is needed to require such applications, which would provide cost savings, provide much improved site under-standing and alternatives assessment, and help ensure range sustainment.

## Acronyms and Abbreviations

AFCEE	Air Force Center for Environmental Excellence
AIA	Artillery impact area
ECB	Environmental Chemistry Branch
AOI	Area of Interest
AMP	Arcadis – Malcolm Pirnie
AP	Ammonium perchlorate
ARAMS	Adaptive Risk Assessment Modeling System
ARCDB	Army Range Constituent Database with TREECS™
ATC	U.S. Army Aberdeen Test Center
bgs	below ground surface
BMP(s)	Best Management Practice(s)
C	crop management factor in the USLE
C <sub>4</sub>	HE consisting of RDX and plasticizers.
CAS	Chemical Abstract Service
CBA	Cost Benefit Analysis
CL-20	IM explosive component, hexanitrohexaazaisowurtzitane (HNIW)
CMS	Contaminant Model for Streams
CN	curve number in the SCS curve number method for computing runoff

CON	Certificate of Networthiness
CSM	Conceptual Site Model
CTS	Chemical Transformation Simulator developed by EPA
D4EM	Data for Environmental Modeling
Demo	Demolition area
DNAN	2,4-dinitroanisole
DoD	U.S. Department of Defense
DODIC	Department of Defense Identification Code
EC(s)	Emerging contaminant(s)
EFS	Environmental Fate Simulator
EL	ERDC Environmental Laboratory
EOD	explosives ordnance disposal
EPA	U.S. Environmental Protection Agency
EPI	Estimation Program Interface
EPED	Environmental Processes and Effects Division
EQT	U.S. Army Environmental Quality Technology
ERDC	U.S. Army Engineer Research and Development Center
ESTCP	Environmental Security Technology Certification Program
FRAMES	Framework for Risk Analysis in Multimedia Environmental Systems
GIS	Geographical Information System

GUI	Graphical User Interfaces
HE	High Explosives
HGCT	TREECS™ Hydro-Geo-Characteristics Toolkit
HLC	Henry's Law Constant, units of atm-m <sup>3</sup> /mole
HNIW	hexanitrohexaaazaiso-wurtzitane
IM	Insensitive munitions
LCL	lower confidence limit for uncertainty analysis
LeC	Las Flores loamy fine sand soil class for ZIA, Camp Pendleton
LS	length-slope-gradient factor in the USLE
MC	Munitions Constituent
MCB	Marine Corps Base
MENA	1,2-methoxy-5-nitroaniline
MEPAS	Multimedia Environmental Pollutant Assessment System
MIDAS	Munition Items Disposition Action System
MMR	Massachusetts Military Reservation
MSL	Mean Sea Level
N	Nitrogen
NCEI	National Centers for Environmental Information of NOAA
NOAA	National Oceanic and Atmospheric Administration
NQ	nitroguanidine

NSN	National Stock Number
NTO	3-nitro-1,2,4-triazol-5-one
OC	organic carbon
ORAP	U.S. Army Operational Range Assessment Program conducted by Army and Air Force
P	conservation practice factor in the USLE
PAL(s)	protective action limit(s) for protection of environmental health in various media
ppb	parts per billion as concentration of a constituent in water, same as $\mu\text{g/L}$
QSAR	Quantitative Structure Activity Relationship
R	rainfall factor in the USLE
RDX	Royal Demolition Explosive, a high explosive, hexahydro-1,3,5-trinitro-1,3,5-triazine
REVA	Range Environmental Vulnerability Assessment conducted by Marine Corps
RMUS	DoD Range Munitions Use Subcommittee
RSEPA	Range Sustainment Environmental Program Assessment conducted by Navy
RTC	range and training complex of USMA
SAFR	Small Arms Firing Ranges
SCS	Soil Conservation Service of the U.S. Department of Agriculture
SERDP	Strategic Environmental Research and Develop Program

---

SPARC	Sparc Performs Automated Reasoning in Chemistry
TEST	Toxicity Estimation Software Tool
T/E	Threatened and Endangered
TNT	HE trinitrotoluene
TREECS™	Training Range Environmental Evaluation and Characterization System
TSS	total suspended solids
UCL	upper confidence limit for uncertainty analysis
UI(s)	user interface(s) for entering and viewing model inputs
USGS	United States Geological Survey
USLE	Universal Soil Loss Equation
USMA	United States Military Academy
UXO	unexploded ordnance
WQCMB	Water Quality and Contaminant Modeling Branch
WSS	Web Soil Survey
WFF	water flux files within TREECS™
ZIA	Zulu Impact Area of Marine Corps Base Camp Pendleton

### **Symbols**

$f_{oc}$	fraction organic carbon for TSS and benthic sediment
$K_d$	sorption distribution coefficient for partitioning an MC between soil or sediment particles and water, L/kg
$K_{oc}$	organic carbon normalized soil–water sorption partition coefficient, L/kg

$K_{ow}$	octanol–water sorption partition coefficient, mL/mL
$K_{sat}$	water-saturated hydraulic conductivity for groundwater flow, length/time
$O$	observed or measured data
$P$	model-predicted data
$RR$	result ratio, a metric for measuring model accuracy
$RE$	relative error, a metric for measuring model accuracy

# 1 Introduction

## 1.1 Background

The Training Range Environmental Evaluation and Characterization System (TREECS™)\* was developed for the Army to forecast the fate of and risk from munitions constituents (MC), such as high explosives (HE) and metals, within and transported from firing/training ranges to surface water and groundwater. TREECS™ consists of time-varying contaminant fate/transport models for soil, vadose zone, groundwater, and surface water to forecast MC export from ranges and resulting concentrations in each medium. TREECS™ allows Department of Defense (DoD) training range managers and/or their environmental specialists to rapidly assess off-site migration of MC and other contaminants to determine if and when range operations could pose risks to human and ecological receptors down-gradient of ranges. Additionally, TREECS™ can be used to evaluate Green Range Best Management Practice (BMP) alternatives where concentrations are presently or are predicted in the future to exceed protective action limits (PALs) for human and ecological health. A detailed description of TREECS™, as well as its performance, are provided by Dortch et al. (2013a).

The physicochemical properties of the MC or contaminants (including emerging contaminants, or ECs) of interest are required for TREECS™ application. Such properties include, for example, molecular weight, solubility, solid phase density, sorption partitioning coefficients, Henry's constant, and degradation rates or half-lives. Although TREECS™ contains three separate databases for constituent physicochemical properties, there are data gaps within these databases.

The Chemical Transformation Simulator<sup>†</sup> (CTS), previously called the Environmental Fate Simulator (EFS), was developed by the U.S. Environmental Protection Agency (EPA) to provide physicochemical properties of complex organic chemicals for both the parent chemical and predicted

---

\*

<http://www.erdc.usace.army.mil/Media/FactSheets/FactSheetArticleView/tabid/9254/Article/476659/training-range-environmental-evaluation-characterization-system.aspx>

<sup>†</sup> [https://cfpub.epa.gov/si/si\\_public\\_record\\_Report.cfm?dirEntryId=310644](https://cfpub.epa.gov/si/si_public_record_Report.cfm?dirEntryId=310644)

transformation products. The CTS has capabilities for estimating properties in the absence of experimentally obtained properties; thus, CTS can help fill data gaps for properties, particularly for emerging contaminants with limited experimental data.

The CTS currently consists of three major components: (1) Chemical Editor that allows for the entry of the chemical of interest through either provision of the common name, smiles string notation, Chemical Abstract Service (CAS) registry number, or chemical structure; (2) Reaction Pathway Simulator, which is based on description of the environmental conditions (e.g., anaerobic vs. aerobic), provides the major transformation products based on the execution of reaction libraries for abiotic reduction, hydrolysis, aerobic biotransformation, and mammalian metabolism; and (3) Physicochemical Properties Calculators, which through access to SPARC (SPARC Performs Automated Reasoning in Chemistry), EPI (Estimation Program Interface) Suite, Toxicity Estimation Software Tool (TEST), and ChemAxon's plug-in calculators, provides the necessary physicochemical properties required for predicting environmental concentrations. Information from CTS is made available to TREECS™ to provide the constituent properties necessary for modeling contaminant fate.

TREECS™ and CTS were applied jointly to three DoD study sites to validate the capability to predict MC concentrations in receiving waters down-gradient of training/firing ranges and to demonstrate the utility of these modeling systems for forecasting the fate of MC, as well as ECs, within and off-site of DoD installations. The utility of the modeling system for evaluating BMPs was also demonstrated. The overall benefit of this work is to help transition these powerful tools to the appropriate user community so that they can be used to help ensure range compliance and sustainability into the future.

## **1.2 Objective of the demonstration**

The objectives of this study were to demonstrate and validate the scientific approach of the TREECS™ and CTS modeling systems to show that the performance is consistent, reliable, and cost effective and that TREECS™-CTS advances the ability to reliably quantify the potential of environmental risks of MC on, and down-gradient of DoD training and testing ranges. The scope of the project included identifying active DoD training ranges, determining the nature and extent of MC, analyzing potentially complex

exposure pathways, validating TREECSTM-CTS to predict MC concentrations in receiving water, evaluating potential risk from exposure to MC, developing user guidance in applying the TREECSTM-CTS for the environmental risk assessment, and providing transition and technology transfer for environmental specialists and range managers.

### **1.3 Regulatory drivers**

All DoD ranges must be managed and operated to support their long-term viability and to meet the national defense mission while protecting the environment and human health (DoD Directives 3200.15 and 4715.11). In support of these policies, DoD Instruction 4715.14 requires all DoD Components to determine whether there has been a release or a substantial threat of a release of munitions constituents of concern from an operational range to an off-range area, to determine whether such a release creates an unacceptable risk to human health or the environment, and to enhance the Components' ability to prevent or respond to such a release. As a result, all DoD Components routinely perform range assessments. The Army and Air Force conduct the Operational Range Assessment Program (ORAP); the Marine Corps perform Range Environmental Vulnerability Assessment (REVA); and the Navy performs Range Sustainment Environmental Program Assessment (RSEPA).

As per DoD Instruction 4715.14, to ensure the long-term viability of operational ranges while protecting human health and the environment, all operational ranges must be periodically re-evaluated to determine if there is a release or substantial threat of a release of munitions constituents of concern from an operational range to an off-range area. This reevaluation shall occur at least every five years, or whenever significant changes (e.g., changes in range operations, site conditions, applicable statutes, regulations, DoD issuances, or other policies) occur that affect determinations made during the previous assessment. Also as part of this instruction, if data are insufficient to determine a potential MC source – receptor interaction, then further analysis, such as modeling, shall be conducted to evaluate this potential.

## 2 Technology

This section provides an overview of the technology that was demonstrated, including an in-depth explanation of the development.

### 2.1 Technology description and development

TREECS™ consists of time-varying contaminant fate/transport models for soil, vadose zone, groundwater, and surface water to forecast MC export from ranges and resulting concentrations in each medium. These disparate models are dynamically linked within a modeling framework, which is the Framework for Risk Analysis in Multimedia Environmental Systems (FRAMES) (Whelan et al. 1997) (<http://mepas.pnnl.gov/FramesV1/index.stm>). The conceptual site model (CSM) as well as the schematic of TREECS™ model linkages is shown in Figure 1 for Tier 2. There are two levels of capability. Tier 1 consists of screening-level methods that assume highly conservative, steady-state MC loading and fate. Tier 1 requires minimal input data requirements and can be easily and quickly applied. Tier 2 provides time-varying analyses and solves mass balance equations for both solid and non-solid phase MC mass with dissolution. Additionally, MC residue loadings to the range soil can vary from year-to-year based on munitions use. Thus, media concentrations computed with Tier 2 should be closer to those expected under actual field conditions. There is also an Advanced Tier 2 option that allows the user to construct complex media pathways using the FRAMES CSM workspace (Figure 2). Developmental documentation reports for TREECS™ are provided by Dortch et al. (2009, 2011a, 2012, 2013a, 2013b), Dortch and Johnson (2012), Johnson and Dortch (2014a), and Dortch and Gerald (2015), as well as a user manual (Gerald et al. 2012). TREECS™ has been applied and validated substantially over its development (Dortch et al. 2011b, Dortch 2012, Dortch 2013, Dortch et al. 2013a, Johnson and Dortch 2014b, and Dortch 2016).

A source loading model provides the source mass loading rate within an area of interest (AOI). There are three options within the AOI loading model: 1) estimate MC residue loadings within an impact area stemming from munitions items fired on range; 2) estimate MC loadings at range firing points; and 3) specify generic source loading that could represent any other scenario not pertaining to firing ranges. The latter option is simply a table of loading rates per year (grams/year) for each constituent of concern; thus, this option could be used for applications that do not pertain to

firing/training ranges. For each munitions item used on a range, the user first selects the munitions identification using the munitions type and the Department of Defense Identification Code (DODIC) or National Stock Number (NSN). The amount of MC mass in each munitions item must be known to compute the MC residue loading. This information can be obtained from the Munition Items Disposition Action System (MIDAS) (<https://midas.dac.army.mil/>) based on DODIC or NSN. However, extraction of information from MIDAS can be slow and tedious. A utility was developed for automatically pulling this information into the TREECS™ application. The munitions MC mass is distinguished between that used at firing points and that used at impact areas. For each munitions item fired into the impact area, the user provides the following for each year of input: number fired; percent of duds (no explosion); percent of low order detonations (partially exploded); percent yield (portion of MC used up when munitions explode) for low order detonations; percent of duds that are sympathetically exploded by another detonation; percent yield for sympathetic detonations; and percent yield for high order detonations. Guidance is provided within TREECS™ for estimating dud rates, low order rate and yields, and high order yields. Little information is available to date for sympathetic detonations. For firing points, the user must enter for each item fired either the emission factor, which is the mass of un-used MC deposited per item, or the percent of unexpended firing point MC for each item fired. The user must also enter the numbers fired each year for each item. The other inputs that are required for impact areas are not required for firing points. Once the MC mass delivered to the impact area or firing point is known for each munitions item used and the other input parameters are entered, the calculation of residue mass loadings becomes a straightforward summation.

**Figure 1.** Conceptual Site Model and schematic of model linkages within TREECS™, Tier 2 (red denotes features in Tier 2 that are not in Tier 1).

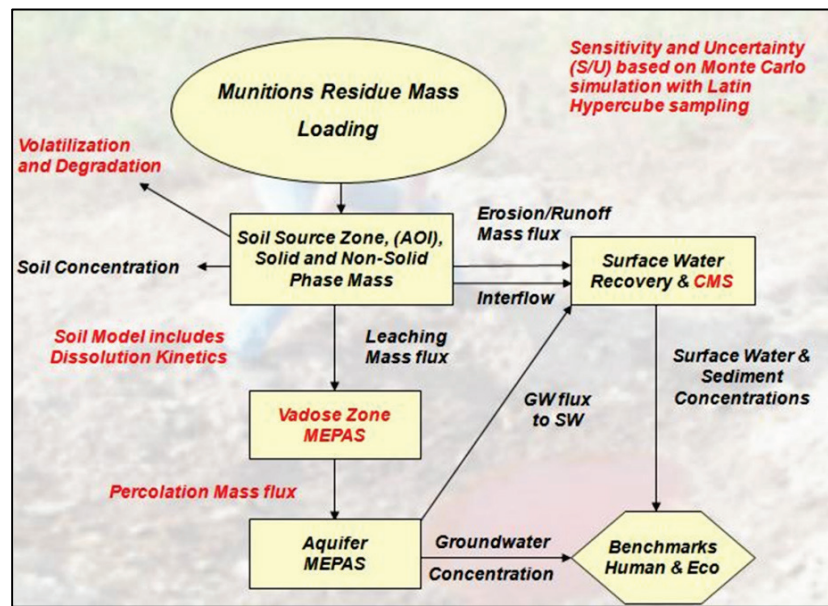
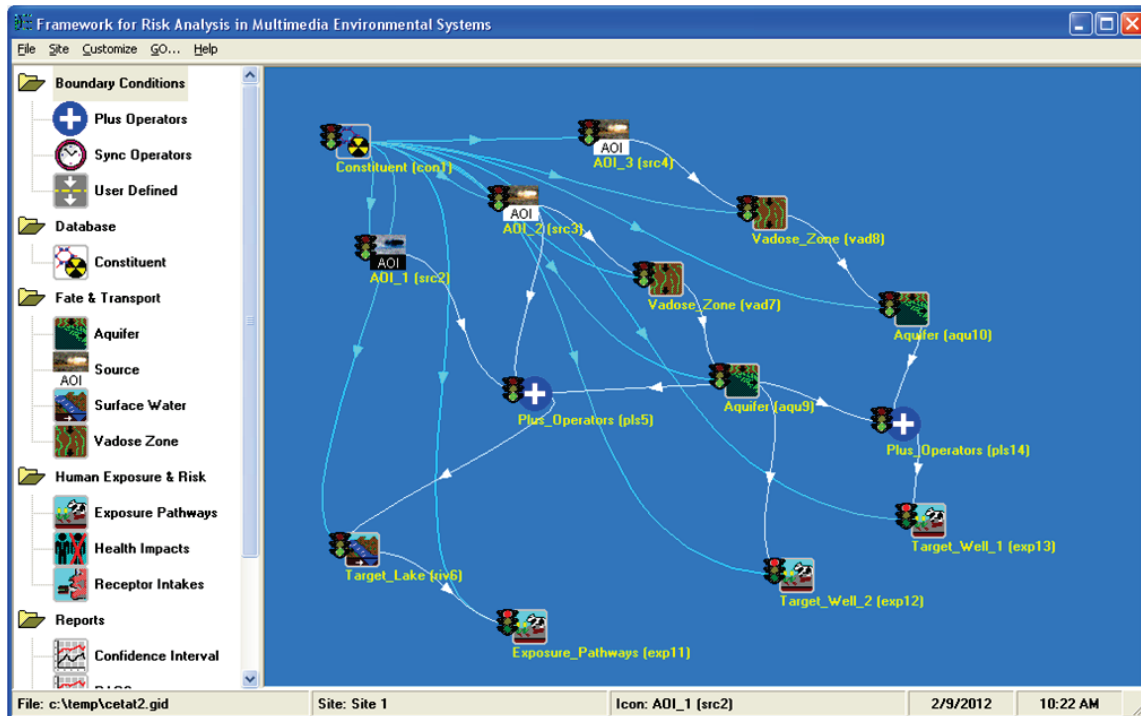


**Figure 2.** FRAMES CSM workspace within TREECS™ Advanced Tier 2 option.



All of the multi-media fate models are based on mechanistic mass balance principles. The soil model simulates a layer of surface soil that has a constituent concentration that varies with time but is fully mixed over a given

AOI, such as the impact area of a live fire range. The soil model accounts for MC transport and transformations due to rain induced erosion, surface runoff, leaching, degradation, and volatilization processes. The constituent can exist in solid and non-solid (dissolved) phases. A dissolution process is included to transfer solid-phase MC to the non-solid phases. The non-solid phase mass exists in equilibrium distributed as dissolved in water within the water filled soil pore spaces, as adsorbed from water to soil particles, and as a vapor in air within the air filled pore spaces. The soil model computes time-varying soil concentrations and mass export fluxes for erosion, rainfall extracted runoff, and infiltration to the vadose zone.

The fate processes in the soil model are presently driven by either average annual or daily hydrology (i.e., precipitation, runoff, infiltration, and erosion), and the user selects which option to use. There is a TREECS™ utility, referred to as the Hydro-Geo-Characteristics Toolkit (HGCT) to estimate average annual and daily hydrologic inputs. Formulations and methods used for estimating average annual and daily hydrology are described by Johnson and Dortch (2014a) and Dortch (2014).

The vadose zone model uses the infiltration, or leached mass influx rate, from the soil model to compute the time-varying mass flux moving through the vadose zone and entering groundwater. The vadose and groundwater, or aquifer, models are legacy models originally used within the Multimedia Environmental Pollutant Assessment System (MEPAS) (Buck et al. 1995). The MEPAS version 5.0 models (<http://mepas.pnl.gov/mepas/maqu/index.html>) compute fluxes through the vadose zone and aquifer and resulting aquifer concentrations at specified well locations. The vadose zone model solves the vertically one-dimensional (1D), reactive, transport equation for partially saturated conditions. The aquifer model solves the reactive, transport equation for 1D, longitudinal advection and three-dimensional (3D) dispersion for saturated conditions. First-order degradation and reversible, linear, equilibrium partitioning are used in both models. The scientific documentation of the MEPAS groundwater models is provided by Whelan et al. (1996) and Dortch et al. (2011a).

There are two options for modeling contaminant fate in surface water and sediments: RECOVERY (Ruiz and Gerald 2001) and the Contaminant Model for Streams, or CMS (Fant and Dortch 2007). Both models are legacy ERDC models. RECOVERY is best suited for pooled surface water, such as ponds and lakes, while CMS is best suited for streams and rivers.

Descriptions of these two models are provided by Dortch et al. (2011a). Both models solve time-varying, mass balance equations for total (dissolved and particulate) contaminant mass in surface water and bottom sediments with reversible linear equilibrium partitioning between dissolved and adsorbed particulate forms. First-order degradation kinetics are used in both models. For the RECOVERY model, the water column is treated as a fully mixed single compartment. The bottom sediments are layered into two types: a single, mixed sediment layer at the sediment-water interface; and multiple, 1 cm thick, deep sediment layers below the mixed layer. This treatment results in three mass balance equations with three unknown variables, which apply to the water column, the mixed sediment layer, and the deep sediment layers. Two coupled ordinary differential equations are solved for the surface water and the mixed sediment layer. A partial differential equation is solved for the deep sediment layers. Fate processes include: water column flushing; sorption partitioning in the water column and benthic sediments; degradation in water and sediments; volatilization from water; water column sediment settling and bottom sediment resuspension; deep sediment burial; mass transfer of dissolved constituent between the water column and mixed sediment layer pore water; bioturbation between the mixed sediment layer and top layers of the deep sediments; and pore-water diffusion within the deep sediments. Loading boundary conditions include inflowing contaminant mass due to export from the soil model, which includes rainfall extraction and runoff, erosion, and soil interflow fluxes. There is also an option to enter user-specified constant external loadings. The model produces output for total and dissolved concentrations in the water column and sediment bed.

The CMS is very similar to RECOVERY with the primary difference being the dimensionality and its orientation. CMS divides the stream into 1D longitudinal (stream-wise direction) segments. A single, fully mixed compartment is used to represent the benthic sediments underneath each 1D stream water segment. There is exchange between the sediment compartment and the overlying water just as in RECOVERY, but there is no longitudinal exchange between benthic sediment compartments except that associated with surface water fate and transport. The model solves a partial differential equation for the 1D, advection-diffusion-reaction (mass balance) equation of the surface water cells and an ordinary differential equation for each benthic sediment compartment. The CMS assumes steady, uniform flow. Stream flow can vary over time, but there is no hydraulic or hydrologic flow routing involved. There are various options for

estimating the flow cross-sectional area and depth based on flow rate. The modeled fate processes are the same as those in RECOVERY except that bioturbation is not included since there is only one benthic layer.

The fate models within TREECS™ are also available within the Adaptive Risk Assessment Modeling System (ARAMS™)\*, which was developed prior to TREECS™ for the Army by ERDC under the Environmental Quality Technology (EQT) research program. The compatibility of TREECS™ models within ARAMS is possible due to the fact that the two systems use FRAMES as the underlying model linkage, operation, execution framework. Thus, as new models are developed for TREECS™, they can be wrapped in a manner so that they can be operational in both TREECS™ and ARAMS™. Likewise, models/modules within ARAMS™ can be shared within TREECS™. ARAMS™ provides the capability to conduct comprehensive human and ecological health risk assessment associated with multimedia exposure to contaminants. The human health risk models (i.e., exposure, intake, and health impacts) within ARAMS™ were added to TREECS™ and can be used by selecting the Advanced Tier 2 Modeling option within TREECS™. The ecological risk models/modules/databases of ARAMS™ have not been added to TREECS™ due to the greater complexity associated with these items. Range applications of TREECS™ typically will not require a comprehensive human or ecological health risk assessment, and the screening level assessment that is readily available and easily used within TREECS™ will be sufficient, especially given the fact that the screening level protective health benchmarks are highly conservative.

If a more comprehensive ecological health risk assessment is required for a range application, then there are two options for doing this. These two options also apply to conducting a comprehensive human health risk assessment in addition to the third option made available by applying TREECS™ Advanced Tier 2 as described above. One option is to apply ARAMS™ using TREECS™ fate models within ARAMS™. The other option is to apply TREECS™, and then supply the TREECS™-predicted media concentrations to ARAMS™ by using the *User Defined* modules within ARAMS™ that allow use of known concentrations within media. The latter option is preferred since TREECS™ has many other features (tools and information) to facilitate range applications that are not available within

---

\* <http://www.erdc.usace.army.mil/Media/FactSheets/FactSheetArticleView/tabid/9254/Article/500113/adaptive-risk-assessment-modeling-system-arams.aspx>

ARAMS™. Additionally, the time required to learn to use TREECS™ Tier 2 is much less than that of ARAMS™ due to the more structured development approach of TREECS™. All risk characterizations within the scope of this project will be screening level and will be based on the conservative, protective, health benchmarks available within TREECS™. The benchmarks are within the TREECS™ DoD Health Benchmarks Database and were provided by the DoD Range Munitions Use Subcommittee (RMUS).

The CTS Environmental Systems Modules and Workflows are illustrated in Figure 3. Figure 4 provides an illustration of the front page of CTS that provides the user with options for the selection of the CTS workflows and descriptions of the CTS modules, physicochemical property calculators, and reaction libraries. When executing a CTS workflow, the user enters the system through the Chemical Editor (Figure 5) which allows for entry of the chemical of interest through either provision of the common name, smiles string notation, CAS registry number, or chemical structure. The user then defines the environmental conditions of interest (e.g., aerobic versus anaerobic). Based on the environmental conditions selected by the user, the Reaction Pathway Simulator (Figure 6) will provide the major transformation products based on the execution of reaction libraries for abiotic reduction, hydrolysis, and/or aerobic biotransformation. The parent chemical and the generated transformation products are then passed to the Physicochemical Properties Calculator (Figure 7) which through access to SPARC (SPARC Performs Automated Reasoning in Chemistry) (Hilal, 2003), EPI Suite (Boethling and Constanza, 2010), TEST (Martin, 2016), and ChemAxon's plug-in calculators, will provide the necessary physicochemical properties required for predicting environmental concentrations. The fully functional version of the CTS will include a Reaction Rate Calculator that will provide reaction rate constants based on the parameterization and execution of available quantitative structure-activity relationships (QSARs). In this version of the CTS, the user will also have the ability to generate environmental descriptors through execution of the Earth Systems Module. This module uses Data for Environmental Modeling (D4EM) to search on-line databases (e.g., the United States Geological Survey (USGS) Water Quality Database) for environmental descriptors, such as groundwater temperature, organic carbon content, and pH.

The most recent version of TREECS™ that is available to the public is Version 5, which was released in October 2013. There is another developmental version that has not been released to the public which contains BMP

modules. The newer version will be released in early 2017. The CTS is a web-based tool that is currently running on cloud-based servers behind the EPA's firewall. The most recent version of CTS will made available to the public in early 2017. The prototype CTS was used during 2014 to expand the Army Range Munitions Constituents Database (ARCDB) to include additional physicochemical properties (e.g., ionization constants), as well as the degradation products (including their physicochemical properties) resulting from reductive transformations.

Figure 3. The primary modules and work flow diagram for CTS.

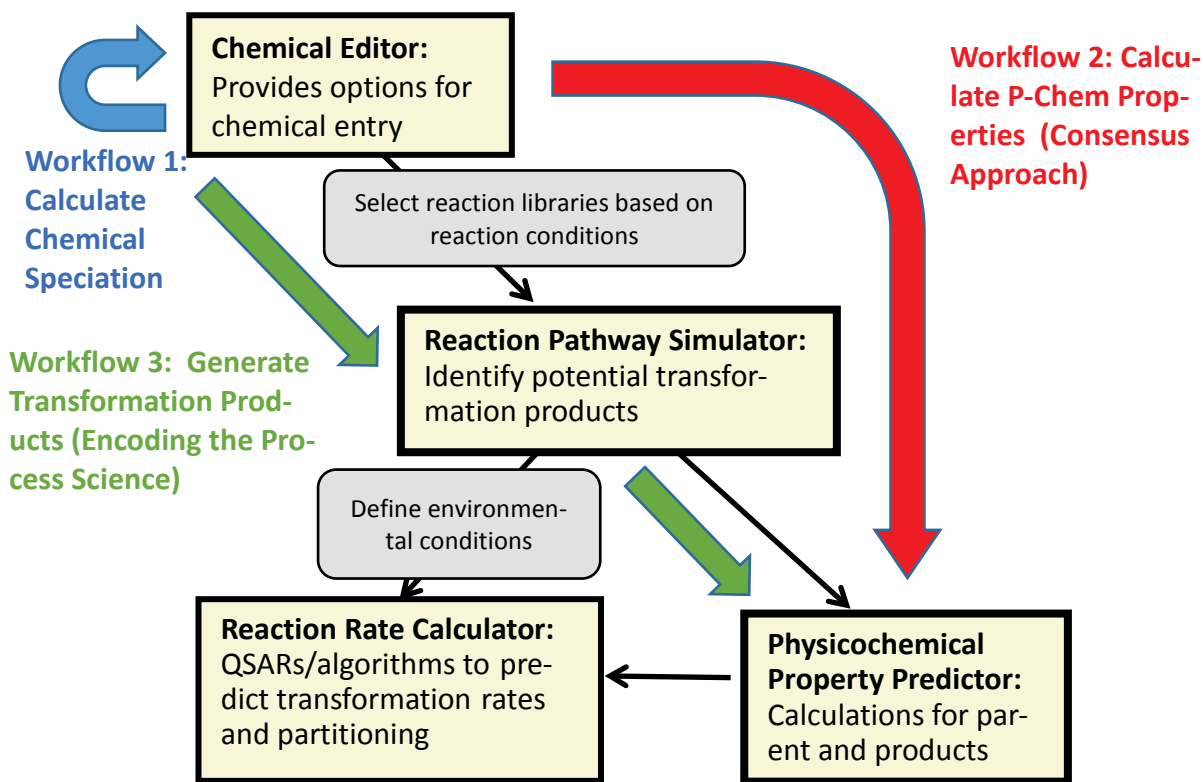
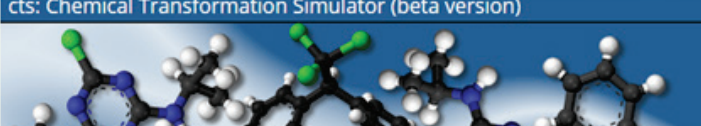


Figure 4. Front page of CTS providing the user with options for the selection of the CTS workflows and descriptions of the CTS modules, physicochemical property calculators and reaction libraries.

cts: Chemical Transformation Simulator (beta version)



The screenshot shows the front page of the Chemical Transformation Simulator (CTS) beta version. At the top, there's a banner with molecular models and the EPA logo. Below the banner, the title "cts: Chemical Transformation Simulator (beta version)" is displayed. On the left, a sidebar titled "CTS Workflows" lists three options: "Calculate Chemical Speciation", "Calculate P-Chem Properties", and "Generate Transformation Products". The "Generate Transformation Products" option is highlighted with a green background. The main content area contains descriptive text for each workflow. To the right, there are three vertical columns of links: "Description of CTS Modules" (Chemical Editor, P-Chem Properties, Reaction Pathway Simulator), "Description of P-Chem Calculators" (EPI Suite, SPARC, ChemAxon, TEST), and "Description of Reaction Libraries" (Abiotic Reduction, Abiotic Hydrolysis, Mammalian Metabolism). A "Get User's Guide" button is located at the bottom right of the main content area.

This web site is under development. It is available for the purposes of receiving feedback and quality assurance from personnel in the EPA.

The Chemical Transformation Simulator (CTS) provides the calculated physico-chemical properties of the parent chemical and transformation products, which are predicted as a function of the reaction system of interest. This is accomplished through the integration of cheminformatics applications for the encoding of process science underlying transformation pathways; computational chemistry tools for the calculation of physico-chemical properties; and software technologies that provide access to on-line databases for environmental descriptors required for estimating environmental concentrations.

The user interacts with the alpha-version of the CTS through the execution of one of three available work flows (green tabs in left column) described below. Each workflow invokes the CTS modules required to provide the data requested by the user. Descriptions of the individual modules are provided by the tabs in the left-hand column.

**Calculate Chemical Speciation Workflow:** Invokes the Chemical Editor (CE) Module which provides the user options for chemical entry and calculates the speciation (i.e., ionization, tautomer distribution and isomerization) for the chemical of interest.

**Calculate Physico-Chemical Properties Workflow:** The User inputs chemical information through the CE and then invokes the Physico-Chemical Properties Calculator (PCP) Module. The PCP Module then calls upon four stand-alone widely recognized calculators (EPI Suite, SPARC, ChemAxon, and Test), all of which calculate p-chem properties by mutually exclusive methods.

**Generate Transformation Products Workflow:** The User inputs chemical information through the CE and then invokes the Reaction Pathway Simulator (RPS) Module to generate transformation products through the execution of reaction libraries based on user-specified conditions. The User is then given the option to invoke the PCP Module for the calculation of p-chem properties for one or more parent or product chemicals.

**Description of CTS Modules**

- Chemical Editor
- P-Chem Properties
- Reaction Pathway Simulator

**Description of P-Chem Calculators**

- EPI Suite
- SPARC
- ChemAxon
- TEST

**Description of Reaction Libraries**

- Abiotic Reduction
- Abiotic Hydrolysis
- Mammalian Metabolism

**Get User's Guide**

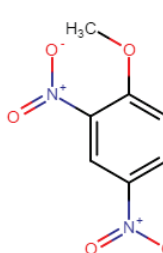
**Figure 5.** CTS Chemical editor module.

Chemical Editor | Reaction Pathway Simulator

Enter a SMILES, IUPAC or CAS#, or draw a chemical, then click the button located in the top right of the chosen method to get results. Click the "next" button below or click the "Reaction Pathway Simulator" link above to continue through the workflow.

**Lookup Chemical**      Enter a SMILES, IUPAC or CAS# and Click Here  
COC1=CC=C(C=C1[N+](=[O-])=O)[N+]([O-])=O

**Draw Chemical Structure**      Draw a chemical structure and Click Here

A chemical structure diagram showing a benzene ring with two nitro groups (-NO2) at positions 2 and 4, and a methoxy group (-OCH3) at position 1.

**Results**

SMILES:	<chem>COC1=CC=C(C=C1[N+](=[O-])=O)[N+]([O-])=O</chem>
Initial SMILES:	<chem>COC1=CC=C(C=C1N(=O)=O)N(=O)=O</chem>
IUPAC:	1-methoxy-2,4-dinitrobenzene
Formula:	C7H6N2O5
Weight:	198.134

**Clear**      **Next**

Figure 6. CTS Reaction Pathway simulator module.

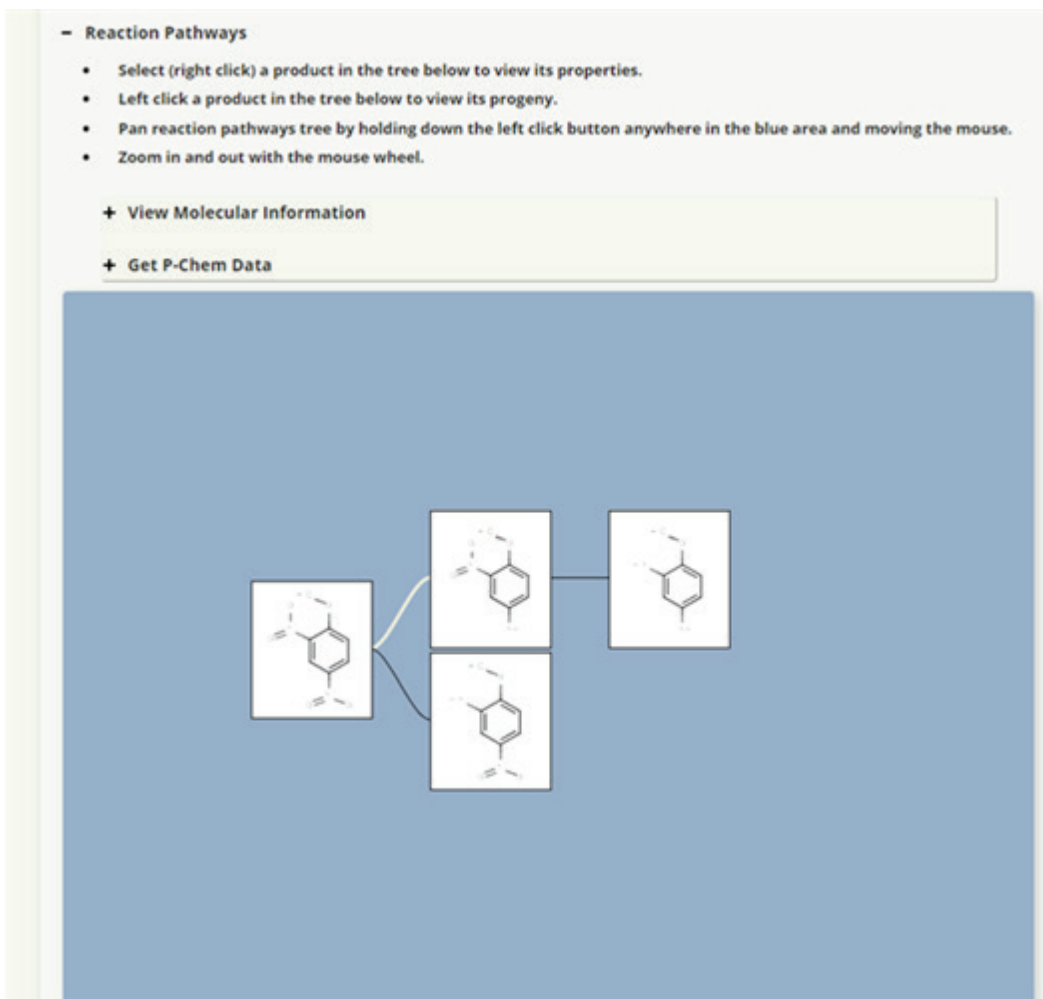


Figure 7. Example output from the CTS Physicochemical Properties calculator module.

The screenshot shows the 'Calculate P-Chem Properties Output' interface. At the top, there are tabs for Description, Inputs, Batch, and Output, with 'Inputs' selected. Below the tabs, it says 'Calculate P-Chem Properties Version 1.0 (Beta)' and the date 'Wednesday, 2016-August-31 11:27:00 (EST)'. On the right, there are download buttons for PDF, HTML, and CSV.

**User Inputs:**

- Molecular Information:
  - SMILES: COC1=CC=C(C=C1[N+](O-[O-])=O)[N+](O-[O-])=O
  - IUPAC: none
  - Mass: 198.134
  - Formula: C7H6N2O5

**P-Chem Properties Results:**

Checkboxes for data sources: ChemAxon, EPI Suite, TEST, SPARC, Measured. The 'All' checkbox is checked.

	ChemAxon	EPI Suite	TEST	SPARC	Measured
<b>Neutral Species Inputs:</b>					
<input checked="" type="checkbox"/> Melting Point (°C)	96.56				94.50
<input checked="" type="checkbox"/> Boiling Point (°C)	319.62		309.90	206.00	
<input checked="" type="checkbox"/> Water Solubility (mg/L)	2.68e+2	6.32e+2		1.24e+3	1.55e+2
<input checked="" type="checkbox"/> Vapor Pressure (mmHg)		1.38e-4		1.28e-3	property not available
<input checked="" type="checkbox"/> Molecular Diffusivity (cm <sup>2</sup> /s)				7.58e-6	
<input checked="" type="checkbox"/> Ionization Constant	pKa: none			pKa: none	
<input checked="" type="checkbox"/> Henry's Law Constant (atm·m <sup>3</sup> /mol)		3.01e-7		2.69e-7	property not available
<input checked="" type="checkbox"/> Octanol/Water Partition Coefficient (log)	1.74 KLOP 1.70 VG 1.65 PHYS	1.71		2.22	property not available
<b>pH-Dependent Inputs at pH: 7.4</b>					
<input checked="" type="checkbox"/> Octanol/Water Partition Coefficient (log)	1.74 KLOP 1.70 VG 1.65 PHYS			2.22	
<input checked="" type="checkbox"/> Organic Carbon Partition Coefficient (L/kg)		229.90			property not available
	Available	Unavailable			

Buttons at the bottom: Cancel, Clear data, Get data.

## 2.2 Advantages and limitations of the technology

The primary advantage of TREECS™ is that it provides a single, standardized suite of tools for specifically assessing military training and firing range operations and management to provide long-term viability to meet the national defense mission while protecting the environment and human health. Although the Marine Corps has used a variety of public domain contaminant fate models in their REVA process, none of these models are customized specifically to address range environmental issues like TREECS™. Thus, TREECS is unique from this application standpoint. However, TREECS™ is still general enough that it can be used for non-military applications.

Advantages of TREECS™ are highlighted via the following unique, TREECS™-specific features:

- Tiered analysis to allow staged assessments from initial screening to more comprehensive.
- Geographic Information Systems (GIS) module to facilitate applications with linkage to HGCT for estimating model inputs.
- Range munitions residue loading estimation module.
- Internal munitions data base indexed by DODIC and/or NSN based on a sub-set extraction from MIDAS for providing MC mass within each type of munitions.
- Three databases for providing constituent physicochemical properties, including the ARCDB which is tailored to range-specific contaminants.
- DoD RMUS ecological and human protective health benchmarks database.
- Automated linkages among multimedia contaminant fate models to facilitate ease-of-use for assessing source-to-receptor exposure.
- Special internal tools for estimating fate process input parameters, such as HGCT and soil-water and sediment-water adsorption partitioning coefficients.
- Sensitivity and uncertainty analysis via use of the built-in Monte Carlo simulation module.
- Specialized viewers to facilitate rapid examination and presentation of results.
- Reference indexing and tracking system and input summary report to document sources and values of input data.
- Database editors to allow development of user-specific databases for constituent properties, protective health benchmarks, and munitions component masses.
- Graphical user interfaces (GUIs) on all models to facilitate model set-up.
- BMP assessment modules.

Given the above features, TREECS™ can be applied in a relatively short period of time to determine range vulnerability for release of MC of concern from an operational range to an off-range area. Furthermore, TREECS™ can be used to determine when such a threat could occur; thus, providing the capability to evaluate future potential threats for existing or proposed ranges. For ranges that pose a threat for MC exposure in off-range areas, it can be used to evaluate alternatives to reduce or negate that

exposure. The primary limitation of TREECS™ is that it does require a level of understanding environmental modeling, which is true for applying any type of model. However, many features have been provided to try to minimize the time required for a user to become proficient. TREECS™ utilizes models of reduced form to minimize input requirements and the level of model complexity. Limiting the number of spatial dimensions and/or assuming property uniformity are a means of reducing model form. Models of reduced form can provide insightful information rapidly with first-order accuracy; however, the primary limitation of such models is that they may not be able to capture the effects of complex site features, and in such cases, a more comprehensive model may be required.

CTS is a unique product for providing a wide range of physicochemical properties for organic contaminants and for their predicted transformation products. This capability is especially of interest for emerging contaminants of which less is known regarding their properties. The limitations of CTS are that it is not applicable to metals and it does not predict degradation rates for organic chemicals.

### 3 Performance Objectives

The demonstration performance objectives and success criteria for this project are shown in Table 1. Each objective, its data requirements, and its success criteria are discussed in further detail. It is noted that each performance objective will be evaluated for each study site except for the second qualitative objective, which is independent of study sites.

**Table 1. Demonstration performance objectives and success criteria.**

Performance Objective	Data Requirements	Success Criteria
<b>Quantitative Performance Objectives*</b>		
TREECS™ accurately simulates long-term fate of MC on ranges	<ul style="list-style-type: none"> <li>• Receiving water MC concentrations</li> <li>• Information to estimate historical firing rates of munitions on range, such as firing records</li> <li>• Various site characteristics required for modeling MC fate</li> </ul>	<ul style="list-style-type: none"> <li>• Highly successful: model concentrations within a factor of 3 of observed</li> <li>• Successful: model concentrations within a factor of 5 of observed</li> <li>• Unsuccessful: model concentrations greater than a factor of 5 of observed</li> </ul>
TREECS™-CTS can be used to quantify uncertainty in inputs	<ul style="list-style-type: none"> <li>• Receiving water MC concentrations</li> <li>• Information to estimate historical firing rates of munitions on range, such as firing records</li> <li>• Various site characteristics required for modeling MC fate</li> </ul>	<ul style="list-style-type: none"> <li>• Model sensitivity and uncertainty feature can be used to bracket observed field MC concentrations at the 95% confidence level</li> </ul>
TREECSTM-CTS can be quickly set up and run with readily available data	<ul style="list-style-type: none"> <li>• Information to estimate historical firing rates of munitions on range, such as firing records</li> <li>• Various site characteristics required for modeling MC fate</li> </ul>	<ul style="list-style-type: none"> <li>• TREECS™, including CTS use, can be set up for a site within 80 labor hours using readily available information</li> </ul>

---

\* Observed data are too limited to do anything more robust for comparison, such as various statistical metrics.

Performance Objective	Data Requirements	Success Criteria
Training requirements are reasonable	<ul style="list-style-type: none"> <li>• Installation personnel or contractors that are available and willing to participate in TREECSTM-CTS training and will apply the system</li> <li>• Interviews with personnel and contractors following system training and use</li> </ul>	<ul style="list-style-type: none"> <li>• Engineer or scientist with general background in modeling, hydrology, and water quality can be trained to use system in 3 days to apply the system</li> </ul>
TREECSTM-CTS can be applied to evaluate range management and/or remediation strategies	<ul style="list-style-type: none"> <li>• Data noted above to accomplish model setup and validation</li> <li>• Future uses of range</li> <li>• Information pertaining to the specific management or remediation alternative to be addressed</li> </ul>	<ul style="list-style-type: none"> <li>• TREECSTM-CTS can be used to evaluate three management and/or remediation strategies to reduce MC concentrations in target receiving water</li> </ul>
TREECSTM-CTS can be applied to evaluate the fate of emerging MC	<ul style="list-style-type: none"> <li>• Input data files for previous application sites</li> <li>• Physicochemical properties of emerging MC to be evaluated</li> </ul>	<ul style="list-style-type: none"> <li>• TREECSTM-CTS can be used to evaluate the fate of four emerging contaminants that are used in new insensitive munitions (IM) by comparing results to those of conventional MC, such as RDX</li> </ul>

The last qualitative performance objective was added after the original work plan development. This objective will demonstrate the capability of TREECSTM-CTS to evaluate the fate of MC for new IM formulations relative to conventional MC, such as RDX. Five emerging contaminants (EC), 2,4-dinitroanisole (DNAN), 3-nitro-1,2,4-triazol-5-one (NTO), nitroguanidine (NQ), ammonium perchlorate (AP), and hexanitrohexaazaiso-wurtzitane (HNIW), also known as CL-20, will be tested and fate results will be compared against Royal Demolition Explosive (RDX) for three study sites. This demonstration will show the powerful utility of the modeling system for evaluating the fate and exposure of EC in the environment.

### 3.1 **Obective: TREECSTM accurately simulates long-term fate of MC on ranges**

It is imperative to demonstrate that TREECSTM can accurately simulate the long-term fate of MC on firing ranges so that there will be confidence in

the user community for its application for range vulnerability and sustainment. Multiple decades can pass between MC residue deposition on a firing range and subsequent migration to off-range receiving waters. Thus, the ability to assess long-term MC fate is a necessary requirement. Although migration to surface waters is expected to occur more rapidly than to groundwater in most cases, it can still take decades before concentrations can reach detection levels in surface water depending on source AOI loading rates and dissolution process rates. Model validation for real world conditions is an important step for model acceptance. This objective is dedicated to this step in model acceptance.

### **3.1.1 Data requirements**

Observed off-range receiving media concentrations are required for model comparison and validation. This project does not provide funding for collecting data; thus, observed/measured MC concentrations must already exist.

Additionally, site characteristics are required to supply the input data for model application. Such information can usually be obtained from previous work, such as ORAP and REVA studies, as well as information on the World Wide Web. Site information includes meteorology/climate, surface hydrology, hydro-geology, soil properties, topography, and land use and cover.

The MC mass loading rate (mass/time) within the AOI must be known in order to calculate the MC mass fate and off-range concentrations. Ideally, it is highly advantageous to have observed concentrations of MC in the AOI soil over time with which to estimate mass, but such data is rarely available for operational ranges. Therefore, it is necessary to estimate the source mass loading rates of MC residue using firing records if available. Installations have been actively maintaining firing range records during the past 10 to 15 years and records can usually be obtained from the installation.

### **3.1.2 Success criteria**

Success criteria should be based on quantitative metrics for a quantitative performance objective; however, quantitative metrics generally require more than a few data points. Unfortunately, there are most often only a

few data points for observed data associated with off-range concentrations, and in many cases, there are no such observations. Thus, success criteria are limited to rudimentary quantitative metrics. Statistical metrics for comparing model versus prototype require at least three observations for each time point and spatial location. Off-range measurements of MC concentrations are limited to a few spatial stations at usually one point in time, and the measurements usually involve only one sample for each station; therefore, statistical comparisons are not possible. Quantitative metrics are limited to simply comparing the model-computed value against the observed value for each spatial station at one, or perhaps two at most, points in time. These comparisons will be reported as ratio of model to prototype value, or the factor by which the model agrees with observed. Agreement of model with observed within a factor of three is considered highly successful given that models of reduced form are being used and given limited information on range firing rates and various model data uncertainties, such as degradation rates. Agreement within or above a factor of five denotes success or failure, respectively.

### **3.2 Objective: TREECS™-CTS can be used to assess uncertainty in inputs**

Given the uncertainties in model inputs, it is necessary to have the capability to provide confidence limits on model output associated with uncertain inputs. Information on site characteristics can be highly variable but relatively certain, such as stream flow rate. Some contaminant fate parameters, such as degradation rate, can be highly uncertain, even if there is little variation. This performance objective will focus on input uncertainty and not variability. The input variables that were treated as uncertain in the Monte Carlo uncertainty analysis of TREECS™ varied for each study site. For example, for the groundwater study site, uncertainty analysis included the soil-to-water adsorption, partitioning, distribution coefficient,  $K_d$ , and the degradation rate or half-life in various media; CTS was used to help quantify physicochemical properties. There were several media-specific input parameters that were not as well-known as other inputs for the other study sites, and these were treated as uncertain. AOI source mass loading rates are uncertain, but these were not treated as uncertain in the analysis since it is well known that media concentrations are directly and linearly related to mass loading rate (Dortch et al. 2010; Dortch et al 2011b). Sensitivity analyses were conducted first to assess the relative sensitivity of less certain inputs, and this information was used to guide the uncertainty analysis.

### **3.2.1 Data requirements**

The data requirements for this performance objective are the same as those required for the first performance objective discussed in section 3.1 above. The only additional requirement was successful completion of the sensitivity analyses that was needed to guide the uncertainty analysis.

### **3.2.2 Success criteria**

This performance objective will be judged as successful if the model output confidence band at the 95% level encompasses the observed data point or mean of the observed data for multiple observed data points.

## **3.3 Objective: TREECS™-CTS can be quickly set up and run with readily available data**

An important aspect of TREECS™-CTS acceptance is that they can be set up relatively quickly and run using readily available data. This aspect is qualitative, but it is important since there are many operational ranges that could require evaluation.

### **3.3.1 Data requirements**

The data requirements for this objective are the same as the two previous objectives with the exception that observed MC concentrations are not required for model set up. Adequate and readily available site information were available as determined during the site selection phase of this study.

### **3.3.2 Success criteria**

Past experience with TREECS™ has shown that the models can usually be set up, adjusted, and made ready for management scenario testing within about 80 labor hours. Thus, 80 hours for model set up and adjustment is deemed the success criteria for this objective.

## **3.4 Objective: training requirements are reasonable**

Another important, qualitative aspect of TREECS™-CTS acceptance is that personnel can be trained relatively easily and quickly to apply the systems. Such personnel should represent the DoD installation community as either

environmental staff of the installation, or contractors working for the installation. The goal was to conduct at least one, perhaps two, training sessions lasting three days.

### **3.4.1 Data requirements**

Completion of this objective will require that there are installation personnel or contractors that are available and willing to participate in TREECS™-CTS training and will apply the system. Additionally, trained personnel must complete a survey following the training. The personnel to be trained must have completed a minimum of a BS degree in engineering and/or science and have a general understanding of mathematical modeling of hydrology and water quality.

### **3.4.2 Success criteria**

This performance objective will be deemed successful if the students can be trained in three days to apply the system. The training survey completed by the students will be used to determine if they can apply the system and where more emphasis should be placed in future training sessions.

## **3.5 Objective: TREECS™-CTS can be applied to evaluate range management and/or remediation strategies**

It is important that TREECS™-CTS can be used to evaluate range management and BMP strategies to reduce or negate the threat of future off-range exposure to MC. The work under this objective was directed to the conventional MC RDX.

### **3.5.1 Data requirements**

The data requirements for this performance objective are the same as those required for the first performance objective discussed in section 3.1. It would have been helpful if installation personnel had provided insights for future range use and any potential range management and/or BMP alternatives considered appropriate to reduce future threats of off-range MC exposure. However, historically it was not imperative to have such insights, as in this case, reasonable and cost effective strategies were selected and evaluated. The assumption was made that future range use will be the same as that experienced in the recent past. The level of future range use was also one of the range management strategies evaluated.

### **3.5.2 Success criteria**

TREECS™-CTS will be used to evaluate three management and/or remediation strategies to reduce MC concentrations in target receiving water for each study site. This demonstration will be conducted for the existing MC of concern. All management scenarios will be compared to baseline, existing conditions without any management or BMP strategies so that effectiveness of each strategy can be evaluated.

## **3.6 Objective: TREECS™-CTS can be applied to evaluate the fate of emerging MC**

It is important that TREECS™-CTS can be used to evaluate the fate of emerging contaminants or munitions constituents associated with new IMs. Much is not known about the fate of these ECs, and models should be used to obtain an improved understanding. The fate of five ECs; DNAN, NTO, NQ, AP, and CL-20, will be evaluated with the system.

### **3.6.1 Data requirements**

The data requirements for this performance objective are the same as those required for the first performance objective discussed in section 3.1. In addition, the physicochemical properties must be either known or estimated and provided as model input. CTS will be used to obtain improved estimates for some of the properties. However, CTS cannot be used to provide one of the most uncertain and sensitive inputs, the EC degradation rate or half-life. Also, soil and sediment adsorption partitioning distribution coefficients cannot always be estimated from organic carbon and/or octanol partitioning coefficients. Therefore, two types of assessments will be performed for the ECs at each study site. One will use the best available estimates for property input that are already within TREECS™-CTS, and the second will use improved estimates for partitioning coefficients and degradation rates based on a literature review.

### **3.6.2 Success criteria**

TREECS™-CTS will be used to evaluate the fate of EC relative to RDX. These demonstrations will be conducted for five EC at all three study sites. CTS will be used when possible to improve property estimates of the ECs.

## 4 Site Description

The approach calls for applying the TREECS™/CTS systems to three DoD sites where receiving water concentrations of MC have been measured, thus allowing demonstration and validation of the models against observed data. Three sites were selected for study as detailed in the Site Selection Memo for this project. The three study sites are: Demolition (Demo) Area 2 of Camp Edwards of Massachusetts Military Reservation (MMR), MA.; the Artillery Impact Area (AIA) of the U.S. Military Academy (USMA), West Point, NY.; and Zulu Impact Area (ZIA) of Marine Corps Base (MCB) Camp Pendleton, CA. The MC of interest at all three sites is the HE hexahydro-1,3,5-trinitro-1,3,5-triazine, referred to as RDX.

Groundwater was modeled for Demo Area 2 of MMR. Surface water (Popolopen Brook) was modeled down-gradient of the AIA at West Point. Surface water and groundwater were modeled for the Las Flores watershed that contains the ZIA. Demo Area 2 is the only site that has more than two observed receiving water concentrations of RDX, but all three sites do have observed values exceeding detection limits, which is rarely the case at most installations where either sampling has not been performed for receiving waters, or receiving water samples are below detection. All three sites were useful for investigative modeling of ECs associated with new IMs with comparison to RDX.

Since there are three study sites, the format of this report must depart some from the ESTCP guidance, in which it is assumed that there is one study site. Separate major sections are devoted to the description of each site. Additionally, this project involved modeling, rather than field sampling and demonstration of a site remediation technology. This aspect further required departing from the ESTCP final report format. For these reasons, the ESTCP guidelines for sections 4 and 5 could not be followed, rather the information pertaining to those sections is captured within each of three major sections that deal with each study site. Before presenting the details of each study site, it is necessary to first explain the overall approach and testing protocol, which follows in the next section.

## 5 Test Design

This section provides the detailed description of the system design and testing conducted during this demonstration project. As explained in the previous section, it is impossible to follow the ESTCP final report format since this project is vastly different from the typical ESTCP Environmental Restoration project that involves field sampling and demonstration of a restoration technology. The sub-sections that follow are closely tied to the performance objectives of Table 1.

### 5.1 Overall concept

Accomplishment of the first quantitative performance objective dealing with model validation is the key to successful accomplishment of the other objectives with the exception of the first qualitative performance objective associated with model set up. There is an important aspect of validation in this study that is common to all three study sites. Model inputs were set initially based on the best available information without regard to how well model results compared with observed data. In other words, input data were not manipulated to force the model to agree exactly with the observed data. Adjustments were made to any inputs that were determined to be inappropriate or were discarded due to improved information or understanding of the modeled system. However, there was no attempt to force calibrate each site model to agree with measured results. Thus, model *calibration* was not performed, and any model input adjustments herein should not be interpreted as calibration (e.g., adjustment of an instrument for taking measurements). TREECS™ was developed to predict or forecast MC fate and concentrations in the environment based on past and future range operations. It is impossible to calibrate the models for such predictions. For this reason, it is far more important to validate the use of TREECS™ for predictive use than to force calibrate it to exactly match past observations. Thus, there is no forced model calibration, rather, the focus is on model validation using the best available and reasonable information for model inputs.

### 5.2 Model validation

The accuracy of each validation was quantified to the extent possible, which depends on the amount of available field-measured data. A set of metrics were needed for evaluating model validation success. Due to the

scarcity of observed MC concentration data, statistical comparisons were not possible in most cases; thus, model results are compared to observed data in two other ways, result ratio (*RR*) and relative error (*RE*). The *RR* is the ratio of model-predicted (*P*) to observed (*O*), or the inverse, as follows,

$$RR = \frac{P}{O}, \text{ if } P \geq O \quad \text{or} \quad RR = \frac{O}{P}, \text{ if } P < O \quad (1)$$

The *RR* provides the factor by which the model either over or under predicts the observed value, and it is always greater than 1.0 unless the prediction is perfect, in which case *RR* = 1. The *RE* is a percent of error computed from

$$RE = 100 \frac{|P - O|}{O} \quad (2)$$

The *RR* and *RE* are related, but relating them can be somewhat misleading. For example, consider two model results that over-predict and under-predict by a factor of 2 (i.e., *RR* = 2). For the over-prediction, *RE* = 100%, but for the under-prediction, *RE* = 50%. Similarly, consider two model results that over-predict and under-predict by a factor of 3 (i.e., *RR* = 3). For the over-prediction, *RE* = 200%, but for the under-prediction, *RE* = 66.7%. An *RE* of 50% (or 66.7%) appears to be allot better than an *RE* of 100% (or 200%), but in reality, the model disagreement with observation is the same, but only over-predicted in one case and under-predicted in the other. Thus, the *RR* will be used to determine whether or not the performance objective has been met, where the criteria for highly successful for the first quantitative objective is *RR* = 3. However, *RE* will also be reported to document the amount of model error relative to the observation.

### 5.3 Baseline characterization

The final validated model for each of the three study sites serves as the baseline condition for sensitivity and uncertainty analyses. The final validated model is also used for the baseline conditions for demonstration and evaluation of range management and BMP alternatives. The media concentrations for each management alternative are compared with no-action baseline concentrations. In the absence of future range use plans, recent range use (i.e., munitions firing rates or MC loading rates) are assumed for future years to establish future no-action baseline conditions. All other inputs are the same as the final validated model. The alternative action conditions, which include input modifications for each alternative

management strategy, were run and compared against the no-action baseline condition. Similarly, baseline conditions are used to assess the fate of each of the ECs for each study site relative to that of RDX.

## 5.4 Field data

Field sampling and testing were not conducted during this project, rather, existing field data were used for assessing the accuracy of model-computed results. Model output for the appropriate media and location, year, and concentration units compared with observed data for that media, location, time, and units. The comparisons that are made are summarized in Table 2.

**Table 2. Available observed data for model comparison.**

Study Site	Media	Year	Type of observation concentration for RDX
Demo Area 2, MMR	AOI <sup>1</sup> soil	1998	Total
Demo Area 2, MMR	Groundwater	2003	Dissolved
AIA, USMA	Surface water creek	2003	Total
AIA, USMA	Surface water creek	2012	Total
Zulu impact area, Camp Pendleton	Surface water creek	2011	Total
Zulu impact area, Camp Pendleton	Groundwater	2012	Dissolved

<sup>1</sup> AOI = area of interest, such as in impact area of firing ranges

## 5.5 Uncertainty analysis

Following model validation, the uncertainty analysis capability of TREECS™ will be demonstrated for the MC of interest at each study site. TREECS™ uses Monte Carlo simulation with Latin Hypercube sampling for assessing uncertainty in model inputs. The inputs to be treated as uncertain will be selected based on some sensitivity testing; the overall understanding for what inputs are driving the results and their values are also not well known. The performance objectives call for delineating the 95% confidence band for predictions and determining if the observed data fall within that band.

## **5.6 Fate of emerging MC (EC) associated with IM**

The third component of each study site application involves applying the systems for emerging contaminants or constituents (ECs), which include components of newer IM. The applications for ECs are provided to demonstrate the utility of TREECS™ - CTS for forecasting the fate of newer MC relative to the fate of traditional MC, (e.g., HE RDX). The physicochemical properties of newer MC are not as well known, and field data are non-existent.

Insensitive munitions contain explosive constituents that are less sensitive to heat and shock. Three IMs receiving attention include IMX 101, IMX 104, and PAX 21. The ingredients of IM include 2,4-dinitroanisole (DNAN), 3-nitro-1,2,4-triazol-5-one (NTO), nitroguanidine (NQ), and ammonium perchlorate (AP). RDX is included in some IMs, such as IMX 104 and PAX 21. Another new HE of interest is HNIW, also known as CL-20. The fate of these five MCs is evaluated at each study site relative to RDX.

## **5.7 BMP assessment**

The fourth component of each study site application involves demonstration of the capability of the systems to assess BMP alternatives, including remediation strategies, for reducing environmental risk. Three or more BMP alternatives will be evaluated for each site using the original MC of interest (RDX) for that site.

Each of the three major sections that follow are devoted to a study site. Within each major section, there are sub-sections explaining site description, model inputs for validation, validation results, uncertainty analysis, fate of ECs, and BMP assessment.

## 6 Demo Area 2, MMR

### 6.1 Site description

The Massachusetts Military Reservation (MMR) is located in Barnstable County in the Cape Cod region of Massachusetts. The installation has been in use since 1911 for Army training and maneuvers, military aircraft operations, maintenance, and support. There are currently units or members of the National Guard operating at the MMR.

Demo Area 2 is located in the northern section of Camp Edwards, which is within the MMR as shown in the site map of Figure 8. Demo Area 2 was used for light demolition training for roughly 10 years, (beginning in about 1978 and continuing until about 1988). The area was used for demolition training, not for demolition of loaded munitions; thus, non-munitions objects were blown up rather than munitions containing explosives. Range records show that the explosives used in this area were limited to blocks of Composition 4 (C4) and trinitrotoluene (TNT) demolition charges. Thus, C4, which contains RDX and plasticizers, was a prevalent explosive at this site. Some charges may not have experienced full, high-order detonation, thus resulting in unexploded HE residue. RDX residue from these explosives infiltrated the groundwater beneath the demolition range.

The soils in this region are sandy and highly permeable allowing for rapid movement of groundwater at rates up to 0.6 m/day (AFCEE, 2006). The MMR is located over the recharge area of the Sagamore Lens, which is a large aquifer about 91 m thick (AFCEE, 2006). Demo Area 2 is divided into four main soil regions, but the source zone area is characterized as Enfield soil type (denoted as 265B), which is silty loam down to 30 cm, a mixture of silty loam and sandy loam from 30 to 79 cm, and mostly sand at depths below 79 cm.

Soil and groundwater concentrations of RDX were measured at the site about 10 to 15 years after demolition training had ceased. The RDX groundwater plume delineation relative to monitoring wells near Demo Area 2 is shown in Figure 9. The darker shade indicates concentrations greater than 2 parts per billion (ppb), which was the public health advisory concentration at the time, and the lighter shade indicates concentrations above non-detection but less than or equal to 2 ppb.

Figure 8. Demo Area 2 of MMR, Cape Cod, MA (modified from AMEC Earth and Environmental, 2004).

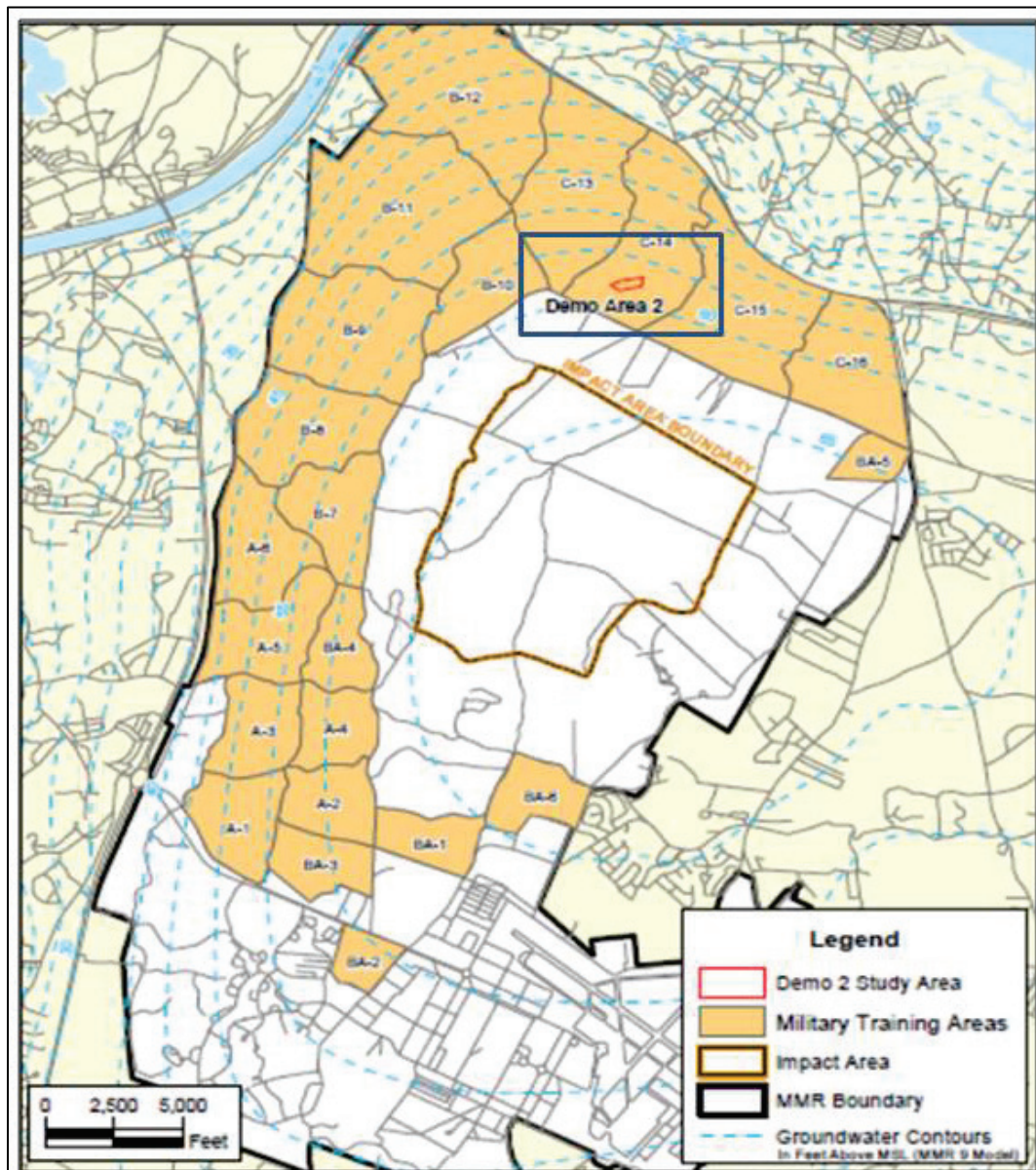
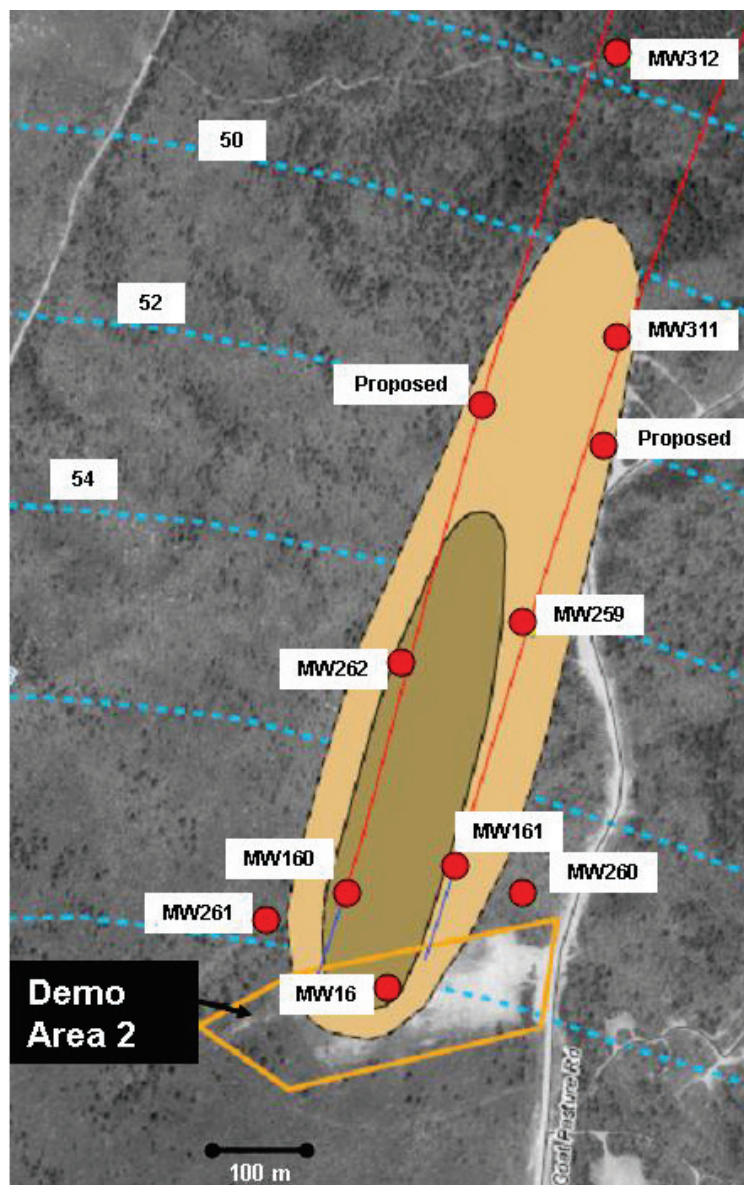


Figure 9. RDX plume delineation and monitoring wells for Demo Area 2 with groundwater contours in feet National Geodetic Vertical Datum (NGVD) (modified from AMEC Earth and Environmental, 2004).



## 6.2 Model inputs for validation

Demo Area 2 and the receiving groundwater were modeled previously with TREECS™ (Dortch et al. 2007; Dortch 2012). This study site was modeled again (Dortch 2015) as part of this ESTCP project. Although most of the model inputs for the ESTCP application are the same as those documented previously (Dortch et al. 2007; Dortch 2012), a few inputs were corrected as described by Dortch (2015).

Three modeling components of TREECS™ were used, which included the Tier 2 soil model, the Multimedia Environmental Pollutant Assessment System (MEPAS) vadose zone model, and the MEPAS aquifer model. The background information for the model input values are not repeated here since this information is presented in the previously referenced publications (Dortch et al. 2007; Dortch 2012; Dortch 2015). However, for completeness, the input values are provided in Table 3 through Table 5. Throughout this report, the term AOI is used to refer to the soil source zone area where MC has been deposited due to military training/firing.

Key features of the model inputs for this application are noted here. The option for average annual hydrology, rather than daily varying hydrology, was used in the soil model for this application. A constant RDX residue loading rate of 1,500 g/yr was applied for 10 years, starting in 1978. This loading rate is an estimate based on the types of detonation charges used (Dortch et al. 2007). The particles of low-order detonations are on the order of a centimeter in size (Pennington et al. 2005; Taylor et al. 2004). A particle diameter of 6,000 micrometers or 0.6 cm was used for this application.

The model was run for 30 years during validation starting in 1978 when there was assumed to be zero soil contamination of RDX. Surface soil runoff was assumed to be zero for the highly permeable soils, thus, all precipitation resulted in evapotranspiration and infiltration into the soil layer. The half-life for degradation of dissolved phase RDX in soil, vadose zone, and groundwater was assumed to be 100 years, whereas the solid and adsorbed phase RDX was assumed to be non-degradable (a high value of 1E20 years was used for half-life). Soil properties for silty loam and sand were used for surface soil and vadose/aquifer, respectively. All chemical-specific properties of RDX were obtained from the Army Range Constituent Database (ARCDDB) within TREECS™. The well location for monitoring model output coincided with the location of monitoring well 161 (MW161), which is one of the wells where RDX concentrations were measured in the field.

CTS was not used during model validation to set the chemical-specific properties for RDX since those properties are fairly well known and were available in the TREECS™ constituent databases. However, values derived from CTS were used during model sensitivity analysis and assessment of the fate of IM components as discussed later.

**Table 3. Tier 2 soil model input values for Demo Area 2, MMR.**

Input Description	Value
<b>Site Characteristics</b>	
AOI dimension that is parallel to the groundwater flow, m	110
AOI dimension that is perpendicular to the groundwater flow, m	110
AOI surface, m <sup>2</sup>	12,100
Active soil layer thickness, m	0.4
Average annual temperature of soil-water matrix, °C	11.0
MC mass residue loading versus time, g/yr	1,500 Assumed to be constant for 10 years
Initial solid phase MC concentration in soil on a soil mass basis at time 0, mg/kg	0 for all constituents
Initial total non-solid phase MC concentration in soil on a soil mass basis at time 0, mg/kg	0 for all constituents
<b>Soil Properties</b>	
Volumetric soil moisture content, percent	15.5
Soil dry bulk density, g/cm <sup>3</sup>	1.43
Soil porosity, percent	46
<b>Hydrology</b>	
Average annual precipitation, m/yr	1.22
Average annual rainfall, m/yr	1.22 (set to precipitation since no runoff)
Average annual soil erosion rate, m/yr	Assumed to be 0.0 since no runoff

Input Description	Value
Average annual water infiltration rate (groundwater recharge for no interflow), m/yr	0.762
Average annual surface water runoff rate, m/yr	Assumed to be 0.0
Percent of annual water infiltration flow rate and mass flux that goes to soil interflow, fraction	0
Average number of rainfall events per year	100
Fate/Transport Parameters for RDX	
Soil exchange layer thickness for rainfall ejection of pore water, m	0.005
Soil detachability for rainfall ejection of pore water, kg/L	0.4
Diffusion layer thickness for volatilization, m	0.4
Soil-water constituent partition coefficient, $K_d$ , L/kg	0.203
Decay/degradation half-life of liquid (water) phase constituent, yrs	100
Decay/degradation half-life of adsorbed (particulate) phase constituent, yrs	1.0E20
Initial mean diameter of solid phase constituent residue particles (assume spherical particles), $\mu\text{m}$	6,000

Input Description	Value
Volatilization rate, m/yr	39.0 as computed by soil model user interface from molecular diffusivity in air
Switch for solid phase erosion	off
Chemical-Specific Properties for RDX	
Aqueous solubility limit, mg/L	29.52 (based on average annual soil temperature of 11 deg C)
Henry's law constant, atm-m <sup>3</sup> /g-mol	6.32E-8
Molecular weight (molar mass or averaged molecular mass), g/mol	222.12
Solid phase constituent mass density, g/cm <sup>3</sup>	1.82
Model Options	
Time length of simulation, yrs	30
Time step, yrs	0.001
Methods used for equation solution	Constant time step

Table 4. MEPAS vadose model input values for Demo Area 2, MMR.

Input Description	Value
Inputs passed from soil model	
AOI dimension that is parallel to the groundwater flow, m	110
AOI dimension that is perpendicular to the groundwater flow, m	110
Water flow rate due to infiltration from soil (rainfall flow rate into vadose zone), m <sup>3</sup> /yr	9220
MC mass flux versus time due to leaching from soil to vadose zone, g/yr	Time-varying
Soil Composition	

Input Description	Value
Percentage of sand, %	91.83
Percentage of silt, %	5
Percentage of clay, %	3
Percentage of organic matter, %	0.17
Percentage of iron and aluminum, %	Unknown, set to 0
Soil Characteristics	
pH of pore water, pH units	7
Total porosity, %	38
Field Capacity, %	9
Saturated hydraulic conductivity, cm/day	570
Thickness of the vadose zone layer, m	39.6
Longitudinal (vertical direction) dispersivity, cm	0.396
Dry bulk density, g/cm <sup>3</sup>	1.64
Constituent Properties for RDX	
Sorption partitioning coefficient, $K_d$ , ml/g	0.024
Water solubility of constituent, mg/L	59.8
Half-life of constituent in groundwater, yrs	100

Table 5. MEPAS aquifer model input values for Demo Area 2, MMR.

Input Description	Value
Inputs passed from vadose zone model	
AOI dimension that is parallel to the groundwater flow, m	110
AOI dimension that is perpendicular to the groundwater flow, m	110
Water flow rate due to percolation (groundwater recharge), m <sup>3</sup> /yr	9220
MC mass flux versus time due to percolation from the vadose zone to the aquifer, g/yr	Time-varying

Input Description	Value
Composition	
Percentage of sand, %	91.83
Percentage of silt, %	5
Percentage of clay, %	3
Percentage of organic matter, %	0.17
Percentage of iron and aluminum, %	Unknown, set to 0
Sub-surface Characteristics	
Percentage of constituent flux entering the aquifer, %	100
pH of the pore water, pH units	7
Total porosity, %	38
Effective porosity, %	30
Darcy velocity, cm/day	100
Thickness of aquifer, m	91
Soil dry bulk density, g/cm <sup>3</sup>	1.64
Concentration (well) Locations	
Longitudinal distance to well, m	198
Perpendicular distance from plume center-line to well, m	59
Vertical distance below water table to well intake, cm	0.0
Longitudinal dispersivity, m	1.09
Transverse dispersivity, m	0.109
Vertical dispersivity, m	0.00198
Constituent Properties for RDX	
Sorption partitioning coefficient, $K_d$ , ml/g	0.024
Water solubility, mg/L	59.8
Half-life of constituent in groundwater, yrs	100

### 6.3 Validation results

The model-computed results with the inputs presented in the previous section are shown in Figure 10 and Figure 11 for soil and groundwater, re-

spectively, with comparison to the mean and range of measured concentrations. Groundwater monitoring well MW161 was selected for comparisons although fairly good model agreement with observations was obtained at all wells (Dortch et al. 2007). Groundwater observations (e.g., measurements) of RDX extended over a several years (2001–2004), but they all were assumed to have been collected in one year, 2003, in order to develop the mean and range of observed concentrations. The range of observed soil concentrations of RDX are due to spatial variations in soil concentration rather than any variation over time since all measurements were obtained in the same year, 1998.

As explained previously, there was no model calibration involved in this study. Certainly, the estimated RDX residue loading rate of 1.5 kg/yr could have decreased slightly, which would have forced the model results to agree exactly with the observed concentrations. The loading rate was an estimate based on best available information, and there is certainly error in that estimate. However, as explained previously, the purpose is not to calibrate TREECSTM to match exactly observed data, rather to validate that it can be used to predict media concentrations given best estimates for model inputs.

The performance metrics of the validation results for soil RDX concentration are  $RR = 1.29$  and  $RE = 29\%$ , where  $RR$  and  $RE$  are defined by Equations 1 and 2, respectively. The performance values for aquifer RDX concentration at MW161 are  $RR = 1.11$  and  $RE = 11\%$ . Since  $RR$  is less than 3 in both cases, the first quantitative performance objective is rated as highly successful according to the performance objective criteria in the Demonstration Plan. An  $RE$  of 29% and 11% are actually quite good considering that water quality models which predict nutrient concentrations with  $RE$  values less than roughly 30% are generally judged as acceptably accurate.

**Figure 10. Computed and observed RDX soil concentrations at MMR Demo Area 2.**

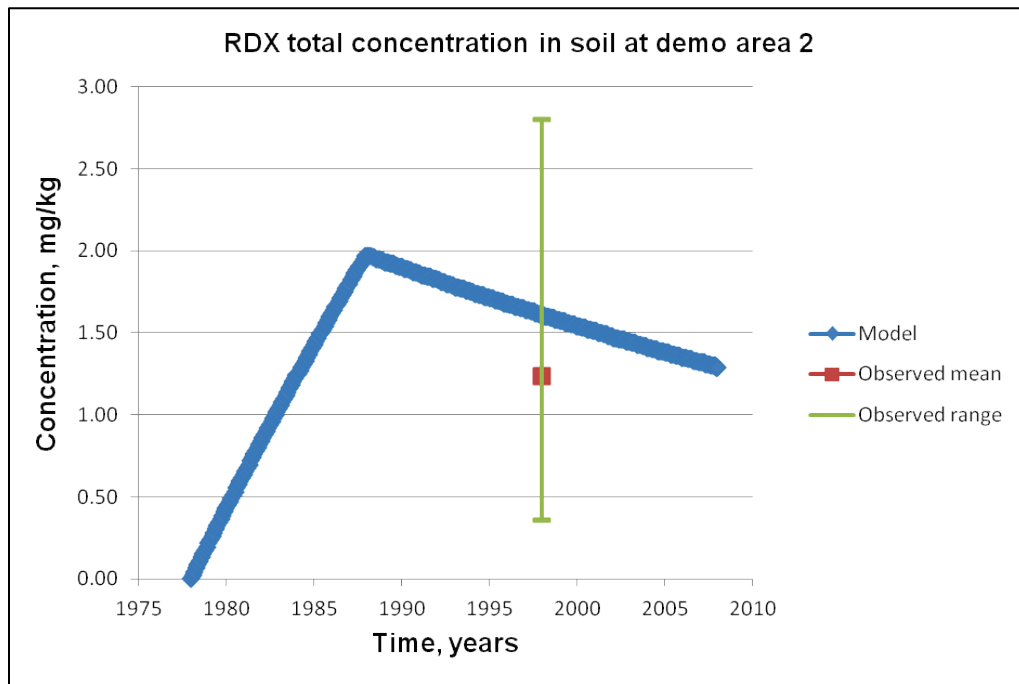


**Figure 11. Computed and observed RDX aquifer concentrations at MW161 down-gradient of MMR Demo Area 2.**

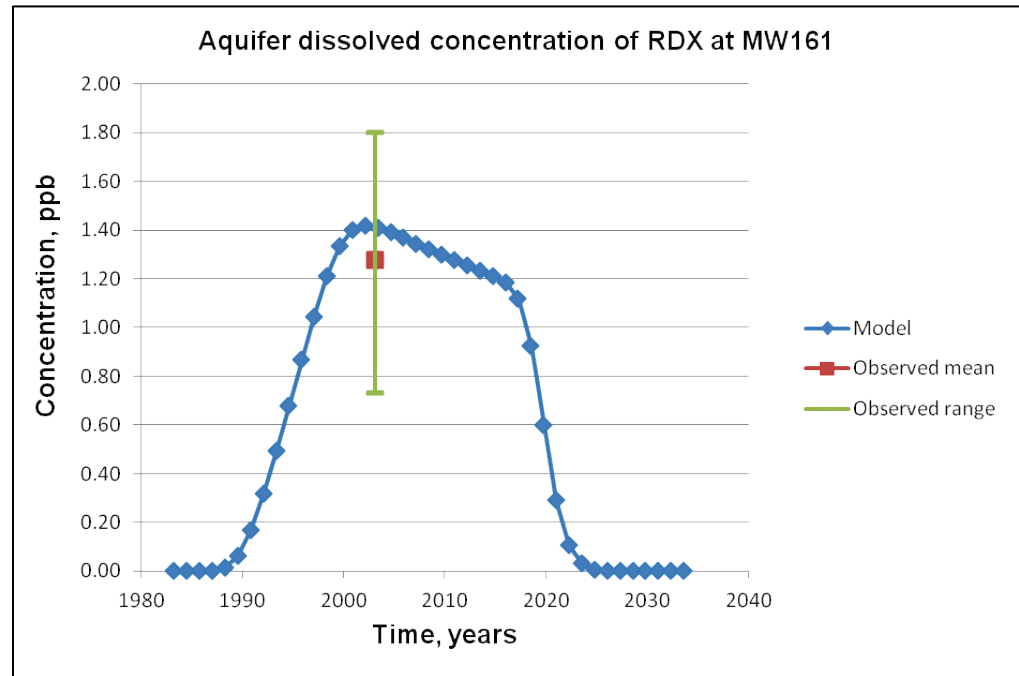


Figure 11 shows the results of running the soil model for 30 years; thus, after 30 years there is no flux of RDX mass from soil to vadose zone. The

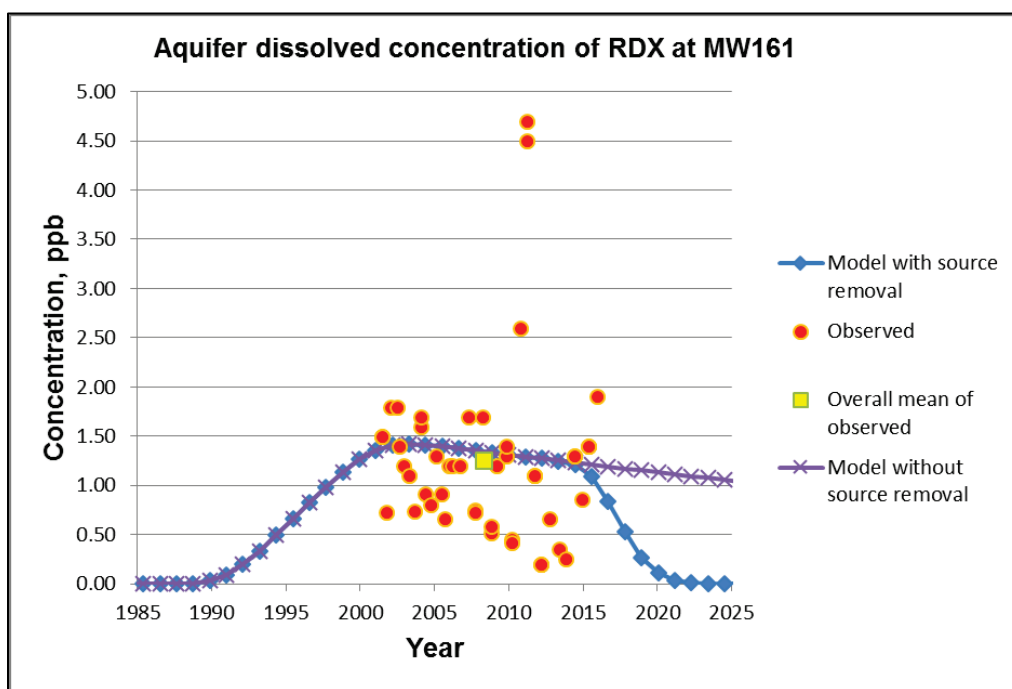
cessation of this flux causes the groundwater concentration of RDX to rapidly decrease toward zero after about 40 years. If the soil model is run longer, the soil concentrations of RDX persist over 100 years while gradually decreasing to zero over that period due to rather slow dissolution of solid phase RDX. Likewise, the RDX concentration in groundwater persists much longer, gradually decreasing towards zero over 120 years or longer. A gradual decrease is expected with a slowly dissolving source mass present.

During the mid-term progress review of this work unit, a member of the review panel recommended that the model be compared with more recent groundwater RDX observations at Demo Area 2. The remediation manager for the Camp Edwards Impact Area Groundwater Study Program of the Army National Guard was contacted to obtain data collected after 2004. As a result, all of the measured RDX concentrations in groundwater for Demo Area 2 were obtained. During the process of obtaining the additional data, it was learned that during 2004 the surface soil at Demo Area 2 was removed and treated to remove source mass of RDX. Thus, TREECS™ was re-applied to the site using the soil model BMP module. The model option *Source Removal BMPs/Selective MC Removal* was selected, and all remaining RDX mass in surface soil was entered for removal during 2004. RDX mass removed during 2004 was specified as 10,400 g in the model input. This mass was computed using the computed surface soil concentration in 2004 of about 1.5 mg/kg times the AOI surface soil volume times the soil dry bulk density.

The results of the re-applied model are shown in Figure 12 along with all of the observed RDX groundwater concentrations measured at MW-161 from 2001 through 2015. Model results are presented for the two cases of with, and without source RDX mass removed in 2004. As shown by the figure, aquifer RDX concentrations persist longer without source removal. The observed RDX concentrations vary widely over time in practically a random manner, although there appears to be a slightly downward trend over time. Some of this variation could be caused by time-varying rainfall and resulting aquifer recharge. Such flow fluctuations can cause fluctuating RDX concentrations due to pulsing mass loading from soil and through the vadose zone, varying amounts of aquifer dilution, and varying plume elevations (and thus concentrations) associated with time-varying flow and water table elevation fluctuations. The MEPAS groundwater models

use steady-state (long-term average annual) water flows, so it is not possible to predict any transient behavior associated with time-varying aquifer recharge. Thus, the model provides concentrations that vary more gradually as associated with long-term, average annual hydrology. The mean of the observed RDX data for time and concentration is plotted in Figure 12, and the model agrees quite well with this mean. It will be interesting to see if the observed concentrations drop over the next few years as the model indicates that they should.

**Figure 12.** Computed (with and without source removal) and observed (2001–2015) RDX aquifer concentrations at MW161 down-gradient of MMR Demo Area 2.



## 6.4 Uncertainty analysis

A sensitivity analysis of various model inputs and their effect on peak RDX concentration at MW161 is discussed by Dortch (2015) for this study site. That study evaluated the effects of uncertainty in the following inputs: RDX residue loading rate; average size of unexploded, solid-phase RDX particles; location of the monitoring well relative to the expected RDX plume centerline in groundwater; and dispersivity factors for groundwater dispersive transport. Model results were sensitive to all the above model inputs, which were substantially uncertain, site-specific, and physically based.

There are other site-specific inputs for the three TREECS™ models used in this application, (e.g., soil texture/composition, meteorology, etc.); however, most of those inputs are much better known or estimated and are not discussed here. None of the uncertain inputs discussed above are chemical-specific. The remainder of this section focuses on the two chemical specific inputs that were determined to be sensitive with some uncertainty; these included the soil-water linear, adsorption, partitioning, distribution coefficient ( $K_d$ , L/kg) and the half-life (which is related to the degradation rate) in the vadose zone. Solubility, another chemical-specific input, affects the particle dissolution rate, but solubility of RDX is well known. The Henry's Law constant (HLC) is a chemical-specific input that affects volatilization loss, but values for it are either known or can be reliably estimated with models, such as those included in the EPI Suite software developed by the U.S. EPA's Office of Pollution Prevention Toxics and Syracuse Research Corporation

(<http://www.epa.gov/oppt/exposure/pubs/episuitedi.htm>). The EPI Suite can also be accessed through CTS. Furthermore, HLC for RDX is so small (6.23E-8 atm-m<sup>3</sup>/mole), there is practically no volatilization.

The half-lives of RDX in soil and groundwater are highly uncertain inputs, but their values are expected to be high in this application. RDX does not readily degrade in aerobic systems (Speitel et al. 2001; Hawari 2000). The soil, vadose zone, and even the groundwater at Demo Area 2 of MMR are aerobic. Half-lives of RDX on the order of years and much longer are reported for aerobic systems (Speitel et al. 2001; Ronen et al. 2008). An RDX half-life of 100 years was used in the validated model for soil, vadose zone, and groundwater. Only dissolved phase RDX in soil pore water and groundwater was allowed to decay in this study. An RDX half-life in AOI surface soil of a year and higher had little to no effect on groundwater concentrations for this study site due to the relatively short retention time of dissolved RDX in the surficial soil layer. Similarly, a half-life of a year or more in groundwater had no effect on groundwater concentrations at this site due to the relatively short travel time of about two months in the groundwater below the source zone to MW161. However, the travel time through the vadose zone from surface soil to the water table is approximately 12 years as determined from the model. Thus, half-lives for the vadose zone of less than 100 years have a profound effect on groundwater concentrations. Half-lives greater than 100 years produced results very similar to those obtained using a 100-year half-life. For example, assuming

no degradation in the vadose zone resulted in a peak groundwater concentration of RDX at MW161 of 1.54 ppb compared with 1.42 ppb for a 100-year half-life, which was the value used for the validated model.

Higher values of  $K_d$  cause greater retardation of constituent transport, which for this study site results in attenuation of the groundwater concentration versus time curve, exhibiting a rounder curve that peaks later at lower concentration. The soil  $K_d$  values for organic chemicals can be estimated within the model user interfaces (UIs) based upon the organic carbon normalized soil–water sorption partition coefficient  $K_{oc}$ , the soil class (e.g., silty loam), which sets the percent sand, silt, and clay, and the percent organic matter content. The surface soil class at the study site is silty loam, whereas the below-ground surface (bgs) soil class required for vadose zone and aquifer modeling is sand. The values used for organic matter content of surface soil and bgs soil were 1.7% and 0.17%, respectively. The recommended value of  $K_{oc}$  is 13.2 L/kg based upon a measured value in one of the TREECS™ constituent databases. These inputs result in an estimated  $K_d$  of 0.203 L/kg for surface soil and 0.024 L/kg for bgs soil; these two values were used for the validated soil and vadose/aquifer models, respectively. Since the model UIs use  $K_{oc}$  to estimate  $K_d$ ,  $K_{oc}$  is actually the uncertain input. Values of  $K_{oc}$  for RDX provided by EPI Suite in CTS were 51.7 and 89.1 L/kg. Estimates for  $K_{oc}$  were considered to vary between approximately 4.6 to 195 L/kg based on values within the TREECS™ three constituent databases and estimates from CTS.

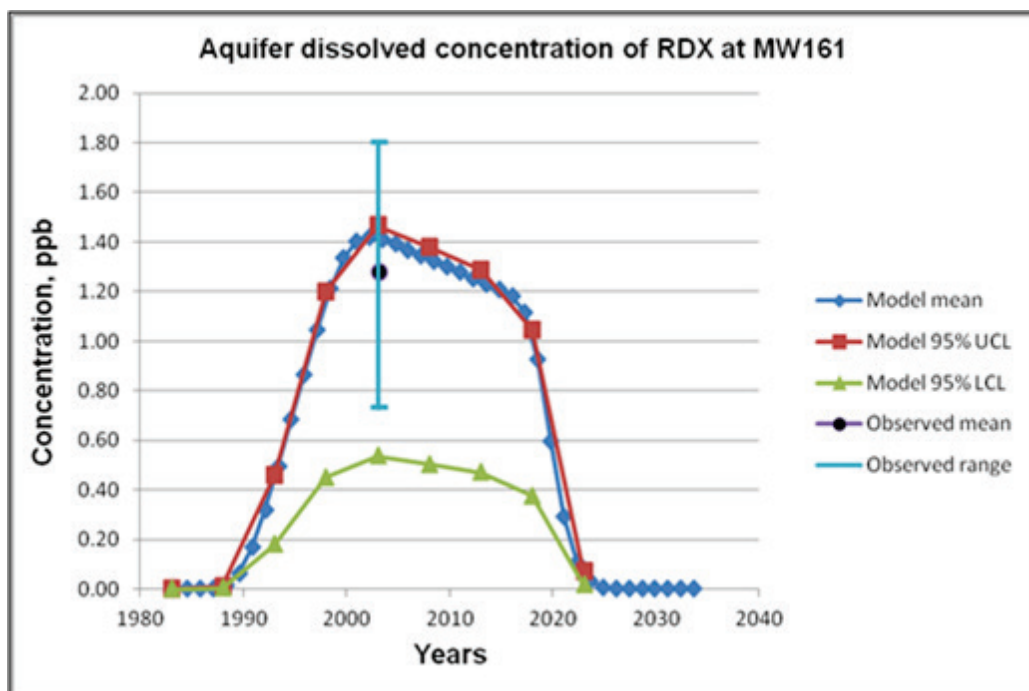
Sensitivity and uncertainty analysis is provided within TREECS™ using Monte Carlo simulation with Latin Hypercube sampling. The user specifies the uncertain input variables and the statistical distributions describing their variability. The sampled output variables are also specified. Uncertainty analysis was conducted separately for RDX half-life in the vadose zone and  $K_d$  for surface and bgs soil. These two analyses are discussed below.

The half-life of RDX in the vadose zone was treated as uncertain with a mean value of 100 years and upper and lower bounds of 300 and 5 years, respectively. A log uniform distribution was assumed since the bounds are so large and there is no clearly known value for half-life; thus, values should receive equal consideration within the entire range of values. The Monte Carlo simulation was set to 100 iterations, although results con-

verged within about 60 iterations. The model results for RDX aquifer concentration versus time at MW161 are compared with the mean and range of observed concentration as shown in Figure 13. This plot is similar to that shown in Figure 11, except that the upper and lower 95 % uncertainty confidence bands are included in the plot. The observed RDX concentrations and upper confidence limit shown in Figure 13 tend to support the use of a rather high half-life.

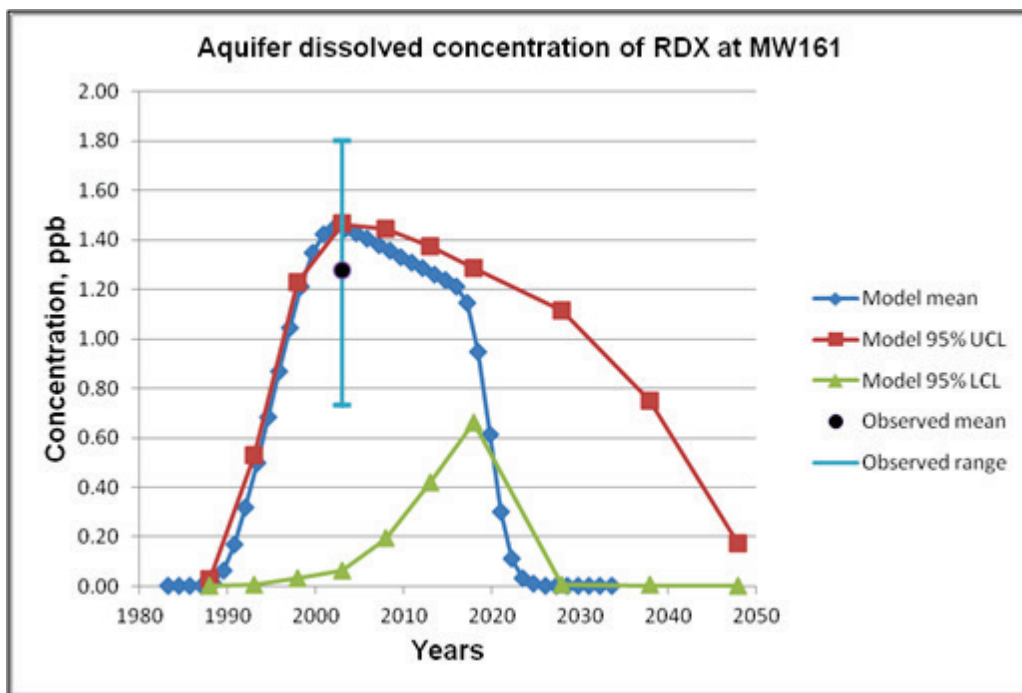
The soil-RDX partition coefficients  $K_d$  for soil, vadose zone, and groundwater were treated as uncertain with a mean value of 0.203 L/kg for soil and 0.024 L/kg for vadose zone and groundwater. A log uniform distribution was used with upper and lower bounds of 0.071 and 3.0 L/kg, respectively, for soil  $K_d$ , and upper and lower bounds of 0.0084 and 0.36 L/kg for  $K_d$  of the vadose zone and aquifer. These  $K_d$  values were estimated via the tools within the model UIs and using upper and lower bound  $K_{oc}$  values of 4.6 and 195 L/kg. The Monte Carlo simulation was run for 100 iterations. The model results for RDX concentration versus time at MW161 are compared with the mean and range of observed concentration as shown in Figure 14 with the inclusion of the upper and lower 95% confidence limits due to uncertainty of  $K_d$  in soil and groundwater.

**Figure 13.** Computed and measured groundwater concentrations of RDX at MW161 down-gradient of Demo Area 2 with upper (UCL) and lower (LCL) confidence limits for uncertainty on RDX half-life.



The lower confidence limit (LCL) in Figure 14 is much farther from the model mean (validation) than the upper confidence limit (UCL) due to the much longer transit time through the vadose zone associated with high  $K_d$  values. The longer transit time allows for greater degradation of RDX. The confidence limits in computed soil concentrations of RDX, which are not presented, were very close to the model validation result shown in Figure 10, indicating variations in the soil  $K_d$  had a minor effect on model results for this application. An additional uncertainty run was made where only the  $K_d$  value for vadose zone was treated as uncertain. The confidence limits for this run were very similar to those shown in Figure 14, thus reinforcing the conclusion that model results are sensitive to vadose zone  $K_d$  values but insensitive to surface soil and groundwater values for this application. Likewise, model results are sensitive to vadose zone half-life of RDX but relatively insensitive to surface soil and groundwater values due to the relatively short transit times in those media. The uncertainty bands bracket the mean of the observed data, thus satisfying the second performance objective.

**Figure 14. Computed and measured groundwater concentrations of RDX at MW161 down-gradient of Demo Area 2 with upper (UCL) and lower (LCL) confidence limits for uncertainty on RDX  $K_d$  in soil and groundwater.**



## 6.5 Fate of emerging MC (EC) associated with IM

The five MCs, DNAN, NTO, NQ, AP, and CL-20 were selected within the TREECS™ validation application of Demo Area 2 for evaluating their fate relative to that of RDX. Each of these five MCs are referred to as an EC for brevity. The inclusion of these five additional ECs in the application required specifying their physicochemical properties, which are not as well-known as are those of RDX. The EPI Suite component of CTS was used to provide some of the properties information for the five ECs, such as HLC and  $K_{oc}$  values. Besides specifying the physicochemical properties and the partitioning distribution coefficients in soil for the EC, the only other additional input that was required was the residue loading rate for each EC, which was set to the same rate as that of RDX, or 1,500 g/yr, and degradation half-life in each media. All other model inputs were the same as the validation application as shown in Tables 3–5.

### 6.5.1 Initial inputs and results

Inputs were initially set using the best available information within TREECS™-CTS without exerting any additional study or literature review, thus relying on default methods within the systems. The additional soil model inputs that were specified for the EC are shown in Table 6. Ammonium perchlorate was declared as miscible due to its very high solubility. The degradation half-life and initial solid-phase particle size was assumed to be the same as that of RDX for comparison purposes. Less is known about the degradation rates of these ECs than is known for RDX, and CTS does not provide estimates for biotic degradation rates. Thus, retaining the same half-lives as for RDX was the only rational alternative.

**Table 6. Additional soil model inputs for the five ECs for Demo Area 2 application.**

Input Description	DNAN	NTO	NQ	AP	CL-20
Site Characteristics					
MC mass residue loading versus time, g/yr, assumed to be constant for 10 years	1,500	1,500	1,500	1,500	1,500
Initial solid phase MC concentration in soil on a soil mass basis at time 0, mg/kg	0	0	0	0	0

Input Description	DNAN	NTO	NQ	AP	CL-20
Initial total non-solid phase MC concentration in soil on a soil mass basis at time 0, mg/kg	0	0	0	0	0
<b>Fate/Transport Parameters</b>					
Soil-water constituent partition coefficient, $K_d$ , L/kg, computed by soil model UI from $K_{oc}$ , soil texture, and percent organic matter for all except CL-20	2.43	1.93	0.18	0.0002	2.0 <sup>1</sup>
Decay/degradation half-life of aqueous phase constituent, years	100	100	100	100	100
Decay/degradation half-life of adsorbed (particulate) phase constituent, years	1.0E20	1.0E20	1.0E20	1.0E20	1.0E20
Initial mean diameter of solid phase constituent residue particles (assume spherical particles), $\mu\text{m}$	6,000	6,000	6,000	NA miscible	6,000
Volatilization rate, m/yr, as computed by soil model UI from molecular diffusivity in air	42.5	65.3	65.8	0 miscible	28.6
<b>Chemical-Specific Properties</b>					
$K_{oc}$ , L/kg	158.5 <sup>a</sup>	125.9 <sup>a</sup>	12 <sup>b</sup>	0.016 <sup>c</sup>	2.7 <sup>d</sup>
Molecular weight (molar mass or averaged molecular mass), g/mol (all from NIST <sup>e</sup> )	198	130	104	117.5	438
Aqueous solubility limit, mg/L	276 <sup>f</sup>	16,600 <sup>g</sup>	3,800 <sup>h</sup>	249,000 <sup>i</sup>	4.33 <sup>j</sup>
Henry's Law constant, atm- $\text{m}^3/\text{g}\cdot\text{mol}$	3.01E-7 <sup>k</sup>	4.07E-13 <sup>l</sup>	4.49E-12 <sup>l</sup>	0	9.39E-25 <sup>m</sup>

Input Description	DNAN	NTO	NQ	AP	CL-20
Solid phase constituent mass density, g/cm <sup>3</sup> (all values except CL-20 were cited by Taylor et al. 2015, which agree with values found via Internet searches)	1.34	1.93	1.72	1.95	2.04 <sup>n</sup>
Molecular diffusivity in air, m <sup>2</sup> /day (all estimated from method by Fuller et al. 1966)	0.56	0.86	0.87	NA Non-volatile	0.37

<sup>1</sup> Mean of range of values reported by Szecsody et al. (2004) for soil

<sup>a</sup> Estimated, Chakka et al. 2010

<sup>b</sup> Average of values estimated with EPI Suite using the MCI and  $K_{ow}$  methods; agrees with estimated value from Hazardous Substances Data Bank (HSDB), <http://tox-net.nlm.nih.gov>

<sup>c</sup> Estimated from  $K_{oc} = 23.83 K_{ow}^{0.544}$  with  $K_{ow} = 1.45E-6$  obtained from EPA (2008)

<sup>d</sup> Chemspider (<http://www.chemspider.com/>) predicted from ACD/Labs Percepta Platform - PhysChem module

<sup>e</sup> National Institute of Standards and Technology (NIST), <http://www.nist.gov/>

<sup>f</sup> Measured, Boddu et al. 2008

<sup>g</sup> Interpolated from measured, Spear et al. 1989

<sup>h</sup> Haag et al. 1990

<sup>i</sup> Agency for Toxic Substances and Disease Registry (ATSDR), <http://www.atsdr.cdc.gov/>

<sup>j</sup> Karakaya et al. (2003)

<sup>k</sup> Estimated with EPI Suite group method

<sup>l</sup> Estimated with EPI Suite bond method

<sup>m</sup> Chemspider (<http://www.chemspider.com/>) predicted from EPI Suite, bond method

<sup>n</sup> Hoffman (2003)

The additional MEPAS vadose and aquifer model inputs for the five ECs are shown in Table 7. The same degradation half-life in groundwater used for RDX was used for the five ECs.

A wide range of values for  $K_{oc}$  was found for CL-20, thus, introducing high uncertainty in estimated  $K_d$  values. Therefore, the  $K_d$  value for CL-20 in surface soil was set to the mean of the range of values reported by Szecsody et al. (2004) for aerobic soil. The  $K_d$  for CL-20 in vadose zone and groundwater was set to a factor of 10 lower than for surface soil due to the organic matter being a factor of 10 lower.

**Table 7. Additional MEPAS vadose and aquifer model inputs for five ECs at Demo Area 2.**

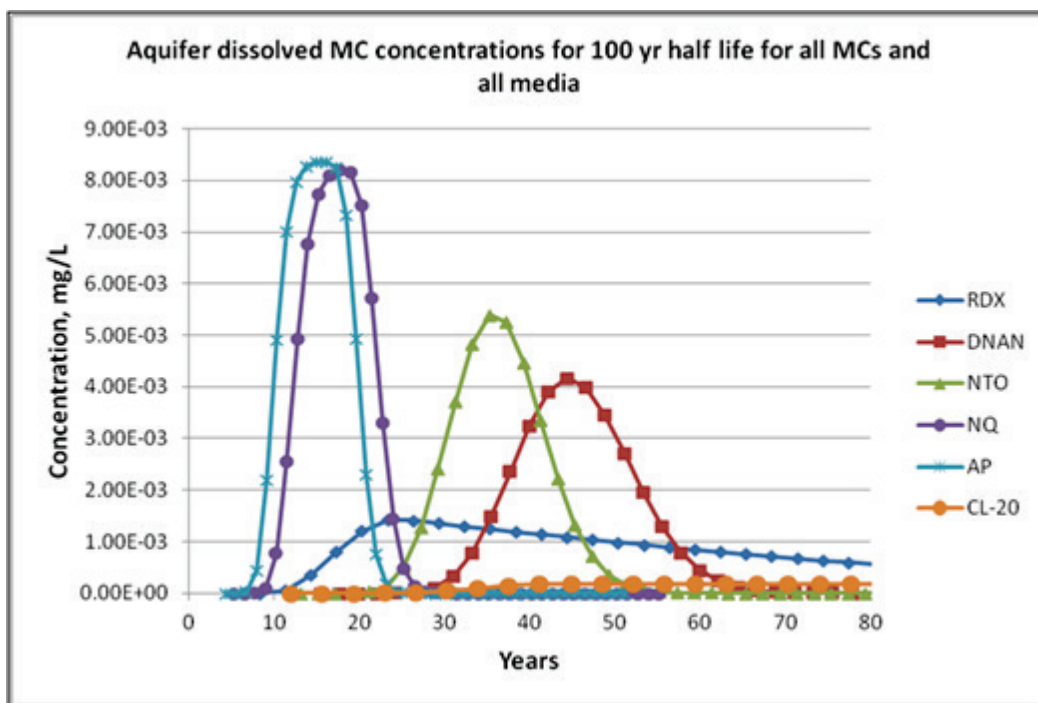
Input Description	DNAN	NTO	NQ	AP	CL-20
Soil-water constituent partition coefficient, $K_d$ , L/kg, computed by model UI from $K_{oc}$ , soil texture, and percent organic matter for all except CL-20	0.29	0.23	0.022	2.9E-5	0.2 <sup>1</sup>
Decay/degradation half-life of dissolved phase in vadose and aquifer	100	100	100	100	100
Aqueous solubility limit, mg/L	276	16,600	3,800	249,000	4.33

<sup>1</sup> A factor of 10 lower than soil  $K_d$  due to organic matter being lower by a factor of 10

The soil model was run for 100 years rather than 30 years so that the results for groundwater could be protracted. The computed groundwater concentrations at MW161 for the five EC are plotted versus time in Figure 15 along with the results for RDX. The low solubility of RDX relative to four of the other MC causes RDX concentrations to persist longer but at lower concentrations. There is still considerable mass of RDX in soil after 60 years, whereas, four of the five ECs have been dissolved and nearly totally flushed out of the soil. Four of the five ECs are transported out of the system faster than RDX, but this occurs with a price of greater peak groundwater concentrations. DNAN and NTO are attenuated more than NQ and AP due to their higher  $K_d$  values.

The EC CL-20 persists in soil well after 100 years since it has the lowest solubility of all six MCs. The peak groundwater concentration of CL-20 is more than an order of magnitude lower than the other MCs due to its very slow migration associated with its low solubility. The low solubility of CL-20 could make it a good candidate as a future HE due to its lower concentration in receiving waters.

**Figure 15.** Computed aquifer concentrations at MW161 down-gradient of Demo Area 2 for five ECs and RDX with half-life of 100 years for all MCs in all media.



### 6.5.2 Refined inputs and simulation results for DNAN and NTO

Additional attention is given to the fate of DNAN and NTO due to the interest in using these two explosive components as potential replacements for TNT and RDX, respectively. There is also uncertainty regarding their properties associated with fate processes. As a result, the physicochemical properties of these MCs are evaluated in greater detail, and the effects on their fate due to refinement in those properties are presented below.

There is relatively high confidence in the values for molecular weight, water solubility, and solid phase density of DNAN and NTO. Although there is some uncertainty in the HLC, values are so low that volatilization is a very minor fate process. Likewise, diffusivity in air, which is an input used to compute volatilization, has low importance. Elimination of these input variables leaves only the soil partitioning coefficient  $K_d$  and the degradation rates as important and uncertain MC-specific inputs.

Unlike most HE, NTO can have a lower adsorption to soils due to its negative charge at environmentally relevant pH values, and it may not correlate well to soil organic carbon (OC) content (Dontsova et al. 2014). The  $K_d$  for DNAN and NTO shown in Table 6 and Table 7 were computed based on

the input values for  $K_{oc}$ , the soil texture (e.g., silty loam), and the soil organic matter content. The input values of  $K_{oc}$  for DNAN and NTO in Table 6 were computational derived from  $K_{ow}$  by Chakka et al. (2010), which can be unreliable, particularly for polar compounds.

Dontsova et al. (2014) have measured batch  $K_d$  values for DNAN and NTO using 11 different soils with widely varying properties. These soils vary from loams with mostly sand, to clay loam with 32% clay. The soil pH ranges from 4.23 to 8.21, and OC content ranges from 0.34% to 5.28%. The surface soil at Demo Area 2 is silty loam with a pH of 4.6 and organic matter content of 1.7% (AMEC Earth Environmental 2004). Organic matter is generally about 40% OC. The deeper soils of the vadose zone and aquifer of Demo Area 2 are mostly sand with one order of magnitude lower organic matter content (i.e., 0.17%) and pH of about 5.9. Silty loam generally has a texture of 20-65-15 percent sand-silt-clay. Sand texture is generally 92-5-3 percent sand-silt-clay.

The characteristics of the 11 soils used in the Dontsova et al. (2014) study were reviewed in an attempt to match as closely as possible the particular soil to the soil texture and pH at Demo Area 2. Matching the soil OC content was considered less important since the measured  $K_d$  values were normalized to OC to provide  $K_{oc}$ . The soils that are the most similar to the surface soils at Demo Area 2 are Catlin (Urbana, IL.), Arnold AFB (Arnold Air Force Base, TN.), Sassafras (Aberdeen Proving Ground, MD.), and Plymouth (MMR, MA). Of course, the Plymouth site is at the same installation as Demo Area 2, but its texture is closer to that of the deeper soils at Demo Area 2.

The characteristics of these four soils and the corresponding measured batch  $K_d$  and OC normalized  $K_{oc}$  values for DNAN and NTO are shown in Table 8 along with the  $R^2$  of the fit for  $K_d$ . The model values of  $K_d$  and  $K_{oc}$  for DNAN in surface soil of 2.43 and 158.5 L/kg, respectively, in Table 6 agree reasonably well with the measured values in Table 8, which range from 1.89 to 5.95 L/kg for  $K_d$  and 113 to 179 L/kg for  $K_{oc}$ . However, due to the low organic matter content, the estimated DNAN  $K_d$  value of 0.29 L/kg for sub-surface soil in Table 7 is an order of magnitude lower than the range of measured values in Table 8. It is noted that the OC content of the four soils in Table 8 ranged between 1.3% for Sassafras to 5.28% for Catlin, which is much higher than the OC content of the sub-surface soils at Demo Area 2. The  $K_{oc}$  of the four soils averages 140.7 L/kg for DNAN. If this

value is multiplied by the fraction of OC content of the Demo Area 2 sub-surface soil (which is about 0.00068), then the estimated  $K_d$  is 0.096 L/kg, which is about the same order of magnitude as the value estimated from the MEPAS model UI of 0.29 L/kg. Thus, the low model  $K_d$  value for sub-surface soil seems reasonable given the very low OC content of those soils. Overall, the values of  $K_d$  used in the original modeling of DNAN seem quite reasonable. Thus, the original  $K_d$  values for DNAN of 2.43 and 0.29 L/kg for surface and sub-surface soil, respectively, were used for the improved simulation.

**Table 8. Soil characteristics, measured batch  $K_d$ , and corresponding  $K_{oc}$  values for DNAN and NTO for four soils similar to Demo Area 2 soils (Dontsova et al. 2014).**

Soils	Sand-silt-clay, %	Soil pH	DNAN $K_d$ , L/kg	$R^2$ , DNAN $K_d$	DNAN $K_{oc}$ , L/kg	NTO $K_d$ , L/kg	$R^2$ , NTO $K_d$	NTO $K_{oc}$ , L/kg
Catlin	9-65-26	7.31	5.95	0.92	113	0.21	0.92	3.98
Arnold AFB	23-66-11	6.66	3.39	0.78	126	0.34	0.94	12.69
Sassafras	41-42-17	4.40	1.89	0.72	145	0.48	0.96	36.92
Plymouth	75-20-5	4.23	4.38	0.94	179	0.50	0.96	20.41

The values of  $K_d$  and  $K_{oc}$  for NTO of 1.93 and 125.9 L/kg, respectively, in Table 6 are about an order of magnitude higher than the measured values in Table 8, which range from 0.21 to 0.5 L/kg for  $K_d$  and 3.98 to 36.92 L/kg for  $K_{oc}$ . Also, the relative range in  $K_{oc}$  for NTO is much greater than it is for DNAN indicating less correlation of partitioning to OC content for NTO. Partitioning of NTO to soil appears to be more closely associated with soil pH with an inverse relationship (Dontsova et al. 2014). An NTO  $K_d$  value of about 0.5 L/kg seems far more appropriate for Demo Area 2 surface soil than the value of 1.93 L/kg that was used originally. With a higher pH in sub-surface soil of 5.9, the  $K_d$  in that region of Demo Area 2 is likely in the range between 0.34 to 0.48 L/kg. Thus, the value of 0.23 L/kg that was originally used in the modeling is not so unreasonable. In retrospect,  $K_d$  values for NTO of 0.5 and 0.4 L/kg for surface and sub-surface soils, respectively, are more appropriate for Demo Area 2; thus, these values were used for the improved simulation.

Although there are recent studies of degradation of DNAN and NTO in enriched cultures, there is little information regarding degradation rates of these two MC in natural environmental settings. Information regarding

the potential for degradation can be gleaned from CTS, but actual degradation rates cannot be predicted by CTS. Degradation half-lives for DNAN and NTO on the order of a few days to a week were reported by Dontsova et al. (2014) for their batch laboratory studies, and they reported even shorter half-lives for NTO in their soil column flow studies.

Perreault et al. (2012) studied the aerobic biotransformation of DNAN using artificially contaminated soil microcosms. DNAN was completely transformed in 8 days in soil slurries supplemented with carbon and nitrogen sources. DNAN was completely transformed in 34 days in slurries supplemented with carbon sources alone. However, DNAN persisted with little degradation in the un-amended microcosms. A strain of *Bacillus* (named 13G) in the soil was determined to transform DNAN by co-metabolism (Perreault et al. 2012). Similarly, Fida et al. (2014) were able to aerobically biodegrade DNAN by *Nocardioides* sp. (strain JS1661), which was isolated from activated sludge.

Although Perreault et al. (2012) stated that DNAN persisted in the un-amended microcosms, there was some small amount of DNAN loss that can be observed in their concentration versus time plot. The slow rate of degradation of DNAN presented by Perreault et al. (2012) for the un-amended microcosm was estimated to have a half-life of about 0.6 years, which is probably more representative of degradation in natural aerobic environments, such as Demo Area 2. Thus, for the improved simulation, it was assumed that DNAN has a half-life of 0.6 years in surface and sub-subsurface soil.

Krzmarzick et al. (2015) were able to readily reduce NTO anaerobically in microcosms using inoculated microbial communities from seven different soils. However, NTO was non-biodegradable in aerobic microcosms with all seven soil inoculated communities. These results are similar to those for RDX; where RDX is degraded under anaerobic conditions but degrades very slowly for aerobic conditions. As with DNAN, microbial enrichment techniques have been used to biodegrade NTO rather rapidly for aerobic conditions. For example, Richard and Weidhaas (2014) showed simultaneous aerobic degradation within 4 days for IM components DNAN, NTO, and NQ in the explosive formulation IMX 101 using soil enrichment cultures involving sludge, soil, and compost. However, for natural aerobic environments like Demo Area 2, it is probably best for now to assume that NTO degrades similar to RDX. Thus, for the improved simulation, it was

assumed that NTO has a half-life of 100 years for surface and sub-surface soil, which is the same as for the initial simulation of the IM components.

In summary, the improved simulation for the EC DNAN and NTO maintained the same inputs as the original simulation with the exception that the  $K_d$  values for NTO were changed from 1.93 and 0.23 L/kg to 0.5 and 0.4 L/kg for surface and sub-surface soil respectively, and the degradation half-life of aqueous phase DNAN was changed from 100 years to 0.6 years for all media (soil, vadose, and aquifer).

The aquifer concentration results at MW161 for the improved simulation of DNAN and NTO are not plotted, but are described as follows. The concentration of DNAN was essentially zero in the aquifer due to the relatively fast degradation rate associated with the lengthy transit time through the vadose zone. The concentration versus time curve for NTO was practically the same as that shown in Figure 15. Even though the  $K_d$  for NTO in surface soil was considerably lower than originally, the high solubility coupled with the relatively short retention time in soil translated into only a very minor effect on flux from soil to vadose zone and resulting aquifer concentrations. Thus, the simulation of improved inputs for DNAN and NTO exhibited no change for NTO and major change for DNAN with essentially zero DNAN present in groundwater. Given that DNAN is similar to TNT and NTO is similar to RDX, it is not surprising that DNAN, like TNT, could potentially be absent in groundwater when NTO, like RDX, could often be present. This application demonstrates the need for better methods and more research for estimating degradation rates in natural environmental media.

## 6.6 BMP assessment

The term best management practice (BMP) is used loosely here to include any management alternative, including remediation strategies, that reduces future concentrations of MC in down-gradient receiving waters.

Three BMPs, or remediation strategies, were evaluated for reducing aquifer concentrations of RDX: surface soil amendment to increase adsorption of RDX to soil; surface soil amendment to increase degradation rate (decrease half-life) of pore water RDX; and groundwater injection to increase degradation rate of RDX in the aquifer plume. Two half-lives were tested for the surface soil amendment to increase degradation rate.

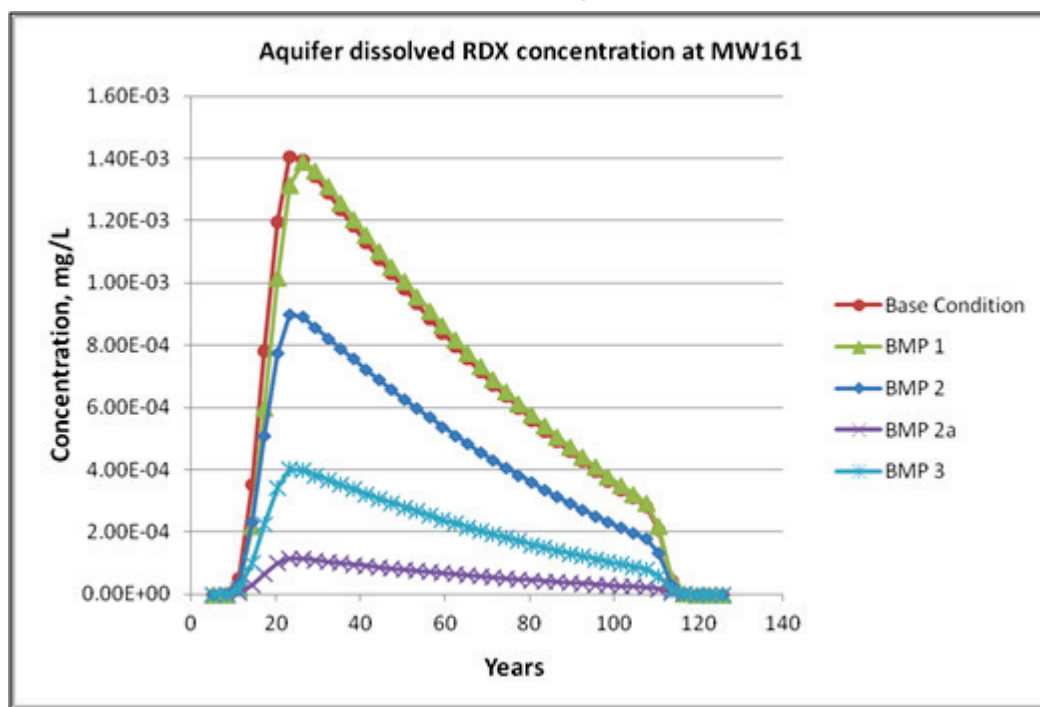
RDX adsorption correlates more closely with clay content than with organic matter content of soils (Boyer et al. 2007). Thus, clay could be added to surface soils at Demo Area 2 to increase the soil-pore water sorption partition coefficient,  $K_d$ . It was assumed for comparison purposes that  $K_d$  of the surface soil could be increased by a factor of 10 from a value of 0.203 L/kg as used in model validation to a value of 2.03 L/kg. All other inputs for the soil model as well as those of the vadose and aquifer models were kept the same as the validation inputs of Tables 3–5. As shown in Figure 16, the results of this first BMP (BMP 1) were practically identical to those of the validation application, (i.e., there was no reduction in aquifer concentrations of RDX), only a slight delay in aquifer concentrations compared with the base condition (i.e., the validation result). This BMP causes the surface soil to hold RDX a little longer, but this effect alters the groundwater concentrations very little.

For BMP 2, it was assumed that an amendment, such as rich organic matter with microbes, is added to the surface soil to increase biological degradation of RDX, thus, decreasing the half-life to about one month, or to 0.1 year. Therefore, the aqueous dissolved RDX half-life in soil was changed from 100 years to 0.1 year, and all other inputs remained the same as the base (validation condition). The results of BMP 2 are shown in Figure 16 for aquifer concentration at MW161 compared to the base results. As the figure shows, the peak RDX concentration is reduced from about 1.4E-3 mg/L (1.4 ppb) to about 0.9 ppb. Greater reductions in RDX concentration do not occur due to the relatively short residence time of RDX in surface soil pore water. The rapid drop in RDX concentration after 110 years is due to running the soil model for only 100 years.

A variation of BMP 2 was run where the surface soil aqueous dissolved RDX half-life was reduced further. Enhanced RDX degradation and transformation can be achieved with hydrated lime (calcium hydroxide, as well as quicklime calcium oxide) added to the soil that induces alkaline hydrolysis (Larson et al. 2008; Johnson et al. 2011) to abiotically transform RDX and other HE. Alkaline hydrolysis via soil liming produced a degradation half-life of 2592 minutes (0.005 year) for RDX on a grenade range at Ft. Lewis, WA. (Johnson et al. 2011). The dissolved phase RDX half-life in soil was set to 0.005 year for BMP 2a. The results of this test are shown in Figure 16 along with the base results for comparison. The peak RDX aquifer concentration is reduced by more than a factor of 10 to 0.11 ppb for BMP 2a.

The third BMP involved reducing the RDX half-life in groundwater from 100 years to 0.1 year. Such a reduction is feasible through injection of organic substrate and microbes into the groundwater RDX plume to reduce RDX via enhanced biodegradation. All other model inputs were the same as the validation or base condition. The results of BMP 3 are shown in Figure 16. BMP 3 has the effect of reducing RDX concentrations at MW161 from about 1.4 ppb to 0.4 ppb.

**Figure 16.** Computed aquifer concentrations of RDX at MW161 down-gradient of Demo Area 2 for four BMPs compared to base condition.



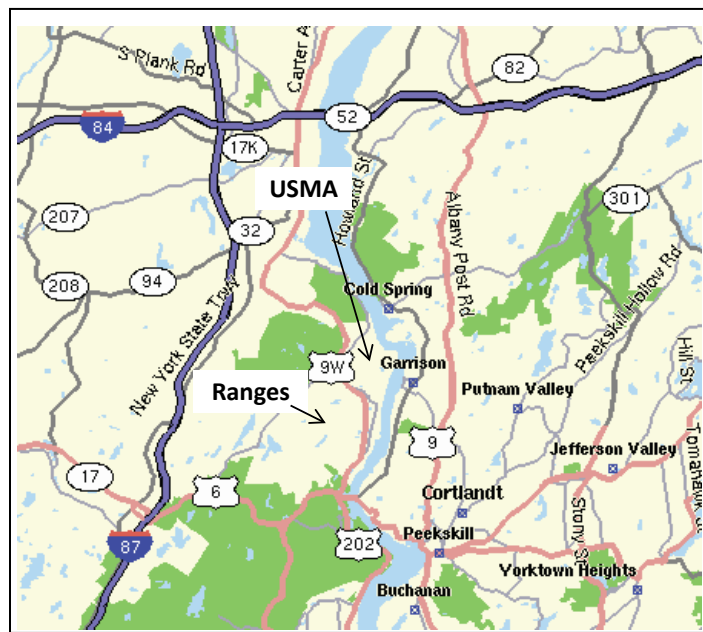
Since it is difficult to immobilize the movement of RDX in water, the more promising BMP or remediation strategies involve degradation, or reduction, of RDX. The BMP tests conducted here show that RDX reduction strategies could be beneficial when applied only to the surface soil or only within the aquifer. It is noted that the degradation BMPs in soil require implementation before RDX has migrated to the vadose zone and groundwater, which was the assumption in these BMP applications. An RDX reduction strategy was not applied to the vadose zone due to the perceived high costs of implementing such a strategy, thus, making the practicality of such an alternative questionable. These BMP applications demonstrate that TREECS™ can be applied to assess the potential effectiveness of various BMP strategies.

## 7 Artillery Impact Area (AIA), USMA

### 7.1 Site description

The site description information presented here was obtained from U.S. Army Aberdeen Test Center (ATC) (2004a). The U.S. Military Academy (USMA) is located at West Point in southeastern New York on the west side of the Hudson River (see map in Figure 17), approximately 45 miles north of New York City. The academic, administrative, and housing areas are located on the main post. The training area and firing ranges consists of approximately 14,000 acres and serves primarily as the summer training facility for the cadets. The area surrounding the USMA is dominated by residential, agricultural, and recreational land uses.

Figure 17. Site map of USMA (modified from ATC 2004a).



The climate of the area is temperate with cold winters and moderately warm summers. The average annual precipitation is about 1.14 m/yr (45.2 in/yr). Average seasonal snowfall is 0.95 m, which has a water equivalency of about 0.14 m. Surface water on the training ranges generally flows to the south and drains into Popolopen Brook which discharges into the Hudson River. Shallow soil, glacial geology, and abundant rainfall produce a regionally high water table, resulting in numerous swamps, lakes, and ponds.

The USMA is located in the Hudson Highlands where underlying rocks consist of granite, gneiss, and diorite. Overlying the bedrock are glacially deposited till and alluvium. The un-stratified till was deposited from glacial ice and consists of large boulders and lesser amounts of clay, sand, and gravel. The stratified alluvium consists primarily of sand and gravel that were deposited in glacial streams and lakes. Overlying the deposits are recent-age stream deposits that consist of clay, silt, and sand. The deposits range from approximately 0.3 to 30 m in thickness.

The dominant soil type at the installation is Hollis-Rock Outcrop, which is characterized by well drained, sloping to moderately steep, medium-texture soils that overlie crystalline bedrock. The Hollis soils are gravel-sand loams, which have a fairly high permeability.

The groundwater at USMA exists as unconfined within the alluvial deposits and within a confined bedrock aquifer. Depth to groundwater varies significantly with depths ranging from less than 1 m to 30 m. The aquifer systems have low well yields and limited extent so they are incapable of municipal supply.

The range and training complex (RTC) of the USMA is largely undeveloped and primarily wooded. The RTC is used each year from June through August by approximately 2500 cadets for training. The RTC is located in the Hudson-Wappinger watershed and is drained by many small tributaries which discharge into the Hudson River. Popolopen Brook is a prominent stream in this watershed that receives much of its drainage from the RTC as shown in Figure 18. The ranges that fire into the AIA of the RTC are Ranges 2, 12, and 13. Range 2 is used for 105 mm artillery, and Ranges 12 and 13 are used for 81 and 60 mm mortars.

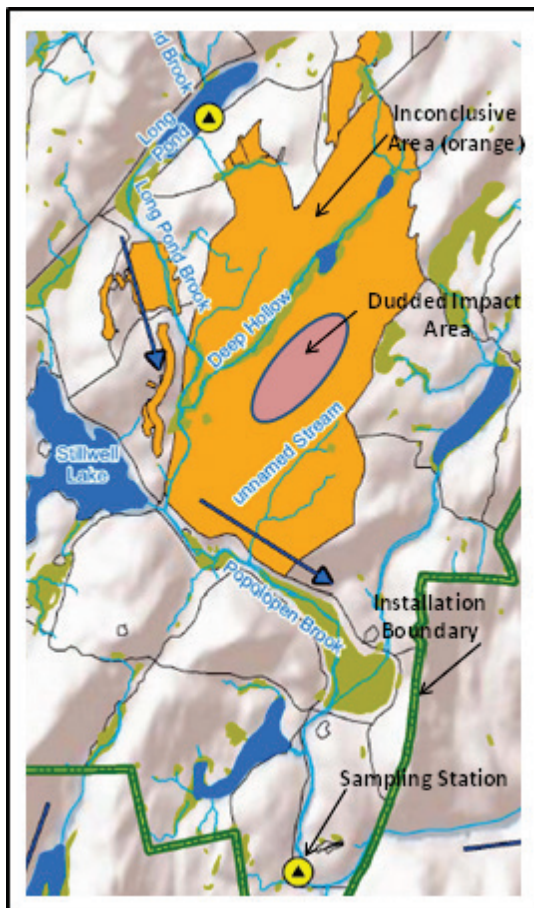
The AIA borders Deep Hollow, also referred to as Zint's Brook. Zint's Brook is joined by Long Pond Brook before joining Popolopen Brook as shown in Figure 18. The AIA resides on a hillside slope that drains into Zint's Brook.

## 7.2 Model inputs for validation

The HE RDX is the primary MC of interest in this application and the application focused on soil and surface water media. Groundwater was not considered since the upper aquifer is close to the ground surface, unconfined, and has a shallow depth. Additionally, a relatively high runoff rate is suspected since the AOI ground surface is rather steep with a slope of

about 19% draining to the northwest into Zint's Brook. There is also considerable bedrock close to the ground surface with a very low permeability. Infiltrated water is assumed to move as soil interflow that quickly resurfaces to surface water. The two models applied within Tier 2 of TREECS™ were the Tier 2 soil model and the Contaminant Model for Streams (CMS), which represented Popolopen Brook. The inputs for each of these two models are described below. All mass flux of RDX from the AOI is assumed to be immediately available and unaltered at the upstream end of the modeled Popolopen Brook reach.

**Figure 18.** Map showing inconclusive range area, artillery duded impact area, and streams of the RTC (modified from EA 2011).

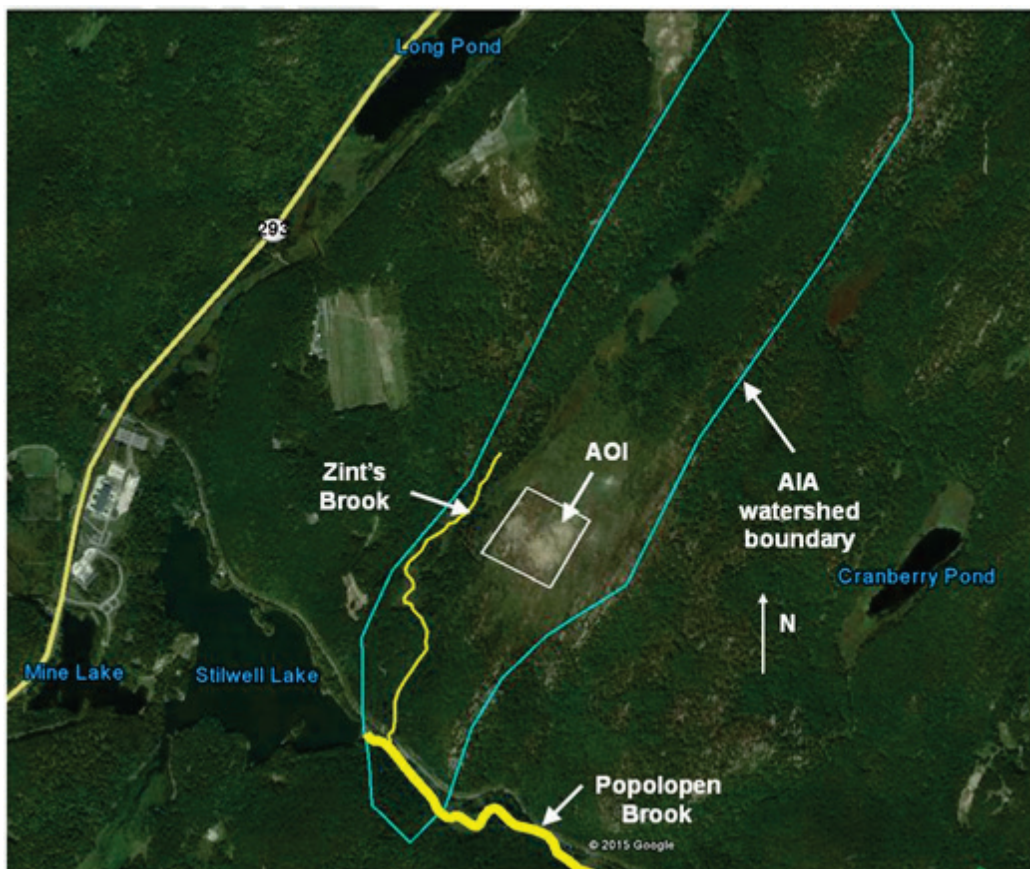


### 7.2.1 Soil model inputs

The AOI was delineated through examination of Google Earth™ images revealing impact craters and barren landscape. The delineations of the AIA watershed and the AOI as polygons are shown in a Google™ Earth satellite view in Figure 19. The duded impact area of the AIA is clearly visible within the AOI polygon in the figure. The approximate dimensions of the

AOI polygon are 300 m by 310 m with an area of 102,000 m<sup>2</sup> (25 acres). AOI length and width are defined as the dimensions that are parallel and perpendicular to the runoff flow path, respectively. The slope of the AIA terrain is such that most of the runoff flows into Zint's Brook.

Figure 19. Delineation of AIA watershed and AOI in Google™ Earth.



Web Soil Survey (WSS\*), which was developed for World Wide Web applications by the Natural Resources Conservation Service of the U.S. Department of Agriculture, was used to obtain AOI soil characteristics. The AOI soils are mostly Hollis-Rock Outcrop. The AOI has an average slope of about 19%. The depth of bedrock below the surface soil is about 0.4 to 2.0 m. The Hollis soil is a gravelly, sandy loam of about 10% clay, 30% silt, and 60% sand for the soil (non-rock) portion having a soil erodibility K factor of about 0.2. The soil pH is about 5.5, and the soil has relatively high organic matter content. The saturated hydraulic conductivity of the surface soils is about 190 cm/day, but the conductivity decreases dramatically to

\* <http://websoilsurvey.nrcs.usda.gov/app/WebSoilSurvey.aspx>

about 0.1 cm/day over the next 0.4 to 2.0 m of soil depth due to the confining bedrock layer below the surface. The estimated dry bulk density and porosity of the surface soil for the texture noted above, is 1.48 g/cm<sup>3</sup> and 44%, respectively. The Hollis soils are classified as well drained and within hydrologic soil group D for the Soil Conservation Service (SCS) curve number runoff method.

Daily precipitation and minimum and maximum daily air temperatures were obtained from a meteorological station near West Point (Station C309292) for the period 1950 through 2008. Meteorological data can be freely downloaded on the World Wide Web from the National Oceanic and Atmospheric Administration's National Centers for Environmental Information (NCEI), formerly the National Climatic Data Center (NCDC). The daily average air temperature was assumed to be the average of the minimum and maximum daily air temperatures. The mean and maximum daily air temperatures, daily precipitation, site latitude of 41.367 degrees north, and a SCS curve number of 87 were used within the TREECS™ HGCT to compute local average annual hydrology. The computed hydrology used by the TREECS™ Tier 2 soil model included: average annual precipitation = 1.13m; average annual rainfall = 1.05 m; average annual infiltration = 0.23 m; average annual surface runoff = 0.51 m; average annual soil volumetric moisture content = 0.12; average annual number of rainfall events = 141; and average annual soil-water matrix temperature = 10.78° C. All infiltrating flow was assumed to transition into soil interflow, thus resurfacing as surface water runoff.

The soil erosion rate was computed within HGCT using the Universal Soil Loss Equation (USLE). Inputs used for the USLE included: a regional rainfall factor of 135; a land slope of 0.2 and LS factor of 8.35; a crop management factor of 0.1; a soil erodibility factor of 0.2; and conservation practice factor of 1.0 (the default value for military ranges). The sediment delivery ratio correction to the USLE result was used. The USLE within the HGCT computed an erosion rate of 0.0028 m/yr.

The soil-water partitioning distribution coefficient,  $K_d$ , for RDX was estimated to be 0.38 L/kg based on the above stated soil texture and 4.5% organic matter. The half-life of RDX in soil for degradation was assumed to be 10 years, and the calculated volatilization rate was 62 m/yr. The RDX solid phase residue particle size was set to 12,000 µm based on TREECS™ guidance. The soil model UI-computed RDX solubility for the soil-water

matrix temperature was 29.18 mg/L. A constituent database within TREECS™ was used to obtain values of 6.32 E-8 atm-m<sup>3</sup>/mol, 222.1 g/mol, and 1.8 g/cm<sup>3</sup> for HLC, molecular weight, and solid phase density, respectively. Solid phase erosion was turned off since the residue particles are relatively large, and it is suspected that most of the eroded particles are deposited in the local drainage area before reaching Popolopen Brook.

Model default values were used for soil exchange layer thickness for rainfall ejection of pore water, soil detachability for rainfall ejection of pore water, and soil diffusion layer thickness for volatilization. The soil model was executed for 100 years starting in 1940. The adaptive time step feature was used with a minimum time step of 0.001 yr. All soil model inputs are summarized in Table 9.

**Table 9. Tier 2 soil model input values for AIA, USMA.**

Input Description	Value
Site Characteristics	
AOI dimension that is parallel to the groundwater flow, m	300
AOI dimension that is perpendicular to the groundwater flow, m	310
AOI surface, m <sup>2</sup>	102,000
Active soil layer thickness, m	0.4
Average annual temperature of soil-water matrix, °C	10.78
MC mass residue loading versus time, g/yr	49,844 Assumed to be constant for all years (see section on residue loading rate)
Initial solid phase MC concentration in soil on a soil mass basis at time 0, mg/kg	0 for all constituents

Input Description	Value
Initial total non-solid phase MC concentration in soil on a soil mass basis at time 0, mg/kg	0 for all constituents
Soil Properties	
Volumetric soil moisture content, percent	12
Soil dry bulk density, g/cm <sup>3</sup>	1.48
Soil porosity, percent	44
Hydrology	
Average annual precipitation, m/yr	1.13
Average annual rainfall, m/yr	1.05
Average annual soil erosion rate, m/yr	0.00246
Average annual water infiltration rate (groundwater recharge for no interflow), m/yr	0.227
Average annual surface water runoff rate, m/yr	0.514
Percent of annual water infiltration flow rate and mass flux that goes to soil interflow, fraction	100
Average number of rainfall events per year	141
Fate/Transport Parameters for RDX	
Soil exchange layer thickness for rainfall ejection of pore water, m	0.005
Soil detachability for rainfall ejection of pore water, kg/L	0.4

Input Description	Value
Diffusion layer thickness for volatilization, m	0.4
Soil-water constituent partition coefficient, $K_d$ , L/kg, computed by soil model UI from $K_{oc}$ , soil texture, and percent organic matter	0.385
Decay/degradation half-life of liquid (water) phase constituent, yrs	10
Decay/degradation half-life of adsorbed (particulate) phase constituent, yrs	1.0E20
Initial mean diameter of solid phase constituent residue particles (assume spherical particles), $\mu\text{m}$	12,000
Volatilization rate, m/yr	62 as computed by soil model UI from molecular diffusivity in air
Switch for solid phase erosion	off
Chemical-Specific Properties for RDX	
Aqueous solubility limit, mg/L	29.18 (computed by soil model UI based on average annual soil temperature of 10.78 deg C)
Henry's Law constant, atm- $\text{m}^3/\text{g}\cdot\text{mol}$	6.32E-8
Molecular weight (molar mass or averaged molecular mass), g/mol	222.1
Solid phase constituent mass density, g/ $\text{cm}^3$	1.8
Model Options	

Input Description	Value
Time length of simulation, yrs	100
Minimum time step, yrs	0.001
Methods used for equation solution	Adaptive time step

### 7.2.2 Stream model inputs

As stated above, the CMS was used to model the target surface water, which is Popolopen Brook. The CMS is a one-dimensional, longitudinal contaminant fate/transport model for streams. The total length of the modeled stream reach was only 50 m, which extended from the confluence of Zint's Brook with Popolopen Brook to the sampling location on Popolopen Brook. Zint's (or Deep Hollow) Brook joins Long Pond Brook before it empties into the headwaters of Popolopen Brook, which begins at the tail water of Stilwell Lake, which is about 100 m upstream of the confluence with Zint's Brook (Deep Hollow). Ten computational segments or nodes were used to represent the very short 50 m modeled reach of Popolopen Brook. The maximum time step was set to 0.25 years. Smaller maximum time steps did not affect results. The longitudinal dispersion coefficient was set to 1.0 m/sec, and the stream total suspended solids (TSS) concentration was set to 3 mg/L based on data reported by ATC (2004a). The fraction of organic carbon ( $f_{oc}$ ) of the TSS in the water column was assumed to be 0.02, which is a fairly typical value. The depth of the mixed sediment layer was assumed to be 0.1 m with porosity of 0.7 and  $f_{oc}$  of 0.02. The dry sediment particle density was set to 2,650 g/L.

The stream was assumed to have a uniform width of 10 m and depth of 0.3 m based on a site visit observation. The stream flow was set to 0.49 m<sup>3</sup>/sec, which was based on an estimate of 1.53E7 m<sup>3</sup>/yr for the average annual flow rate. The average annual flow rate was computed from the product of the watershed area of 29.9 km<sup>2</sup> and the average annual runoff depth of 0.514 m/yr. The watershed area was estimated from examination of terrain and elevations of the region within Google™ Earth. This flow rate and stream geometry results in an average flow velocity of 0.16 m/sec (0.53 ft/sec).

The stream benthic sediment burial rate was set to an extremely small value (1.0 E-20 m/day) to represent essentially no burial for this small stream that is most likely in equilibrium for sedimentation. The TSS settling rate was set to 216 m/day, which is the approximate settling rate of very fine sand to coarse silt. The resuspension rate was computed from a steady-state solids balance resulting in a rate of 0.00081 m/day that was used in the model. Sediment mass deposition was in balance with sediment mass resuspension.

The RDX octanol – water partitioning distribution coefficient,  $K_{ow}$ , was set to 7.41 ml/ml based on the value within the ARCDB that resides within TREECS™. The  $K_{ow}$  value is used within the CMS UI to compute  $K_d$  given  $f_{oc}$ ; the computed  $K_d$  used in the model was 0.091 L/kg for water column TSS and benthic sediments. The ARCDB values for molecular diffusivity in water of 7.07 E-6 cm<sup>2</sup>/sec and HLC of 6.32 E-8 atm-m<sup>3</sup>/g-mole were used. A wind speed of 5 m/sec was assumed. The CMS UI was used to compute the RDX volatilization rate of 0.0012 m/day and sediment pore-water – water column diffusive mass transfer velocity of 0.0036 m/day. The decay rate of RDX in stream water and sediment was set to 0.0 day<sup>-1</sup>, representing no degradation. Degradation is not important for this application given the extremely brief residence time in the short stream reach being modeled. All CMS inputs are summarized in Table 10.

**Table 10. CMS input values used for AIA, USMA.**

Input Description	Value	Data source
Number of computational segments, unit-less	10	user choice
Time step, yr	0.25	user choice
Total simulation time, yr	99	user choice
Longitudinal dispersion coefficient, m <sup>2</sup> /sec	1.0	typical value for streams
TSS concentration in stream, mg/L	3.0	ATC (2004a)
Depth of active sediment layer, m	0.1	typical value
Dry sediment particle density, g/L	2,650	typical value for inorganic sediments
Sediment porosity, unit-less	0.7	typical value
Fraction organic carbon in water column TSS, unit-less	0.02	typical value

Input Description	Value	Data source
Fraction organic carbon in bed sediment, unit-less	0.02	typical value
Average annual water temperature, deg C	10	equal to approximate average annual air temperature
Average annual wind speed, m/sec	5	assumed, typical average value for U.S.
Distance from entry point of AOI loads or confluence to end of model reach, m	50	approximate distance to sampling location from confluence
Stream reach average width, m	10.0	estimated based on site visit observation
Stream reach average depth, m	0.3	estimated based on site visit observation
Stream reach average flow rate, m <sup>3</sup> /sec	0.487	see text
Background and initial stream concentrations, mg/L	0	assumed
Decay rates for various phases, per day	0	not important due to very brief residence time in modeled stream reach
RDX $K_{ow}$ , mL/mL	7.41	from ARCDB
Partitioning distribution coefficient for adsorption of RDX to water column TSS, $K_d$ , L/kg	0.091	computed by model UI based on TSS $f_{oc}$ and RDX $K_{ow}$
Partitioning distribution coefficient for adsorption of RDX to bed sediment, $K_d$ , L/kg	0.091	computed by model UI based on sediment $f_{oc}$ and RDX $K_{ow}$
Volatilization rate, m/day	0.0012	computed from model UI based on HLC, wind speed and water flow velocity
Mass transfer velocity between sediment pore water and water column, m/day	0.0036	computed within model UI based on other inputs
Molecular weight of RDX, g/mole	222.1	from ARCDB
Molecular diffusivity of RDX in water at 25 deg C, cm <sup>2</sup> /sec	7.07E-6	from ARCDB
Henry's Law constant of RDX, atm-m <sup>3</sup> /g-mole	6.32E-8	from ARCDB
TSS settling rate, m/day	216	typical value for fine sand-coarse silt sediments

Input Description	Value	Data source
Sediment burial rate, m/day	1E-20	assumed to be very small (bed in equilibrium for deposition and resuspension)
Sediment resuspension rate, m/day	0.00081	computed by model UI from steady-state solids balance

Of all of the CMS inputs, the most important one for this application and probably the most uncertain is the average annual stream flow rate. The computed stream water column concentration is inversely, linearly proportional to the stream flow rate. If the stream flow is halved, the water concentration doubles. Popolopen Brook does not have a flow gage. The rather large and quite hilly watershed complicates estimation of the watershed area draining into Popolopen Brook. Stream flow estimates were based on watershed area. Estimation of watershed runoff, also used in stream flow estimation, is complicated by the potential for infiltrated soil interflow that resurfaces to surface flow. The presence of the series of lakes upstream of the modeled reach also complicates estimation of stream flow rate due to water storage and controlled releases. Finally, the suspected highly variable stream flow rates associated with dry and wet seasonal conditions greatly affect stream concentrations of RDX. TREECS™ has the capability for the user to choose between the options of using average annual hydrology or daily hydrology with daily varying stream flow (Dortch et al. 2012; Dortch 2014). The daily hydrology option provides greater accuracy for resolving fluctuating MC concentrations in streams (Dortch 2014). However, the daily hydrology option was not used in this application due to the need to capture the long-term, 100-year fate of RDX at the AIA study site. Additionally, without a flow gage, there was no way to know if the computed daily stream flows were accurate. Thus, it was more rational to estimate the long-term, average annual stream flow rate and use that value to predict stream concentrations of RDX that are associated with long-term, average annual flows.

### 7.2.3 RDX residue mass loading rate

One additional set of input information is required for this application to the AIA, USMA. This information pertains to firing range munitions usage and the resulting estimates of RDX residue mass loading rate that is needed as an input to the soil fate model.

The RDX residue mass loading rate (grams per year) to the AOI soil was computed based on munitions used on Ranges 2, 12, and 13. Training ammunition usage reports for 2006 and 2009 were provided by the USMA. It was determined from these reports that the munitions fired from these ranges were 105 mm artillery (DODIC C445), 81 mm mortars (DODIC C868), and 60 mm mortars (DODIC B642). The projectiles of these three munitions contain 1252, 548, and 221 g of RDX, respectively, values provided by the extracted/modified version of MIDAS that resides within TREECS™ as a database. MIDAS is maintained by the U.S. Army Joint Munitions Command in McAlester, OK.

The highest numbers of items fired for each DODIC for the two years were used to estimate RDX residue. The numbers fired for each DODIC are shown in Table 11 along with the percentages for duds, low order detonations, low order yields, and high order yields. Yield is defined as the percent of total HE delivered to impact areas that is exploded upon impact. The high order detonation percentage is simply the total fired minus the percent duds and low order. The percentages shown in Table 11 are based on guidance within TREECS™ for each munitions type. TREECS™ has various built-in help menus. The MC residue is calculated based upon the projectile MC mass delivered to the impact area and the numbers and percentages shown in Table 11. The total RDX residue loading rate was calculated to be 49.84 kg/yr, with the 105 mm being by far the greatest contributor. The total loading rate was assumed to be constant each year for the entire 100-year simulation, starting in 1940.

**Table 11. Munitions usage and detonation characteristics for the AIA, USMA.**

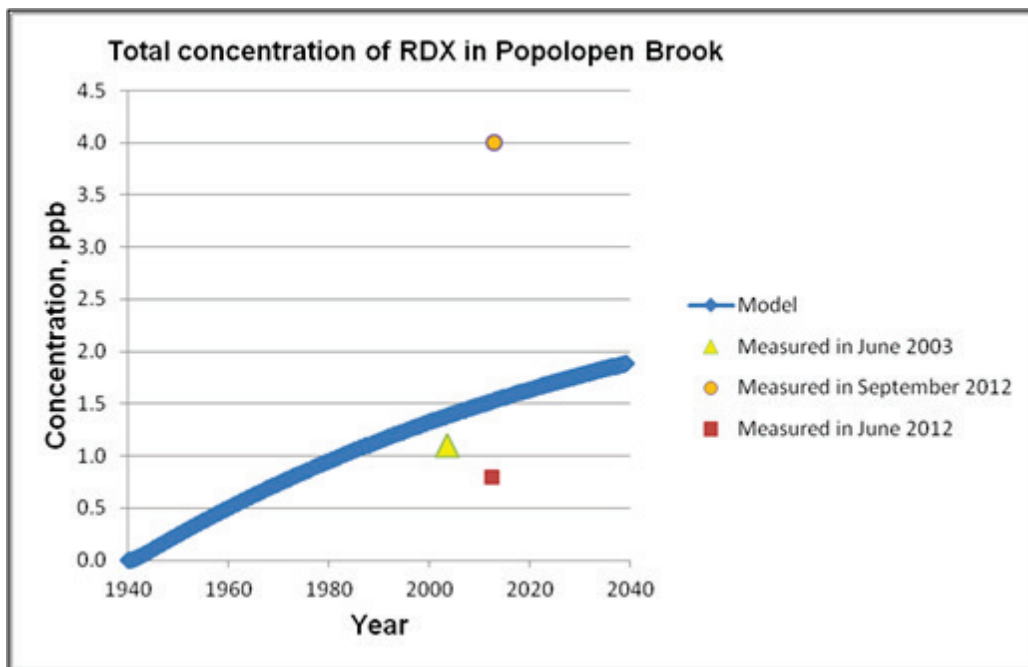
DODIC	Numbers of rounds fired per year	Duds, %	Low order, %	Low order yield, %	High order yield, %
C445	7855	2.8	1	50	99.999993
C868	3164	2.9	0.06	50	99.999993
B642	2314	2.9	0.06	50	99.999993

### 7.3 Validation results

Using the inputs described in section 7.2, the TREECS™ models were executed and the results were plotted using viewers within TREECS™. The model-computed results for stream water total concentration of RDX at

the terminus of the modeled reach of Popolopen Brook versus year are plotted in Figure 20. The concentrations measured in 2003 and 2012 at approximately the same location are also shown in Figure 20 for comparison.

**Figure 20. Computed and measured concentration of RDX in Popolopen Brook down-gradient of the AIA, USMA.**



The measured value in 2003 was obtained by ATC (2004b), and the measured values in 2012 were obtained through grab samples collected by USMA personnel and analyzed by the Engineer Research and Development Command (ERDC) Environmental Laboratory (EL) Environmental Chemistry Branch (ECB) using EPA Method 8330. Samples were collected from Popolopen Brook at USMA on 9 different dates in the summer and early fall of 2012, but RDX was detected for only two of those sampling dates as shown in Table 12. For both dates that RDX was measured, duplicate samples confirmed the measured values for each date.

The interesting thing about the information exhibited in Table 12 is that RDX was detected only on dates when there was a sizable rainfall the day before and some rainfall on the day of the sampling. The date with the highest measured RDX stream concentration, which occurred on September 6, 2012, had the highest rainfall the day before the sampling. The measured results clearly indicated how flashy RDX stream concentrations can be and how dependent those concentrations are on recent rainfall to

move RDX from AOI soil to receiving water. The model-computed concentrations increase over time due to the build-up of RDX residue on the range associated with continual firings each year.

There appears to be a correspondence between the variation of model prediction relative to observation and actual rainfall just before and during observation relative to average annual rainfall per rainfall event. The ratio of the sampling date rainfall to the average annual rainfall per rainfall event was computed for each observation. The ratio of observed stream concentration to predicted stream concentration was also computed. A comparison of the two ratios showed remarkable agreement. For example, the average annual rainfall per rainfall event is 0.29 inches, which was obtained by dividing the average annual rainfall of 41.3 inches (1.05 m) by 141, the average number of rainfall events per year. The average rainfall for September 5 and 6, 2012, is 0.93 inches. The ratio of 0.93 inches and 0.29 inches is 3.17. The ratio of observed to model-computed RDX concentration on September 6, 2012, is 2.61. Similarly, the ratio of measured to model-computed RDX concentration on June 19, 2003, is 0.79 when the ratio of average rainfall for June 18 and 19, 2003, to average annual rainfall per rainfall event is 0.70. Thus, the model tends to under-predict and over-predict by roughly the ratio of actual rainfall on and just before the sampling date to average rainfall per rainfall event. These results support the concept that the TREECS™, when applied with average annual hydrology, tends to predict stream concentrations coinciding with average rainfall per rainfall event.

**Table 12. RDX concentration and precipitation on day of, and two days preceding sampling for RDX in Popolopen Brook<sup>4</sup>, USMA.**

Date	Measured RDX concentration, ppb	Precipitation on date, inches	Precipitation on day before date, inches	Precipitation two days before date, inches
6/19/2003	1.1	0.06	0.35	0
6/3/2012	0.8 <sup>2</sup>	0.03	0.77	0
6/14/2012	ND <sup>3</sup>	0	0.69	0
6/18/2012	ND	0.07	0	0
6/25/2012	ND	0.39	0	0
7/5/2012	ND	0	0.02	0

Date	Measured RDX concentration, ppb	Precipitation on date, inches	Precipitation on day before date, inches	Precipitation two days before date, inches
7/23/2012	ND	0.32	0.09	0
7/30/2012	ND	0	0	0.58
8/8/2012	ND	0	0	0
9/6/2012	4.0 <sup>4</sup>	0.36	1.5	0

<sup>1</sup> Sampling station is downstream of Stilwell Lake and a short distance below the confluence with Zint's Brook

<sup>2</sup> Value is the average of two values of 0.7 and 0.9 ppb, which are above detection but below the reporting limit of 1 ppb

<sup>3</sup> ND = not detected

<sup>4</sup> Both samples measurements were the same, 4.0 ppb

The measured RDX concentrations in benthic sediment during 2003 were below the methods reporting limit of 0.05 mg/kg. The computed benthic sediment concentrations in the stream peaked at 0.0013 mg/kg after 100 years. Benthic sediment samples were not collected in 2012. The measured water concentrations of RDX in 2003 and 2012 were total, (i.e., dissolved and particulate RDX). Likewise, the model computed values in Figure 20 are also total. The computed dissolved RDX concentrations were almost identical to the total, which indicates very little particulate RDX as expected for the low value of  $K_d$  and low TSS concentration.

The performance metrics for evaluating model accuracy, (i.e.,  $RR$  and  $RE$ ), are shown in Table 13 for stream concentration of RDX down-gradient of the AIA. The  $RR$  is below 3.0 for all three dates resulting in highly successful results according to the performance objective criteria in the Demonstration Plan. The  $RR$  and  $RE$  for June 2003 are quite good, while for the other two dates, they are considered mediocre to less than preferred.

**Table 13. Performance metrics of model accuracy for stream concentration of RDX down-gradient of the AIA, USMA.**

Date	Measured, ppb	Modeled, ppb	RR	RE, %
June 2003	1.1	1.39	1.26	26
June 2012	0.8	1.53	1.91	91
September 2012	4.0	1.53	2.61	62

There are a number of reasons the performance metrics for the two samples are less than preferred. For one, the measured values are a snapshot in time. As discussed above, stream flow rates are highly variable over time, even from day to day, and MC concentrations in streams vary with the flow rate. There are also several uncertain model inputs. Besides stream flow rate, another primary uncertain input is the RDX residue loading rate, which depends on the number of rounds fired each year. A constant firing rate was assumed, whereas, the firing rate is believed to be variable from year to year. Additionally, it is not known how long these ranges have been in use. For this application, it was assumed that these ranges began use in 1940. Stream concentrations are directly and linearly related to residue loading rate, and thus firing rates.

Rainfall extraction and runoff is the predominant AOI export process, with export rates that are about two orders of magnitude (100 times) greater than the soil erosion export rate. The solid phase RDX residue mass is two orders of magnitude greater than the non-solid phase (i.e., aqueous phase dissolved and soil adsorbed) RDX mass after 100 years. The primary reason for this difference is that RDX solid phase dissolution is relatively slow, so there is a delay time between residue particle deposition and export of the dissolved phase. Slow dissolution results in a long recovery time for stream concentrations of RDX should use cease and RDX residue depositional flux becomes zero.

Solid phase MC particle dissolution is dependent on annual precipitation rate, MC solubility in water, particle size, and particle density. The first two variables and particle density are well known, but MC particle size is highly variable and uncertain. The size used for RDX in this application is based on the best available information resulting from firing range research (Pennington et al. 2005; Taylor et al. 2004). However, as an example, assume the size is an order of magnitude smaller, (i.e., 1,200  $\mu\text{m}$ ). Stream concentration of RDX reaches nearly steady-state after about 50 years at a value of 3.2 ppb, which is about double the validation result after 72 years. The higher stream concentrations, as well as reaching steady-state soil and stream concentrations sooner, is due to the higher dissolution rate of RDX.

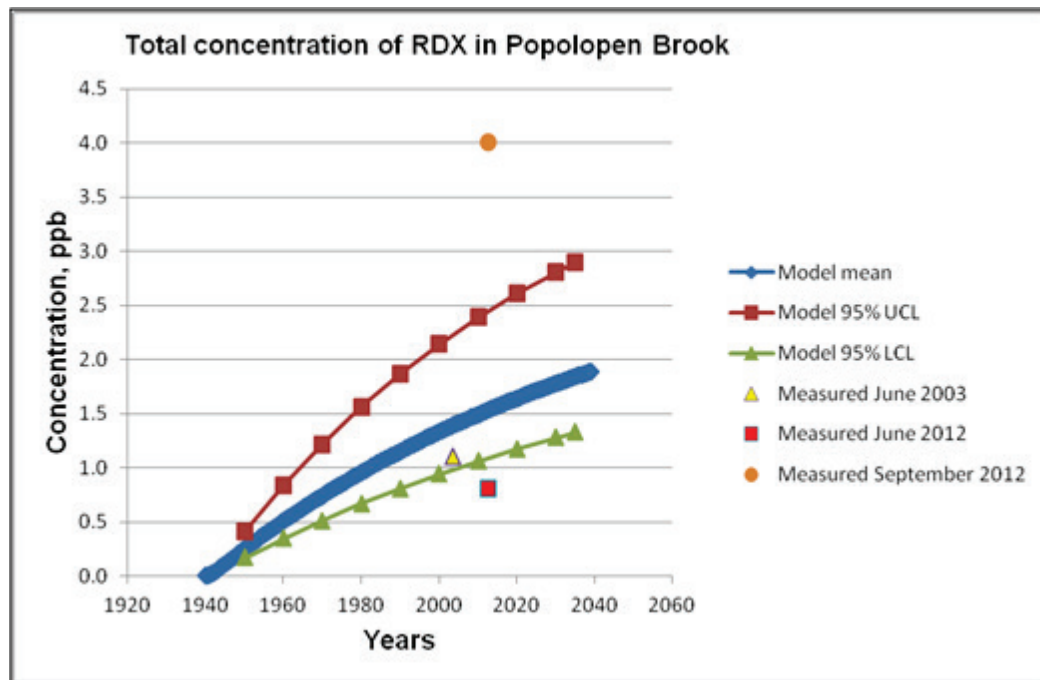
## 7.4 Uncertainty analysis

None of the RDX physicochemical properties are considered highly uncertain, nor are the results sensitive to the less certain value of  $K_d$  for soil and

water TSS. The complexity of the watersheds surrounding Popolopen Brook made estimation of watershed area and therefore runoff volume and stream flow rate difficult. Residue solid phase particle size is also rather uncertain and variable. Model results are sensitive to both average annual stream flow rate and the average initial size of the RDX residue solid phase particles. Thus, these two inputs were treated as uncertain within the Monte Carlo simulation. Each were varied by a factor of two using a normal distribution with the mean of the distribution equal to the validation inputs of  $0.487 \text{ m}^3/\text{sec}$  and  $12,000 \mu\text{m}$  for stream flow rate and particle diameter, respectively. The upper and lower bounds of the distributions were set to double and half of the mean values, respectively. The standard deviations of the distributions were estimated from one sixth of the range between upper and lower bounds, resulting in standard deviation of  $0.122 \text{ m}^3/\text{sec}$  for flow and  $3,000 \mu\text{m}$  for particle diameter. The Monte Carlo simulation was run for 100 realizations, which were enough to accurately define the uncertainty bands.

The uncertainty analysis results for variation in RDX residue particle diameter and stream flow rate are shown in Figure 21. The uncertainty confidence bands capture one measured value but not the other two collected in 2012. Greater variation in the bounds on the two uncertain variables would allow the measured data to be captured within the bounds, but there was no rationale for greater variation than simply doubling and halving the validation inputs.

Figure 21. Computed and measured concentration of RDX in Popolopen Brook down-gradient of the AIA, USMA, with upper (UCL) and lower (LCL) 95% confidence limits for uncertainty on RDX residue initial mean particle diameter and stream flow rate.



Model results are considerably more sensitive to stream flow rate than RDX residue particle diameter. The uncertainty analysis indicated that flow rate explained about two-thirds of the variability. Doubling and halving the stream flow rate causes model stream concentrations that are almost as high as the measured value in September, 2012 and lower than the measured value in June, 2012, respectively. Certainly a little greater variation than doubling and halving stream flow rate alone would lead to model results that capture all measured data. It is concluded that stream flow rate is the single most sensitive and uncertain of the model inputs. Additionally, as explained in the previous section, simulations with average annual hydrology tend to predict stream concentrations coinciding with average rainfall per rainfall event, whereas, actual stream concentrations appear to be highly correlated to amount of rainfall that occurred during and just prior to the sampling event. This latter aspect is a primary driver of large variations in observed stream concentrations.

## 7.5 Fate of emerging MC (EC) associated with IM

The five ECs, DNAN, NTO, NQ, AP, and CL-20 were selected within the TREECS™ validation application of the AIA, USMA, for evaluating their

fate relative to that of RDX in surface water. The inclusion of these five additional constituents in the application required specifying their physicochemical properties, which are not as well-known as are those of RDX. The EPI Suite component of CTS was used to provide some of the properties information for the five EC, such as HLC and  $K_{oc}$  values. The *General Source Zone Loading* option was selected under the *Site Conditions/Operational Inputs* tab for the soil loading option rather than *Impact Zone*, which was used for the validation application for estimating RDX residue loading rates. By selecting this option, the residue loading rates (grams per year) could be specified. The MC residue loading rate for each EC was set to the same rate as that estimated for RDX based on munitions use, or 49,844 g/yr. Besides specifying the physicochemical properties and the partitioning distribution coefficients in soil for each EC, the only other additional input that was required was the degradation half-life in each media. All other model inputs were the same as the validation application as shown in Tables 9 and 10.

### 7.5.1 Initial inputs and results

Inputs were initially set using the best available information within TREECS™-CTS without exerting any additional study or literature review, thus relying on default methods within the system. The additional soil model inputs that were specified for the five ECs are shown in Table 14. Most of the values in this table are the same as those in Table 6 with the exception of the residue loading rate, solid phase particle diameter, soil volatilization rate, soil  $K_d$ , and aqueous phase half-life. The loading rate and particle diameter were the same as that of RDX for the AIA validation application. The volatilization rate was different due to different soil porosity and water content. Except for CL-20, the soil  $K_d$  values in Table 14 were computed by the soil model UI using  $K_{oc}$  and percentages of sand, silt, clay, and organic matter of 57.5, 28, 10, and 4.5, respectively. The degradation half-life in soil was assumed to be the same as that of RDX for comparison purposes, or 10 years for aqueous dissolved and 1.0E20 years for aqueous adsorbed to soil.

**Table 14. Additional soil model inputs of the five ECs for AIA application, USMA.**

Input Description	DNAN	NTO	NQ	AP	CL-20
Site Characteristics					
MC mass residue loading versus time, g/yr, constant for 100 years	49,844	49,844	49,844	49,844	49,844

Input Description	DNAN	NTO	NQ	AP	CL-20
Initial solid phase MC concentration in soil on a soil mass basis at time 0, mg/kg	0	0	0	0	0
Initial total non-solid phase MC concentration in soil on a soil mass basis at time 0, mg/kg	0	0	0	0	0
Fate/Transport Parameters					
Soil-water constituent partition coefficient, $K_d$ , L/kg, computed by soil model UI from $K_{oc}$ , soil texture, and percent organic matter for all except CL-20	4.62	3.67	0.35	0.0005	2.0 <sup>1</sup>
Decay/degradation half-life of aqueous phase constituent, yrs	10	10	10	10	10
Decay/degradation half-life of adsorbed (particulate) phase constituent, yrs	1.0E20	1.0E20	1.0E20	1.0E20	1.0E20
Initial mean diameter of solid phase constituent residue particles (assume spherical particles), $\mu\text{m}$	12,000	12,000	12,000	NA miscible	12,000
Volatilization rate, m/yr, as computed by soil model UI from molecular diffusivity in air	55.0	84.6	85.2	0 miscible	37.1
Chemical-Specific Properties (same as the values in Table 6)					
$K_{oc}$ , L/kg	158.5	125.9	12	0.016	2.7
Molecular weight (molar mass or averaged molecular mass), g/mol	198	130	104	117.5	438
Aqueous solubility limit, mg/L	276	16,600	3,800	249,000	4.33
Henry's Law constant, atm· $\text{m}^3/\text{g}\cdot\text{mol}$	3.01E-7	4.07E-13	4.49E-12	0	9.39E-25
Solid phase constituent mass density, g/ $\text{cm}^3$	1.34	1.93	1.72	1.95	2.04

Input Description	DNAN	NTO	NQ	AP	CL-20
Molecular diffusivity in air, m <sup>2</sup> /day	0.56	0.86	0.87	NA Non-volatile	0.37

<sup>1</sup> Mean of range of values reported by Szecsody et al. (2004) for soil

The only additional inputs required for CMS are within the *Constituent Parameters* screen of the CMS UI. Within that screen, all initial EC concentrations and decay rates were set to zero, same as for RDX. Two additional inputs required within that screen for each EC include  $K_{ow}$ , which is used by the model UI to compute  $K_d$  for water column TSS and benthic sediment, and molecular diffusivity in water, which is used by the model UI to compute the mass transfer velocity for diffusion of dissolved constituent between the water column and benthic sediment pore water. The water volatilization rate is also on this input screen with the option selected to compute it by the model UI from HLC, wind speed, and water flow velocity. The values of the two inputs and the computed parameters are shown in Table 15 for each EC. The value of HLC and molecular weight are also displayed on the *Constituent Parameters* screen of the CMS UI, and these values are supplied by the TREECS™ constituent data base with their values as shown in Table 14.

**Table 15. Additional CMS inputs for the five EC for Popolopen Brook application, USMA.**

Input Description	DNAN	NTO	NQ	AP	CL-20
$K_{ow}$ , mL/mL	43.6 <sup>1</sup>	2.34 <sup>2</sup>	0.13 <sup>3</sup>	1.45E-6 <sup>4</sup>	1.07 <sup>5</sup>
TSS-water constituent partition coefficient, $K_d$ , L/kg, computed by CMS UI from $K_{ow}$ and $f_{oc}$	0.54	0.029	0.0016	1.8E-8	0.013
Benthic sediment-water constituent partition coefficient, $K_d$ , L/kg, computed by CMS UI from $K_{ow}$ and $f_{oc}$	0.54	0.029	0.0016	1.8E-8	0.013
Volatilization rate, m/day, computed by CMS UI from HLC, wind speed, and water flow velocity	0.006	9.0E-9	1.05E-7	0	1.5E-20

Input Description	DNAN	NTO	NQ	AP	CL-20
Mass transfer velocity, m/day, for diffusion of dissolved constituent between water column and sediment pore water, m/day, computed from molecular diffusivity in water and sediment porosity	0.0039	0.0052	0.006	0.0055	0.0023
Molecular diffusivity in water, cm <sup>2</sup> /sec, computed from method by Hayduk and Laudie (1974) except for AP	6.16E-6	8.55E-6	8.45E-6	1.8E-5 <sup>6</sup>	4.18E-6

<sup>1</sup> Measured, Sokkalingam et al. (2008)

<sup>2</sup> Estimated, Sokkalingam et al. (2008)

<sup>3</sup> Measured, Hansch et al. (1995) as cited in EPI Suite

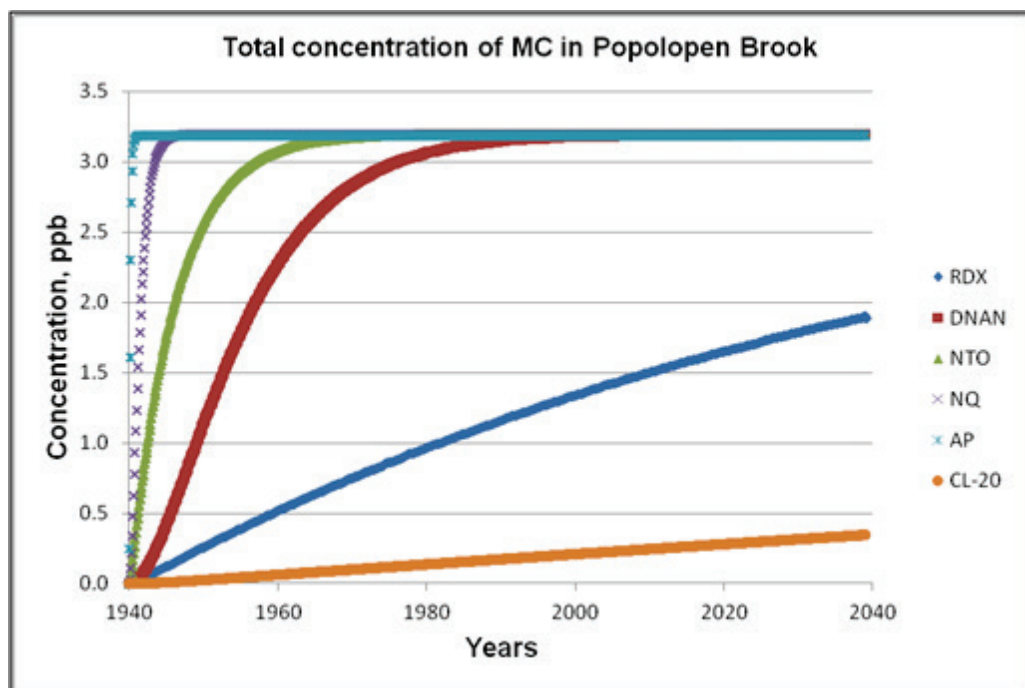
<sup>4</sup> EPA (2008)

<sup>5</sup> Chemspider (<http://www.chemspider.com/>) predicted from ACD/Labs Percepta Platform - PhysChem module

<sup>6</sup> Hlquily and Clifton (1984)

The above inputs, including the other model inputs used in the RDX validation application were used in the EC application. The results of the EC application are plotted in Figure 22 as stream total concentration versus year. The previous results for RDX are included in the plot for comparison. All results approach a constant, steady-state stream concentration over time, which is due to the constant loading rate of MC residue each year. RDX and CL-20 have not reached steady-state because of their much lower solubility and dissolution rates that require a much longer time to dissolve. All of the MC results in Figure 22 follow a trend where steady-state is reached faster as solubility increases. However, NQ and NTO depart from this trend some since NTO has a higher solubility than NQ, but NQ reaches steady-state sooner than NTO. This trend departure is due to NTO having a much higher soil  $K_d$  than NQ, resulting in greater retardation while in AOI soil. The ratios of NTO-to-NQ solubility and soil  $K_d$  are 4.37 and 10.49, respectively; thus,  $K_d$  has a greater effect than solubility for reaching steady-state. The same steady-state concentrations are reached for each MC due to each having the same half-life in AOI soil and receiving stream.

Figure 22. Computed water concentrations in Popolopen Brook down-gradient of AIA, USMA, for five ECs and RDX.



### 7.5.2 Refined inputs and simulation results for DNAN and NTO

DNAN and NTO were chosen for a more focused study in the AIA application, same as for the application for Demo Area 2, MMR. Of all the chemical-specific inputs, the values for  $K_{oc}$ , which affect the estimates of soil  $K_d$ , and soil half-life were considered the most uncertain for DNAN and NTO. Thus, refined estimates for soil  $K_d$  and half-life were made for DNAN and NTO and used to examine the effects on their fate. Stream EC concentrations are insensitive to EC stream degradation rates due to the relatively short travel time from the upstream entry point to the receptor location.

The characteristics of the 11 soils used in the Dontsova et al. (2014) study were reviewed in an attempt to match as closely as possible the particular soil to the soil texture and pH for the AIA soils. Matching the soil OC content was considered less important since the measured  $K_d$  values were normalized by Dontsova et al. (2014) to OC to provide  $K_{oc}$ . The soils that are the most similar to the surface soils at the AIA are Camp Butner (NC.), Limestone Hills (MT.), Fort Harrison (MT.), and Plymouth (MMR, MA.). Soils from the first three sites are all sandy loam like the AIA soils, while the Plymouth soils are loamy sand. WSS was used to estimate the AIA soil pH of 5.5, but most of the small arms firing ranges (SAFRs) at USMA have

pH of about 6.2 or higher (ATC 2004a), which could be due to the presence of weathered lead particles.

The characteristics of the four soils studied by Dontsova et al. (2014) and the corresponding measured batch  $K_d$  and OC normalized  $K_{oc}$  values for DNAN and NTO are shown in Table 16 along with the  $R^2$  of the fit for  $K_d$ . The values of  $K_d$  and  $K_{oc}$  for DNAN of 4.62 and 158.5 L/kg, respectively, in Table 6 agree reasonably well with the measured values in Table 16, which range from 2.05 to 6.32 L/kg for  $K_d$  and 84.8 to 250 L/kg for  $K_{oc}$ . It is noted that the OC content of the four soils in Table 16 ranged between 1.99% for Limestone Hills to 3.88% for Fort Harrison. The OC content of the AIA soils are estimated to be 1.8%. The  $K_{oc}$  of the four soils averages 169 L/kg for DNAN, which is close to the value of 158.5 used originally. Given such similarities, the original  $K_d$  value of 4.62 L/kg for DNAN was retained for the refined simulation.

**Table 16. Soil characteristics and measured batch  $K_d$  and corresponding  $K_{oc}$  values for DNAN and NTO for four soils similar to AIA soils (Dontsova et al. 2014).**

Soils	Sand-silt-clay, %	Soil pH	DNAN $K_d$ , L/kg	$R^2$ , DNAN $K_d$	DNAN $K_{oc}$ , L/kg	NTO $K_d$ , L/kg	$R^2$ , NTO $K_d$	NTO $K_{oc}$ , L/kg
Camp Butner	66-26-8	6.69	2.05	0.92	84.8	0.12	0.72	4.96
Limestone Hills	53-36-11	7.54	4.96	0.92	250	0.21	0.92	10.55
Fort Harrison	55-37-8	6.67	6.32	0.93	163	0.35	0.95	9.02
Plymouth	75-20-5	4.23	4.38	0.94	179	0.50	0.96	20.41

The values of  $K_d$  and  $K_{oc}$  for NTO of 3.67 and 125.9 L/kg, respectively, in Table 14 are about an order of magnitude higher than the measured values in Table 16, which range from 0.12 to 0.5 L/kg for  $K_d$  and 4.96 to 20.41 L/kg for  $K_{oc}$ . Also, the relative range in  $K_{oc}$  for NTO is greater than it is for DNAN indicating less correlation of partitioning to OC content for NTO. Partitioning of NTO to soil appears to be more closely associated with soil pH with an inverse relationship (Dontsova et al. 2014). A  $K_d$  value of about 0.23 L/kg, which is the average  $K_d$  for the Camp Butner, Limestone Hills, and Fort Harrison soils, seems far more appropriate for the AIA surface soil than the value of 3.67 L/kg that was used originally.

The reasoning used previously for degradation rates (half-lives) of DNAN and NTO at Demo Area 2 can be applied for the AIA. Thus, a DNAN half-life of 0.6 years and a NTO half-life of 10 years (same value as used for RDX in this application) were used for the refined simulation. The soil  $K_d$  for DNAN was kept at the original value of 4.62 L/kg, and that of NTO was reduced from 3.67 to 0.23 L/kg for the refined simulation. All other inputs were kept at the same value as for the original EC simulation for the AIA.

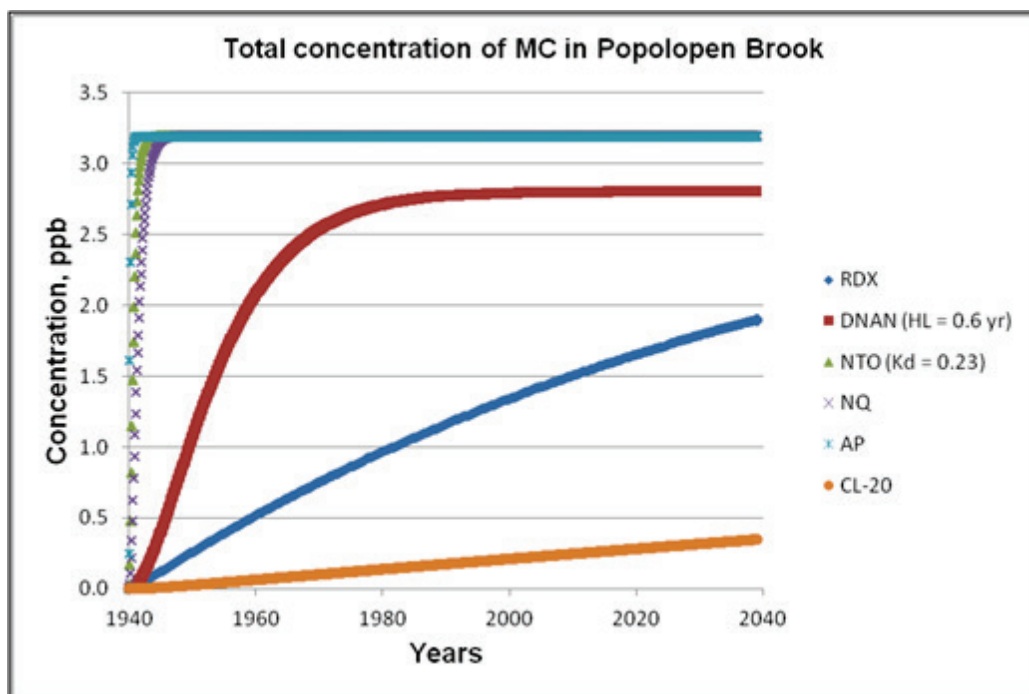
The results of the above refinements (i.e., improvements in input estimates for DNAN and NTO) are shown in Figure 23 along with the previous result for the other three EC and RDX for comparison. NTO now reaches steady-state very quickly, and the steady-state concentration of DNAN is now lower than originally due to degradation in AOI soil.

## 7.6 BMP assessment

Three BMPs were evaluated for RDX at the AIA study site as follows:

- BMP 1 – discontinue range use after the year 2015;
- BMP 2 – amend, repeatedly when necessary, the AOI soil with lime to create alkaline hydrolysis with rapid degradation of RDX; and
- BMP 3 – continuous AOI export treatment of RDX in surface runoff (including soil interflow) through a degradation reactor.

Figure 23. Computed water concentrations in Popolopen Brook down-gradient of AIA, USMA, for five ECs and RDX, with improved inputs for DNAN and NTO.



Each BMP was simulated and results compared against base condition results. The base condition was the same as the validated model with the exception of doubling the simulation time from 100 to 200 years so that results could be more fully evaluated, so each BMP was run for 200 years. BMP 1 had the same inputs as the base condition, except that the firing rates for the three munitions were set to zero in year 2016 for the remainder of the simulation. BMP 2 had the same inputs as the base condition with the exception that the aqueous dissolved RDX in soil pore water had a degradation half-life of 0.005 years due to alkaline hydrolysis of the lime soil amendment applied to the AOI soils (see BMP 2a for the MMR application).

BMP 3 involved application of a porous bed degradation reactor (Dortch and Gerald 2015) to intercept AOI surface runoff and soil interflow and remove via degradation dissolved RDX from the AOI export flux. The validation application revealed that the surface water export flux (including soil interflow flux) of dissolved RDX is about 200 times greater than that associated with particulate (adsorbed) RDX. A degradation reactor model was developed for TREECS™ as an AOI export treatment BMP option (Dortch and Gerald 2015). This model was applied to the AOI RDX export from the AIA with the following reactor specifications:

- length: 30 m
- width: 3 m
- depth: 1 m
- flow rate: 536 m<sup>3</sup>/day
- bed porosity: 0.5
- bed dry bulk density: 1.32 kg/L
- bed solids – water partitioning distribution coefficient: 0.5 L/kg
- degradation rate: 10.0 day<sup>-1</sup>

The flow rate of 536 m<sup>3</sup>/day was calculated from the sum of the average annual water runoff and infiltration rates of 0.514 and 0.227 m/yr, respectively, times the AOI surface area of 102,000 m<sup>2</sup> divided by 141 days per year, which is the average number of days per year with significant rainfall. A bed solids-to-water partitioning distribution coefficient of 0.5 L/kg was used to represent expected typical sorption conditions for RDX. The degradation rate of 10.0 day<sup>-1</sup> can be rather easily achieved for a properly constructed reactor bed using zero valent iron or similar RDX-reductive material. Analysis of experimental results for a meso-scale, laboratory, iron bed reactor (Dortch and Smith 2013) indicates an overall bulk degradation rate of about 240 day<sup>-1</sup>, thus, a value of 10.0 day<sup>-1</sup> should be quite conservative. For the above conditions, the TREECS™ degradation reactor model computed a reactor effluent normalized concentration of 0.1, (i.e., the ratio of effluent to influent RDX concentration is 0.1, or 90% of the RDX concentration is removed). This amount of reduction was used to scale the AOI export fluxes of RDX to surface water which are needed by the stream model. Otherwise, all other inputs for BMP 3 were the same as those of the base condition. At the time of this report, the reactor model was being added to TREECS™ so that there will be a continuous, automated sequence of computations from AOI, through reactor, and into and through the receiving water.

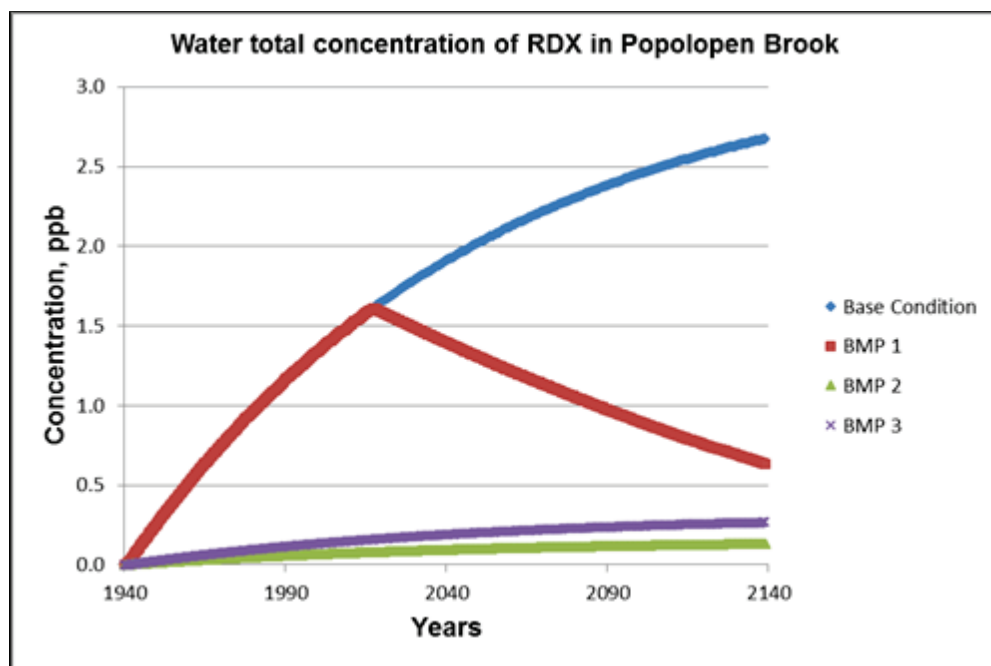
The results of the three BMP simulations are plotted in Figure 24 as water total concentration of RDX in Popolopen Brook versus years. The results of the base condition are included in the plot for comparison of BMP effectiveness.

BMPs 2 and 3 are nearly equivalent in effectiveness for reducing stream concentrations of RDX. Differences within these two BMPs are within the accuracy and assumptions of the BMP approach and ability to model it. BMP 1 is not very effective, and it takes a very long time to realize any benefit it provides. Any RDX residue mass will persist in AOI soils for a long

time due to the relatively slow dissolution rate of RDX. The cessation of range use associated with BMP 1 is probably not a viable alternative anyway.

BMP 2 (amending AOI soil with lime) is probably a cost effective alternative, but it will be hazardous to work AIA soils due to unexploded ordnance (UXO). Additionally, repeated application of soil amendment may be required over time. BMP 3 (AOI export treatment with a degradation reactor) can be implemented with much less exposure to UXO, although it may be necessary to perform some grading down-gradient of the AIA to channel water flow towards the degradation reactor. Additionally, BMP 3 is considered new and still experimental; there could be problems with sediment laden runoff clogging the reactor.

**Figure 24.** Computed water concentrations of RDX in Popolopen Brook down-gradient of the AIA, USMA, for three BMPs compared to base condition.



## **8 Zulu Impact Area (ZIA), Marine Corp Base (MCB) Camp Pendleton, CA.**

### **8.1 Site description**

Quebec, Whiskey, and Zulu impact areas were identified as areas where the most MCs were deposited at MCB Camp Pendleton, CA. The ZIA was selected as a study site for this ESTCP project for the reasons provided in the ESTCP Project ER-201435 Site Selection Memo. The ZIA is located within the Las Flores watershed, whereas, the San Onofre and San Mateo watersheds are associated with the Whiskey and Quebec impact areas.

The CSM developed for Camp Pendleton strongly suggests that surface water flow drives the potential for off-range migration of MCs to human and threatened and endangered (T/E) ecological receptors (AMP 2013). A REVA conducted for the Marine Corps included screening-level surface water and groundwater modeling that predicted low levels of explosives potentially present within the Las Flores and San Onofre watersheds (AMP 2013). As a result, groundwater and surface water sampling were conducted for these watersheds during 2011–2013. Sample results within the Las Flores watershed indicated RDX concentrations above detection limits but below reporting limits and below the screening PALs in both surface water and groundwater. The screening PALs were established by the DoD RMUS. The ZIA is duded with an area of 7,390 acres and receives artillery and mortar fire, as well as fire from small arms, grenades, rockets, guided missiles, aerial gunnery, and aerial bombs (AMP 2013).

Installation profile information was obtained from the latest REVA report (AMP 2013). MCB Camp Pendleton, which began operations in 1942, occupies approximately 125,000 acres of coastal Southern California in San Diego County. It is located about halfway between San Diego and Los Angeles on the California Pacific Coast, along the Interstate 5 highway.

Nearby communities include Oceanside to the south, Fallbrook to the east, and San Clemente to the northwest. The installation shares approximately 8 miles of its northern border with the San Mateo Wilderness Area of the Cleveland National Forest, and it shares its eastern border with the Fallbrook Naval Weapons Station. Aside from the wilderness area and the Naval Weapons Station (which are both largely natural areas), surrounding land use includes urban development, rural residential development,

and working farms and ranches. Camp Pendleton was a crucially important training center for marine amphibious warfare during World War II. The installation is subdivided into 36 training areas (including beaches) and six non-overlapping impact areas, three of which are dud-producing as noted above with HE munitions usage. There are presently 146 fixed range facilities at the installation.

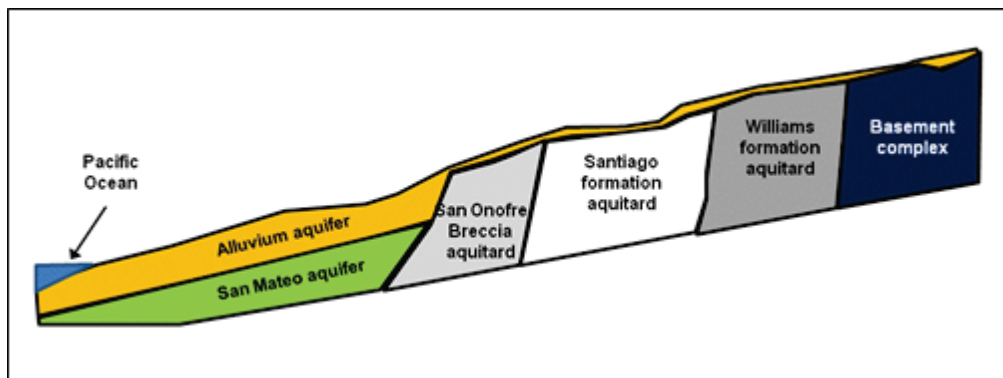
MCB Camp Pendleton has several climatic zones that roughly coincide with the three geomorphic regions present: coastal plain, coastal valley, and mountain. In general, the installation has a semiarid Mediterranean climate with warm, dry summers and mild, wet winters. The annual average daily temperature ranges from a low of 51 degrees Fahrenheit ( $^{\circ}\text{F}$ ) at lower elevations to a high of  $75^{\circ}\text{F}$ . Precipitation varies widely at Camp Pendleton, with higher values in the mountain region averaging about 22 inches per year and lower values along the coastal plain averaging about 10 to 14 inches per year. About 75% of the annual precipitation falls between November and March. Winds generally blow from the west to southwest from the Pacific Ocean. Wildfires occur during the dry season between May and November.

The elevation at MCB Camp Pendleton ranges from sea level at the coastline to approximately 2,900 feet above mean sea level (MSL) in the Santa Margarita Mountains near the north-central boundary of the installation. The majority of the land where operational range areas are located has an elevation ranging from approximately 300 feet MSL to approximately 2,250 feet MSL.

MCB Camp Pendleton contains diverse geologic units, ranging from the oldest metavolcanic rocks and granite to stream or ocean-cut terrace sequences and recent alluvium. In general, the installation is underlain by Holocene to late Pleistocene unconsolidated sedimentary deposits that include alluvium in canyon bottoms and coastal terraces, Eocene to Pliocene sedimentary rocks of marine and non-marine origin, and Cretaceous to Triassic bedrock that includes highly consolidated and cemented sedimentary rock and plutonic and metamorphic crystalline rock. In general, the stratigraphy consists of a series of thick aquitard units extending from the mountains to the foothills towards the coast. Each aquitard is overlain with a thin alluvium aquifer in the ephemeral stream valleys. The alluvium aquifer thickens and lies above the San Mateo aquifer in the lower foothills and coastal plain as shown in Figure 25. The alluvial groundwater basin

and the Mateo aquifer in the coastal plain serve as the principal water sources for the installation.

Figure 25. MCB Camp Pendleton stratigraphy (modified from AMP 2013).



The soils of MCB Camp Pendleton vary substantially, but in general consist of rough broken land and various sandy loams or loamy sands that are well drained with widely varying runoff and erosion potential. Given the wide variability in soils and their characteristics across the installation, the decision was made to use WSS to better define the soil characteristics and properties within the ZIA. Google Earth™ was used to locate the most cratered area within the ZIA. A rough delineation of the ZIA as viewed in Google Earth™ is shown in Figure 26. WSS was then used to define an AOI that covered the most cratered impact area of the ZIA. A soil map with corresponding properties was generated for the AOI with WSS. The WSS-generated AOI and soil map within the ZIA are shown in Figure 27. The lighter shaded feature in the bottom left-hand corner of the figure appears to be a sand-gravel mine. This feature, which can be observed in Figure 26, was used to help locate the cratered ZIA area within WSS. Las Flores loamy fine sand (LeC) (Figure 27), with slope between 2 and 9%, is the predominant soil type and makes up 60% of the AOI area. The other soil classes consist of Las Flores loamy fine sand and sandy loams with steeper slopes. The LeC surface soil consists of the following properties provided by WSS:

- organic matter of 0.75%
- percent sand, silt, clay of 87, 7, 6%
- saturated hydraulic conductivity of 240 cm/day
- water capacity of 0.09 cm/cm
- water content at 15 bar of 5.8%
- moderately well drained soil of soil group D
- ground slope of 6%

- soil erodibility factor K of 0.17
- soil pH of 6.1.

The above soil properties were re-examined when using HGCT in TREECS™ to ensure that the correct properties were used in the soil model.

The streams within the Las Flores watershed are ephemeral and generally flow only during significant rainfall events. These streams recharge the alluvium aquifer in the coastal plain. Most of the infiltration into surface soils within the ZIA quickly returns to surface water stream flow via soil interflow due to the rather impermeable basement units that lie closely beneath surface soils. Las Pulgas Canyon Creek (also referred to as Las Flores Creek) is the main drainage route for the Las Flores watershed.

Approximately 1 mile east of the Pacific Ocean, the Las Pulgas and Piedra de Lumbre Creeks join to form the Las Flores Creek, the headwaters of which originate approximately 10 miles from the Pacific Ocean in the Santa Margarita Mountains. A map of the Las Flores watershed with drainage streams and the location of the ZIA is shown in Figure 28. The Las Flores watershed covers about 17,300 acres (7,000 ha or 7E7 m<sup>2</sup>).

Figure 26. Rough delineation of ZIA as viewed in Google Earth™.

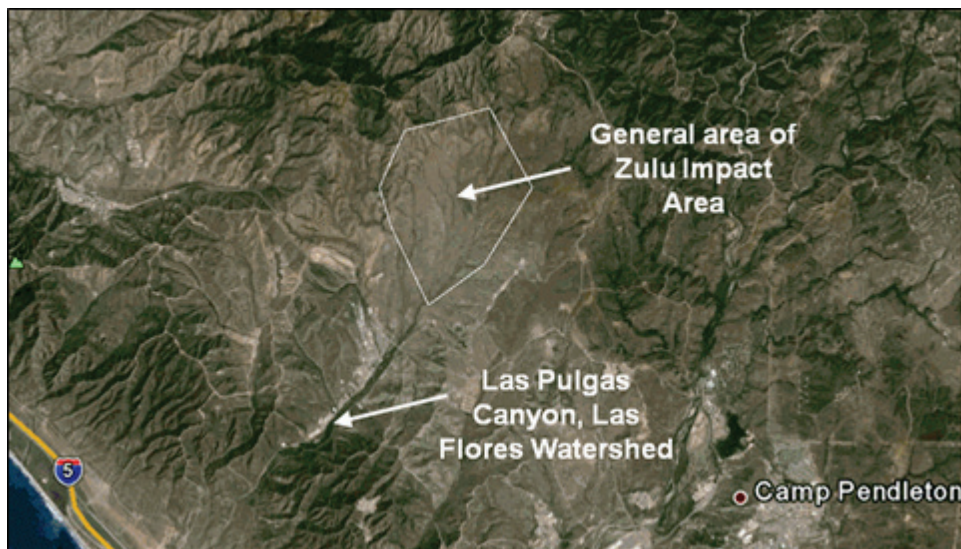


Figure 27. WSS-generated AOI and soil map within the cratered area of the ZIA as viewed in WSS.

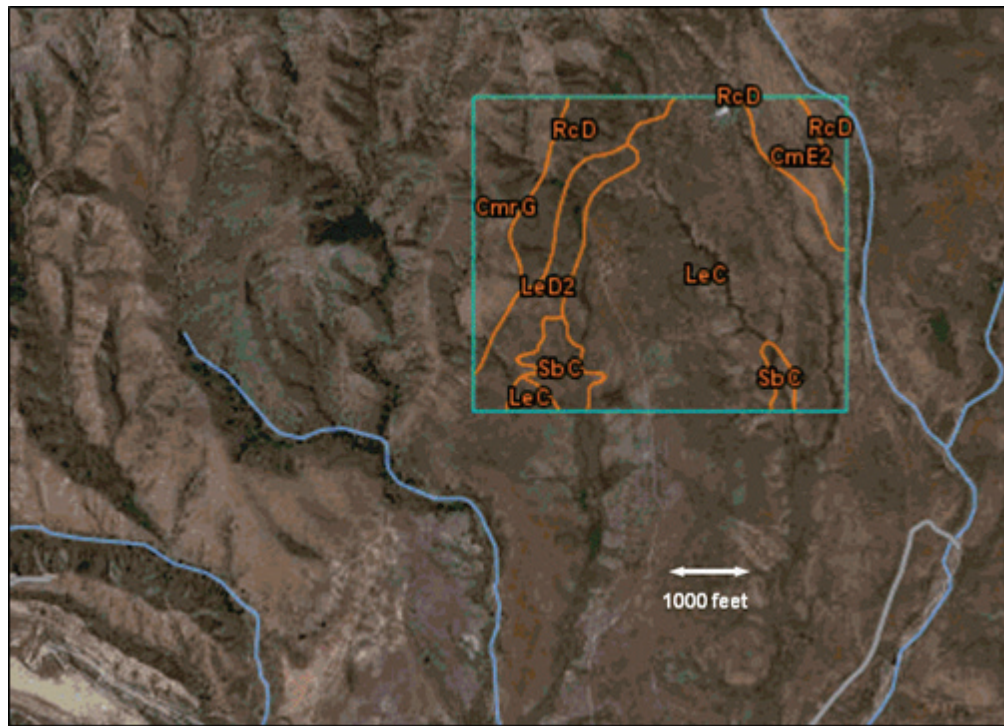
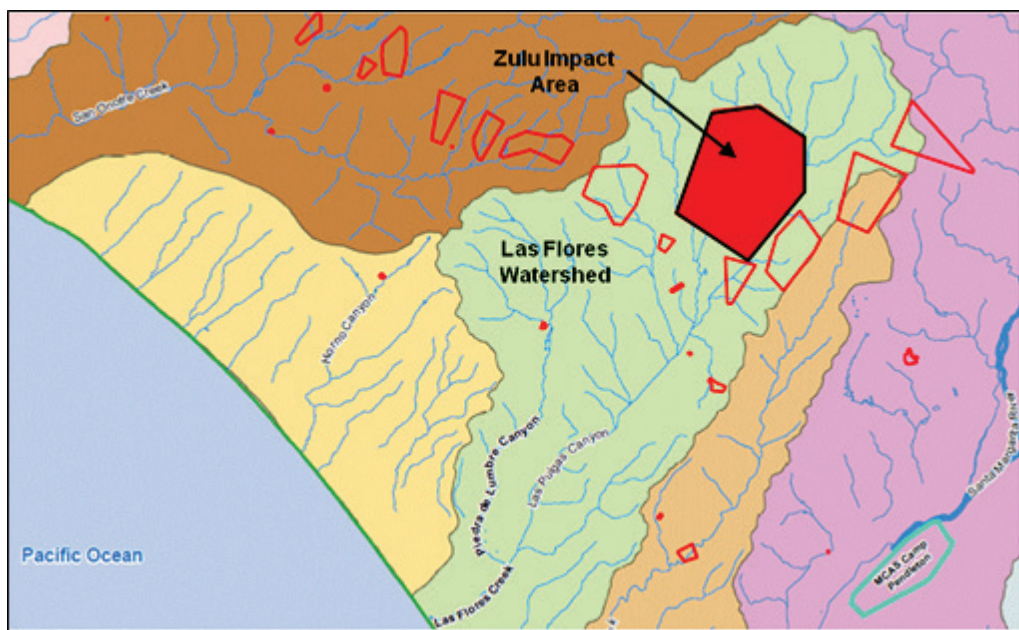


Figure 28. Las Flores watershed, stream network and ZIA (modified from AMP 2013).



The alluvial aquifers in the coastal plain area of the installation are the most important aquifers for REVA due to their connection with both surface water and the San Mateo aquifer. These alluvial deposits are located

in many of the deeply incised mountain valleys and consist of unconsolidated silts, sands, gravels, and conglomerates. The thicknesses of the alluvial aquifers vary from 18 to 105 feet, and the aquifers generally are thickest toward the center of the stream valleys. The alluvial aquifers are recharged by surface stream flow, and the San Mateo aquifer is recharged by the alluvial aquifers. The San Mateo aquifer consists of coarse poorly sorted pebbly sand, and it is the major water producing aquifer of the Las Flores basin. There are four groundwater producing wells in the Las Flores watershed. The depth to groundwater in the Las Flores basin varies between 10 to 58 feet bgs, and the groundwater flow is in the southwest direction. The hydraulic gradient of groundwater in the Las Flores basis varies between about 0.08 in Las Pulgas canyon to about 0.01 near the coast with an average of about 0.068 (AMP 2013). The general Darcy flow velocity in the Las Flores basin groundwater is estimated to be about 22 cm/day based on information provided by AMP (2013). However, Darcy flow velocity may be much higher within the San Mateo aquifer of the Las Flores basin since the saturated hydraulic conductivity has been estimated to range between about 4,000 to 8,000 cm/day based on pumping tests (AMP 2013). With an approximate average gradient of 0.068, the Darcy flow velocity could range between about 269 to 567 cm/day in the San Mateo aquifer. These values are quite high and questionable. AMP (2013) further reports that the aquifer pore velocity was estimated to be about 92 cm/day. For sand porosity of 0.38, this pore velocity would result in a Darcy velocity of 35 cm/day and an associated saturated hydraulic conductivity of 515 cm/day. These latter values are far more reasonable.

Loading rates of residue MC mass were estimated during the REVA study (AMP 2013). The loadings for the Las Flores watershed including the ZIA are summarized in Table 6-22 of that study. These loading estimates are broken down into two time periods, baseline (1989–2005) and five year review (2006–2011). Only the ZIA loading estimate was performed for the baseline period, and the average annual RDX loading estimated for ZIA during that period was 9,708 g/yr. The average annual RDX loadings estimated for the five year review period for all ranges in the Las Flores watershed and for only the ZIA were 75,269 and 60,894 g/yr, respectively. Thus, the ZIA contributed 81% of the estimated RDX loadings within the Las Flores watershed. There is a tremendous difference in RDX mass residue loading for the baseline and five year review periods, and the full reasons for this difference are not readily available. It is known that Range 108, which is within the Las Flores watershed, became the primary explosives

ordnance disposal (EOD) demolition range for the installation in 2009. However, this does not explain why the RDX residue mass loading for the ZIA increased more than six fold between the baseline and five year review periods. It is noted that the RDX loading density within the ZIA increased by a factor of three between the baseline and five year review periods from 3.01E-6 to 9.81E-6 kg/m<sup>2</sup> (AMP 2013). Additionally, the assumed MC loading area of the ZIA doubled from three to over six million square meters from the baseline to five year review periods (AMP 2013). These increases explain the six fold increase in RDX mass loading for the ZIA, but the reasons for the increases in loading density and MC loading area were not explained by AMP (2013).

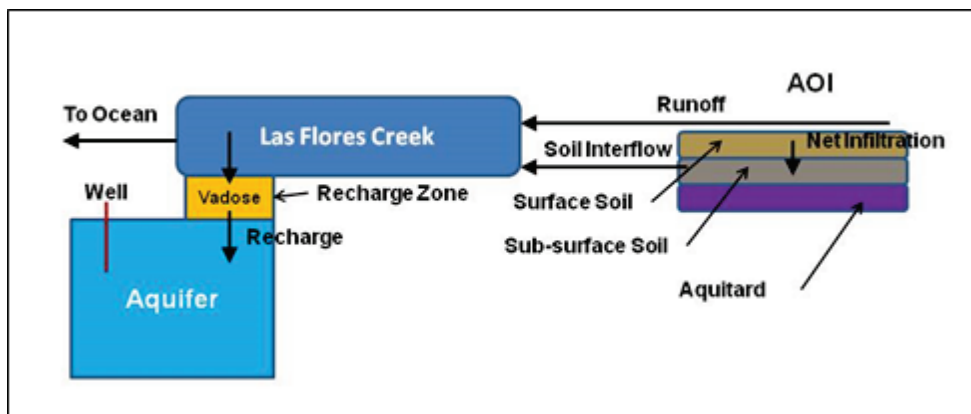
## 8.2 Model inputs for validation

The HE RDX is the primary MC of interest in this application, and the application focused on soil, surface water, and groundwater media. The AOI for this site is located over the dud producing portion of the ZIA within the Las Flores watershed. Although there are contributions of RDX from other ranges within this watershed, the ZIA is by far the greatest contributor. Also, given the expanded REVA-estimated RDX residue loading rates within this watershed for 2006–2011 and the questions associated with that increase, it did not seem beneficial to include other sources of RDX.

The hydrology of this region presents a modeling challenge. The ZIA sits above basement rock that is close to the land surface thus greatly limiting groundwater recharge at that location. The CSM for the Las Flores watershed developed for the REVA by AMP (2013) suggests that the primary pathways for AOI MC residue are overland flow and soil interflow to ephemeral streams that transport MC down to the coastal plain where groundwater recharge to the alluvial aquifer occurs. In previous TREECS™ applications, MC migration to groundwater occurs below the AOI rather than farther downstream, so the downstream recharge aspect presented a unique challenge.

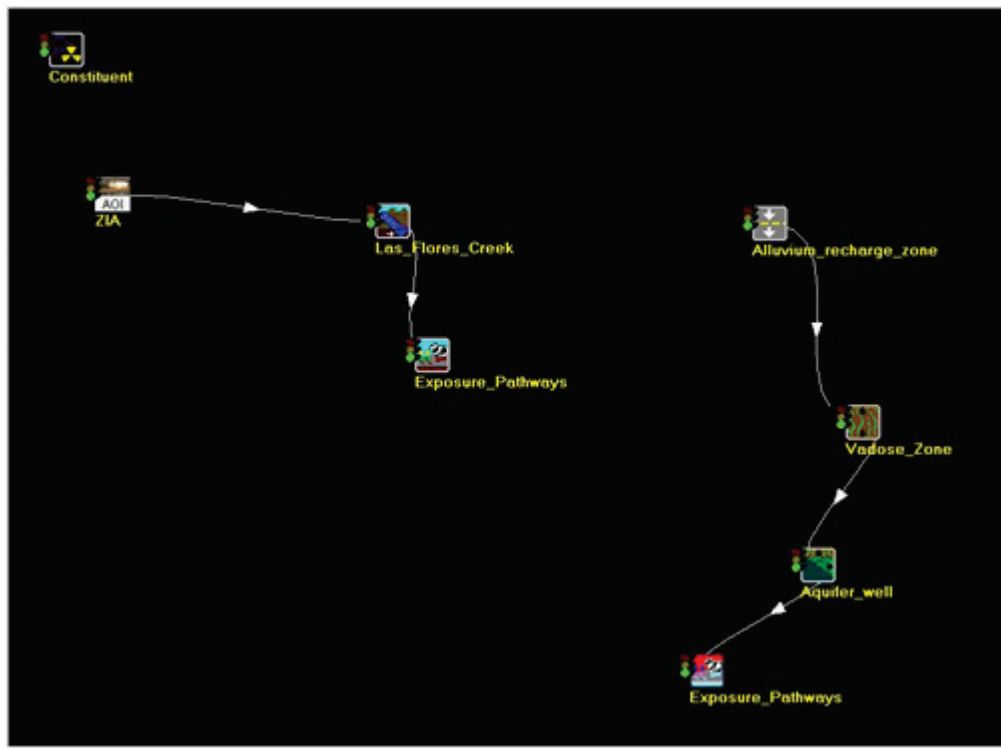
The modeling CSM for this study is presented in Figure 29. As shown by this CSM, net infiltration transitions to soil interflow rather than percolation to deeper groundwater, eventually discharging to Las Flores Creek. Creek water flow, which consists of runoff and soil interflow, travels to the coastal plain where a portion becomes recharge to the Las Flores alluvial aquifer, and the remainder discharges to the ocean.

Figure 29. Modeling CSM for ZIA and receiving waters, Camp Pendleton, CA.



Modeling the AOI soils of the ZIA and the receiving stream, which is Las Flores Creek, is straight forward within TREECS™. The Tier 2 soil model is required for the AOI soils, and the CMS is recommended for the stream. However, modeling the groundwater recharge from the lower reaches of the stream is problematic since TREECS™ presently does not have the capability to allow groundwater recharge from a modeled stream reach. Such a capability could be added, but this would require significant modifications to CMS, as well as additional manipulation of its output. The work-around approach called for using the Advanced Tier 2 option in TREECS™. In this approach, the soil model and the stream models were directly linked. In order to model groundwater recharge and migration of RDX from the stream to the aquifer, output from the CMS were gathered, processed, and entered into the User Defined Module for Vadose Water Flux File (WFF). The Vadose WFF module was linked to the MEPAS vadose zone model, which was linked to the MEPAS aquifer model. This approach for the CSM as set up under Advanced Tier 2 is shown in Figure 30.

Figure 30. CSM as modeled in TREECS™ with Advanced Tier 2 option.



### 8.2.1 Soil model inputs

The ZIA has a surface area of approximately 6.2E6 m<sup>2</sup> (AMP 2013). Thus, the AOI area was set to this value, and the square root of this area was used to set the length and width of the AOI to 2,490 m each. Since the REVA study (AMP 2013) provided estimates of RDX residue mass loading for the ZIA, the general source zone loading module of TREECS™ was used rather than the impact zone module that uses the TREECS™ munitions loading estimator. Based upon the REVA study estimates, the RDX mass residue loading rate was set to 9,708 g/yr for 63 years (1943–2005), and to 60,894 g/yr for the remaining 37 years (2006–2042) of the 100-year simulation. Zero soil concentration of RDX was assumed at the beginning of the simulation.

The AOI soils were described by the LeC class, which is loamy fine sand with a mixture of 87, 7, and 6% sand, silt, and clay, respectively, with 0.75% organic matter. The HGCT provided soil property estimates for loamy sand texture as follows:

- porosity = 43.7%

- field capacity = 12%
- dry bulk density = 1.49 g/cm<sup>3</sup>
- saturated hydraulic conductivity,  $K_{sat}$  = 164 cm/day

The above HGCT-generated soil properties were used in the Tier 2 soil model. The HGCT  $K_{sat}$  of 164 cm/day agrees reasonably well with the value of 240 cm/day obtained from WSS for LeC soil. The water capacity of 0.09 cm/cm reported from WSS in the previous section is the amount of water the soil can store that is available for plant use, which is the water held between field capacity and the wilting point; thus, the wilting point should be around 3%.

AMP (2013) recommended a runoff coefficient of about 0.5. However, the HGCT uses the SCS curve number (CN) method for computing runoff. The SCS guidelines for arid and semi-arid range lands indicate that the CN should be roughly 85 for soil group D in fair condition.

A search of meteorological data for the region was conducted (<http://www.ncdc.noaa.gov/cdo-web/search>) using the National Centers for Environmental Information (NCEI) of the National Oceanic and Atmospheric Administration (NOAA). The only stations in relatively close proximity to the installation are Camp Pendleton (station GHCND:USW00003154) and Oceanside Marina (station GHCND:USC00046377). Daily maximum and minimum air temperatures and daily precipitation data were downloaded for the two stations. The earliest available year of data for the Camp Pendleton station was 1967; thus, daily data for the years 1967 through 2014 were downloaded. Daily data for 1950 through 2014 were downloaded for the Oceanside Marina station. The Camp Pendleton station is about the same elevation and distance from the ocean as the ZIA, while Oceanside Marina is closer to the ocean and cooler and drier. Although the Camp Pendleton station is more representative of conditions at the ZIA, the data for that station are too sparse with too many data gaps to be used directly. Therefore, meteorological data processing was required to generate data that is representative of the ZIA.

The overall meteorological processing approach was to use Oceanside data translocation for Camp Pendleton station, which is assumed to represent the ZIA. The first step in this approach was to fill data gaps within the Oceanside Marina data. This was accomplished by using monthly averaged data for the period of record for the days that were missing data. HGCT requires daily maximum and mean air temperatures. The minimum and

maximum air temperatures each day were averaged to provide an estimate of daily mean air temperature. The Oceanside marina data were next paired with the Camp Pendleton data for the same dates and statistical analyses were conducted. These analyses indicated that a suitable translocation approach was to scale the Oceanside daily precipitation by a factor of 1.28 to generate the appropriate Camp Pendleton (ZIA) values. Translocation of air temperatures involved adding 1.1 °C and 3.9 °C to the mean and maximum daily air temperatures, respectively, to produce the Camp Pendleton, or ZIA, values from Oceanside data.

The final ZIA meteorological data consisted of daily values of precipitation and mean and maximum air temperature for every day in the period 1950–2014. The mean annual precipitation of this record is 12.96 inches/year compared to 12.52 inches/year, which is the mean annual precipitation for the Camp Pendleton station for its period of record. The mean and maximum annual average air temperature for the processed record is 16.96 and 23.75 °C, respectively, compared with 17.05 and 23.44 °C for the Camp Pendleton station period of record. Thus, the processed record was deemed suitable to use at the ZIA and was used as an input file for the HGCT to generate information for hydrology and erosion.

The 65 years of meteorological data were used within HGCT along with the site latitude of 33.37 degrees north and CN of 85 to generate average annual hydrologic information. The HGCT hydrology output consisted of the following average annual values:

- precipitation (all rainfall) = 0.3292 m/yr (12.96 in/yr)
- runoff = 0.1034 m/yr (4.07 in/yr)
- net infiltration = 0.0297 m/yr (1.17 in/yr)
- evapotranspiration (ET) = 0.1963 m/yr (7.73 in/yr)
- number of rain days = 49.2
- mean air temperature = 16.96 °C
- soil volumetric water content = 5%.

Net infiltration is the same thing as percolation, or the depth of water per year penetrating through the soil layer after deducting runoff and ET. Percolation rate is groundwater recharge rate at steady-state. The above HGCT hydrology output was used in the Tier 2 soil model applied for average annual hydrology mode. Within the soil model inputs, 100% of the infiltration was set to return to stream flow via soil interflow.

The USLE was applied within the HGCT to generate the AOI average annual soil erosion rate. The input parameters for the USLE were:

- rainfall factor R = 35
- soil erodibility factor K = 0.17
- slope = 0.06 m/m
- length-slope-gradient factor LS = 1.335
- crop management factor C = 0.25
- conservation practice factor P = 1.0.

The values for K and slope were obtained from WSS as described previously. The values of R, C, and P are the same as those used in the REVA modeling (AMP 2013). The value of LS is computed by HGCT for a maximum allowable slope length of 400 feet. The value of 1.0 for P is the default for impact ranges. The above inputs were used without the sediment delivery ratio option to produce an erosion rate of 2.99E-4 m/yr compared to 8.57E-4 m/yr computed by the REVA modeling (AMP 2013), which used a value of 0.37 for K. The erosion rate of 2.99E-4 m/yr was used in the Tier 2 soil model.

Tier 2 soil model default values of 0.4 m and 17.96 °C (average annual air temperature plus one degree C) were used for active soil layer thickness and average annual soil-water matrix temperature, respectively. Tier 2 soil model UI default values of 0.005 m, 0.4 kg/L, and 0.4 m were used for soil exchange layer thickness for rainfall extracted pore water, soil detachability for rainfall extracted pore water, and diffusion layer thickness for volatilization, respectively.

A tool within the Tier 2 soil model UI was used to estimate the AOI soil  $K_d$  value of 0.079 L/kg for RDX using input of loamy sand with an organic matter content of 0.75 %. No degradation (i.e., half-life of 1E20 years) of RDX in soil was assumed. The initial particle size of RDX solid phase residue was set to 12,000  $\mu\text{m}$  based on guidance with the UI help section. Residue particle shape was assumed to be spherical. The value for the diffusion coefficient of RDX vapor in air of 0.632  $\text{m}^2/\text{day}$  was obtained from the ARCDB. Using this value, the volatilization mass transfer rate of RDX vapor from soil was computed by the UI to be 122.4 m/yr.

The solubility of RDX in water of 41.03 mg/L was computed by the UI based on the soil-water matrix temperature of 17.96 °C. RDX property values for HLC, molecular weight, and solid phase density of 6.32E-8 atm-

$\text{m}^3/\text{mol}$ , 222 g/mol, and 1.8 g/cm $^3$ , respectively, were provided by the ARCDB.

The constant time step solution option was used with a time step of 0.001 year. Inputs for the Tier 2 soil model are summarized in Table 17.

**Table 17. Tier 2 soil model input values for Zulu impact area, Camp Pendleton, CA.**

Input Description	Value
Site Characteristics	
AOI dimension that is parallel to the groundwater flow, m	2490
AOI dimension that is perpendicular to the groundwater flow, m	2490
AOI surface, m $^2$	6.2E6
Active soil layer thickness, m	0.4
Average annual temperature of soil-water matrix, °C	17.96
MC mass residue loading versus time, g/yr	9,708 constant for first 63 years 60,894 Constant for next 37 years
Initial solid phase MC concentration in soil on a soil mass basis at time 0, mg/kg	0 for all constituents
Initial total non-solid phase MC concentration in soil on a soil mass basis at time 0, mg/kg	0 for all constituents
Soil Properties	
Volumetric soil moisture content, percent	5
Soil dry bulk density, g/cm $^3$	1.49
Soil porosity, percent	43.7

Input Description	Value
<b>Hydrology</b>	
Average annual precipitation, m/yr	0.3292
Average annual rainfall, m/yr	0.3292
Average annual soil erosion rate, m/yr	2.99E-4
Average annual water infiltration rate (groundwater recharge for no interflow), m/yr	0.0297
Average annual surface water runoff rate, m/yr	0.1034
Percent of annual water infiltration flow rate and mass flux that goes to soil interflow, fraction	100
Average number of rainfall events per year	49.2
<b>Fate/Transport Parameters for RDX</b>	
Soil exchange layer thickness for rainfall ejection of pore water, m	0.005
Soil detachability for rainfall ejection of pore water, kg/L	0.4
Diffusion layer thickness for volatilization, m	0.4
Soil-water constituent partition coefficient, $K_d$ , L/kg	0.079
Decay/degradation half-life of liquid (water) phase constituent, yrs	1.0E20
Decay/degradation half-life of adsorbed (particulate) phase constituent, yrs	1.0E20

Input Description	Value
Initial mean diameter of solid phase constituent residue particles (assume spherical particles), $\mu\text{m}$	12,000
Volatilization rate, m/yr	122.4 as computed by soil model user interface from molecular diffusivity in air
Switch for solid phase erosion	off
Chemical-Specific Properties for RDX	
Aqueous solubility limit, mg/L	41.03 (based on average annual soil temperature of 17.96 deg C)
Henry's law constant, atm- $\text{m}^3/\text{g}\cdot\text{mol}$	6.32E-8
Molecular weight (molar mass or averaged molecular mass), g/mol	222.12
Solid phase constituent mass density, g/ $\text{cm}^3$	1.8
Model Options	
Time length of simulation, yrs	100
Time step, yrs	0.001
Methods used for equation solution	Constant time step

### 8.2.2 Stream model inputs

The stream flow distance along Las Flores Creek from the proximity of the AOI (i.e., ZIA) to the general recharge area of the coastal plain is about 8,000 m. This distance was segmented into 50 computational cells within the CMS UI. Thus, each cell was 160 m long. There was no information regarding width and depth of Las Flores Creek, so Google™ Earth was used to estimate the width of about 4 m. The average stream depth of 0.86 m was calculated from Manning's equation using the 4 m width, the average annual flow rate of 0.295  $\text{m}^3/\text{sec}$  (10.43 ft<sup>3</sup>/sec), stream bed slope of 0.01,

and Manning's roughness coefficient of 0.045. The bed slope was estimated from Google™ Earth using ground elevations and the distance measuring tool. The average annual stream flow rate was estimated using the precipitation depth that contributes to stream flow of 0.133 m times the Las Flores watershed area of 7.0E7 m<sup>2</sup> and converting the result from cubic meters per year to cubic meters per second. The precipitation depth that contributes to stream flow is the sum of the average annual runoff depth of 0.103 m and infiltration depth of 0.03 m, which returns to surface flow via soil interflow.

The simulation period was set to 100 years, and a time step of 0.1 year was used. The stream longitudinal dispersion coefficient was set to 0.1 m<sup>2</sup>/sec, a typical value for small streams. In the absence of observed data, the stream average TSS concentration was assumed to be 10 mg/L. The active benthic sediment layer thickness, the sediment particle density, and the active benthic layer sediment porosity were set to the default values of 0.1 m, 2,650 g/L, and 0.7, respectively. The TSS and benthic sediment fraction of organic carbon were both set to 0.0035, which is about half of the organic matter content of AOI soils. The average annual water temperature was set to 17 °C, and the average annual wind speed was set to 5 m/sec.

Initial and background stream concentrations of RDX were set to zero, and all RDX degradation rates were also set to zero. The octanol-water partition coefficient of 7.41 mL/mL, which was provided to the CMS UI by the ARCDB, was used by the UI to compute the TSS and benthic sediment partition coefficients of 0.016 L/kg. The UI-computed volatilization rate of 0.0012 m/day and mass transfer coefficient for pore-water and water column diffusion of 0.0036 m/day were used. The molecular weight, molecular diffusivity in water, and HLC of 222.1 g/mol, 7.07E-6 cm<sup>2</sup>/sec, and 6.32E-8 atm-m<sup>3</sup>/g-mol, respectively, were used as provided by the ARCDB.

The benthic sediments were assumed to be in depositional equilibrium. Thus, the sediment burial rate was set to essentially zero (1E-20 m/day). The TSS settling rate was set to 0.5 m/day, which is a value that is typical of fine sediments. The resuspension rate of 6.29E-6 m/day was computed by the CMS UI from a steady-state solids balance for the benthic layer. The CMS inputs are summarized in Table 18.

Table 18. CMS input values for Las Flores Creek, Camp Pendleton, CA.

Input Description	Value
Number of computational segments, unit-less	50
Time step, yr	0.1
Total simulation time, yr	100
Longitudinal dispersion coefficient, m <sup>2</sup> /sec	0.1
TSS concentration in stream, mg/L	10.0
Depth of active sediment layer, m	0.1
Dry sediment particle density, g/L	2,650
Sediment porosity, unit-less	0.7
Fraction organic carbon in water column TSS, unit-less	0.0035
Fraction organic carbon in bed sediment, unit-less	0.0035
Average annual water temperature, deg C	17
Average annual wind speed, m/sec	5
Distance from entry point of AOI loads or confluence to end of model reach, m	8,000
Stream reach average width, m	4.0
Stream reach average depth, m	0.86
Stream reach average flow rate, m <sup>3</sup> /sec	0.295
Background and initial stream concentrations, mg/L	0
Decay rates for various phases, per day	0
RDX $K_{ow}$ , mL/mL	7.41
UI computed partitioning distribution coefficient for adsorption of RDX to water column TSS, $K_d$ , L/kg	0.016
UI computed partitioning distribution coefficient for adsorption of RDX to bed sediment, $K_d$ , L/kg	0.016

Input Description	Value
Volatilization rate, m/day	0.0012
Mass transfer velocity between sediment pore water and water column, m/day	0.0036
Molecular weight of RDX, g/mole	222.1
Molecular diffusivity of RDX in water at 25 deg C, cm <sup>2</sup> /sec	7.07E-6
Henry's Law constant of RDX, atm-m <sup>3</sup> /g-mole	6.32E-8
TSS settling rate, m/day	0.5
Sediment burial rate, m/day	1E-20
Sediment resuspension rate, m/day	6.29E-6

### 8.2.3 Groundwater modeling inputs

The User Defined Known WFF module was used to set input fluxes for water recharge rate (m<sup>3</sup>/yr) and RDX mass loading rate (g/yr) in recharge water. The RDX mass loading rate from stream to vadose zone was based upon output from the CMS of Las Flores Creek at the downstream terminus, which is the groundwater recharge zone. In addition to computing stream water column and benthic sediment concentrations of contaminant, the CMS also computes and outputs stream mass loads (also referred to as mass flux) of contaminant (mass/time). This output was adjusted to provide input mass loads (i.e., mass flux) into the vadose zone model.

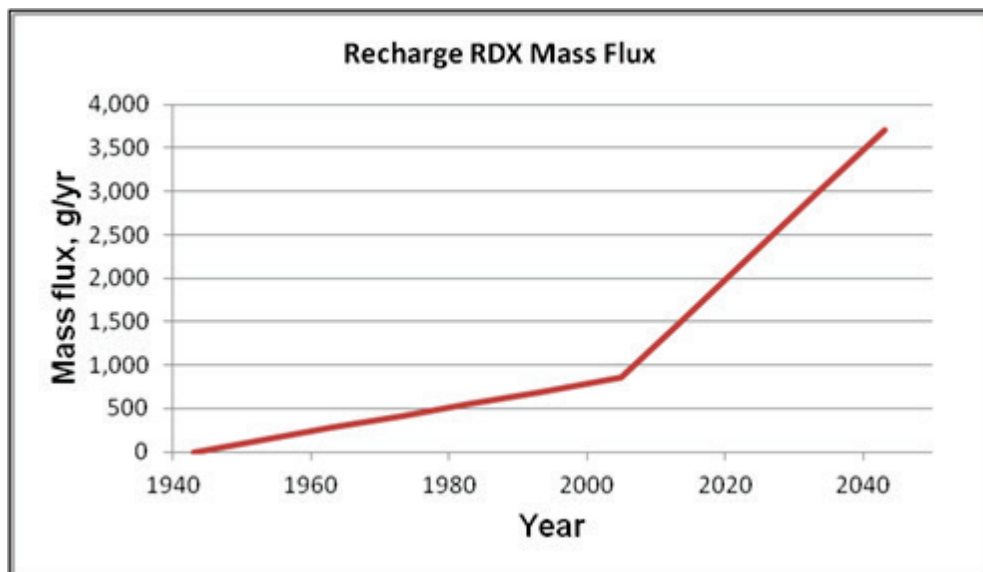
The planar dimensions of the recharge zone had to be specified within the WFF module. The dimensions of the flux plane, which were estimated using Google™ Earth, were set to a length of 3,000 m along the Las Flores Creek flow axis with a width of 100 m across the creek channel. The 3,000 m length is the approximate distance between the end of the foothills (beginning of the coastal plain) and Interstate 5. The width of 100 m is a rough order of magnitude estimate.

The recharge flow rate (cubic meters per year) is another input for the WFF module. The average annual water recharge rate in the coastal plain has been estimated to be about 0.058 m/yr (AMP 2013). This recharge rate is 44 % of the estimated average annual precipitation of 0.133 m/yr

contributing to stream water discharge. For the validation run, the recharge flow rate was set to 4.05E6 m<sup>3</sup>/yr, which is the product of the average annual creek flow rate of 9.31E6 m<sup>3</sup>/yr times the scaling factor of 0.44, the ratio of the average annual precipitation depths contributing to recharge and stream discharge. The mass flux of RDX delivered over time as recharge into the vadose zone is the final set of inputs required by the WFF module. For the validation run, these values were set equal to the RDX mass fluxes computed by the CMS at its terminus times the same scaling factor 0.44. The computed RDX mass recharge fluxes are shown in Figure 31.

The vadose zone soil was set to sand in the MEPAS vadose zone model with an organic matter content of 0.1 %. The model UI was used to establish inputs of 38 % for porosity, 9 % for field capacity, 570 cm/day for saturated hydraulic conductivity, and 1.64 g/cm<sup>3</sup> for dry bulk density. The organic matter content was an assumed value with the justification that the value should be much lower than that of surface soil. The thickness of the vadose zone was set to 6.5 m based on inputs used for the REVA aquifer modeling (AMP 2013). The vertical dispersivity for the vadose zone was set to 0.065 m, which is the recommended default value (1/100 of vadose zone thickness). The soil-water  $K_d$  for the vadose zone was computed by the model UI as 0.019 L/kg. The RDX half-life was set to 1E20 days (assuming no degradation), and the RDX solubility was automatically set to 59.7 mg/L based on the ARCDDB value at 25 °C.

Figure 31. Computed RDX mass flux in recharge into the Las Flores aquifer.



The aquifer soil was also assumed to be sand with 0.1 % organic matter, and the MEPAS aquifer model UI was used to establish inputs of 38 % for porosity and 1.64 g/cm<sup>3</sup> for dry bulk density. The effective porosity was set to 25 %, same as the value used in REVA modeling (AMP 2013).

An estimate of the Darcy flow velocity of 25.6 cm/day was obtained from the product of the saturated hydraulic conductivity of sand (570 cm/day) and the average water table slope between Las Flores Canyon and the coast of 0.045 (AMP 2013). This Darcy velocity is consistent with estimated pore velocities reported by AMP (2013) of 0.0021 ft/min (92 cm/day) and effective porosity of 25 %, which yield a Darcy velocity of 23 cm/day. The aquifer thickness was assumed to be 20 m based on information provided by AMP (2013).

If the estimated recharge flow rate of 4.05E6 m<sup>3</sup>/yr is divided by a recharge area of 300,000 m<sup>2</sup>, the recharge rate for this area is 13.5 m/yr, which is certainly feasible with a saturated hydraulic conductivity of 570 cm/day (2,080 m/yr). A Darcy flow velocity of 19 cm/day was computed by dividing the recharge water flow of 4.05E6 m<sup>3</sup>/yr by a flow area of 60,000 m<sup>2</sup> (based on a width of 3,000 m and aquifer average thickness of 20 m) and dividing the result by 365 days per year to convert time units from years to days. This Darcy velocity of 19 cm/day is not far out of line with the values estimated above of 25.6 and 23 cm/day. A Darcy velocity of 19 cm/day and saturated hydraulic conductivity of 570 cm/day yield a groundwater hydraulic gradient of 0.032, which is fairly close to the average value of 0.045 cited by AMP (2013) for the Las Flores coastal plain aquifer. For the model validation, the Darcy velocity was set to 25.6 cm/day to be consistent with the reported average hydraulic gradient and saturated hydraulic conductivity. It is suspected that there are other potential sources of Darcy flow besides the recharge zone of Las Flores Creek.

The longitudinal distance from the flux zone to the monitoring well was set to 322 m (1056 ft), which is the distance used in the REVA modeling (AMP 2013). Without the benefit of knowing the exact well location, the monitoring well was assumed to lie along the centerline of the plume, and the depth of the well intake was assumed to be at half of the aquifer thickness, or 10 m below the water table; thus, the lateral and vertical distances for the well were set to zero and 10 m, respectively. Testing showed that well concentrations of RDX did not change for this application with variations in these two inputs. The reason for this is due to the relatively large width

of the source zone (3,000 m) and the relatively small aquifer thickness (20 m). The longitudinal, transverse, and vertical dispersivity were set to the default values computed by the model UI of 32.2, 10.6, and 0.08 m, respectively. Sensitivity testing revealed that results were not very sensitive to the dispersivity values for these site conditions. The values for  $K_d$ , solubility, and half-life of RDX in the aquifer were the same as those used for the vadose zone. Inputs for the MEPAS vadose and aquifer model inputs are summarized in Table 19 and Table 20, respectively.

**Table 19. MEPAS vadose zone model inputs for Las Flores aquifer, Camp Pendleton, CA.**

Input Description	Value
Inputs passed from soil model	
AOI dimension that is parallel to the groundwater flow, m	100
AOI dimension that is perpendicular to the groundwater flow, m	3000
Water flow rate due to net infiltration (recharge), m <sup>3</sup> /yr	9.31E6
MC mass flux versus time due to leaching into vadose zone, g/yr	Time-varying, see Figure 31
Soil Composition	
Percentage of sand, %	91.9
Percentage of silt, %	5
Percentage of clay, %	3
Percentage of organic matter, %	0.1
Percentage of iron and aluminum, %	Unknown, set to 0
Soil Characteristics	
pH of pore water, pH units	7
Total porosity, %	38
Field Capacity, %	9
Saturated hydraulic conductivity, cm/day	570
Thickness of the vadose zone layer, m	6.5

Input Description	Value
Longitudinal (vertical direction) dispersivity, cm	0.065
Dry bulk density, g/cm <sup>3</sup>	1.64
Constituent Properties for RDX	
Sorption partitioning coefficient, $K_d$ , ml/g	0.019
Water solubility of constituent, mg/L	59.7
Half-life of constituent in groundwater, days	1E20

Table 20. MEPAS aquifer model inputs for Las Flores aquifer, Camp Pendleton, CA.

Input Description	Value
Inputs passed from vadose zone model	
AOI dimension that is parallel to the groundwater flow, m	100
AOI dimension that is perpendicular to the groundwater flow, m	3000
Water flow rate due to percolation (groundwater recharge), m <sup>3</sup> /yr	9.31E6
MC mass flux versus time due to percolation from the vadose zone to the aquifer, g/yr	Time-varying
Composition	
Percentage of sand, %	91.9
Percentage of silt, %	5
Percentage of clay, %	3
Percentage of organic matter, %	0.1
Percentage of iron and aluminum, %	Unknown, set to 0
Sub-surface Characteristics	
Percentage of constituent flux entering the aquifer, %	100
pH of the pore water, pH units	7
Total porosity, %	38
Effective porosity, %	25
Darcy velocity, cm/day	25.6
Thickness of aquifer, m	20

Input Description	Value
Soil dry bulk density, g/cm <sup>3</sup>	1.64
Concentration (well) Locations	
Longitudinal distance to well, m	322
Perpendicular distance from plume center-line to well, m	0.0
Vertical distance below water table to well intake, m	10.0
Longitudinal dispersivity, m	32.2
Transverse dispersivity, m	10.6
Vertical dispersivity, m	0.08
Constituent Properties for RDX	
Sorption partitioning coefficient, $K_d$ , ml/g	0.019
Water solubility, mg/L	59.7
Half-life of constituent in groundwater, days	1E20

### 8.3 Validation results

TREECS™ was applied for the model inputs described in the previous section. The computed stream concentration of RDX at the stream terminus (i.e., the recharge zone) after 70 years, which corresponds to 2012, was 0.29 ppb. Practically all of the RDX concentration was dissolved. An observed concentration of 0.28 ppb was estimated based on laboratory analysis above the detection limit of a sample collected in lower Las Flores Creek on January 23, 2012 (AMP 2013). The fact that the model-computed and observed concentrations are so close is not totally impressive since concentrations for other stream samples were below detection, and it is believed that stream concentrations are highly variable and dependent on recent rainfall and stream flow conditions as discussed for the AIA application. However, the fact that the computed and observed values are so close is encouraging, especially given the discussion of coincident rainfall in the next paragraph. The computed and measured stream concentrations of RDX versus time are plotted in Figure 32.

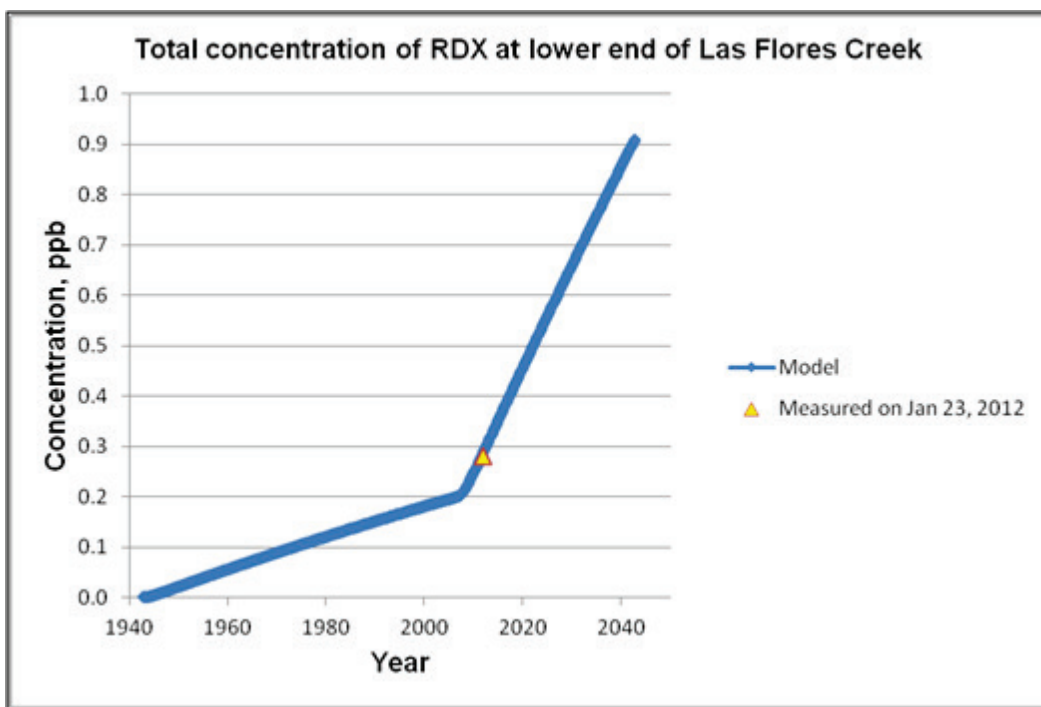
Stream samples were collected on three dates, September 26, 2011, January 23, 2012, and November 19, 2012. Rainfall rates for these dates were investigated, and the following was discovered. There was no rainfall on September 26, 2011, and it had not rained since July 31 prior to that date. There was substantial rainfall on and just before January 23, 2012, when

the observed RDX concentration was estimated to be 0.28 ppb. There were 0.33 inches of rainfall on January 21, zero rainfall on January 22, and 0.35 inches of rainfall on January 23, 2012. There was zero rainfall on November 18 and 19, 2012, but it did rain a trace of 0.08 inches on November 17, 2012. This pattern is similar to the pattern observed at Popolopen Brook, USMA, as discussed in the previous chapter, where stream concentrations of RDX were detected when there was substantial rainfall on and just prior to the sampling dates and below detection on dates when there had not been substantial rainfall. It seems only logical for RDX to be below detection when there has not been significant rainfall on and just prior to the sampling date.

The average rainfall per event for this site was estimated by dividing the average annual rainfall of 12.95 inches by the average number of rainfall events per year of 49.2, yielding 0.26 inches per event. It is interesting that the rainfall on January 23, 2012 of 0.35 inches is relatively close to the average rainfall per event of 0.26 inches. Thus, it may not be a random coincidence that the model-computed stream concentration of RDX is so close to the observed value on January 23, 2012. These results, along with those presented for Popolopen Brook, USMA, support the concept that TREECS™ applied with average annual hydrology predicts stream concentrations associated with average annual rainfall per rainfall event.

The computed RDX concentrations at the groundwater receptor well are plotted versus year in Figure 33. It is noteworthy how quick the receptor well concentrations respond to changes in RDX loadings into the AOI due to the short constituent travel times in the aquifer. With a pore velocity of 103 cm/day (25.6 cm/day Darcy velocity divided by effective porosity of 0.25), RDX can travel to the receptor well in 314 days. The computed RDX concentration at the receptor well in 2011 was 0.24 ppb. As reported by AMP (2013), RDX concentrations were below the detection limit for four out of five groundwater samples obtained and analyzed for RDX during 2011 and 2012. RDX was detected for one sample collected on October 24, 2011, and the concentration was estimated to be 0.09 ppb, which is a factor of 2.67 times smaller than the model-computed concentration in that year. The detection limit for RDX was not reported by AMP (2013), nor is there an explanation for why RDX would be detected in one sample when not detected in four others.

Figure 32. Computed and measured (via analytical estimation) concentration of RDX in Las Flores Creek down-gradient of the ZIA, Camp Pendleton, CA.

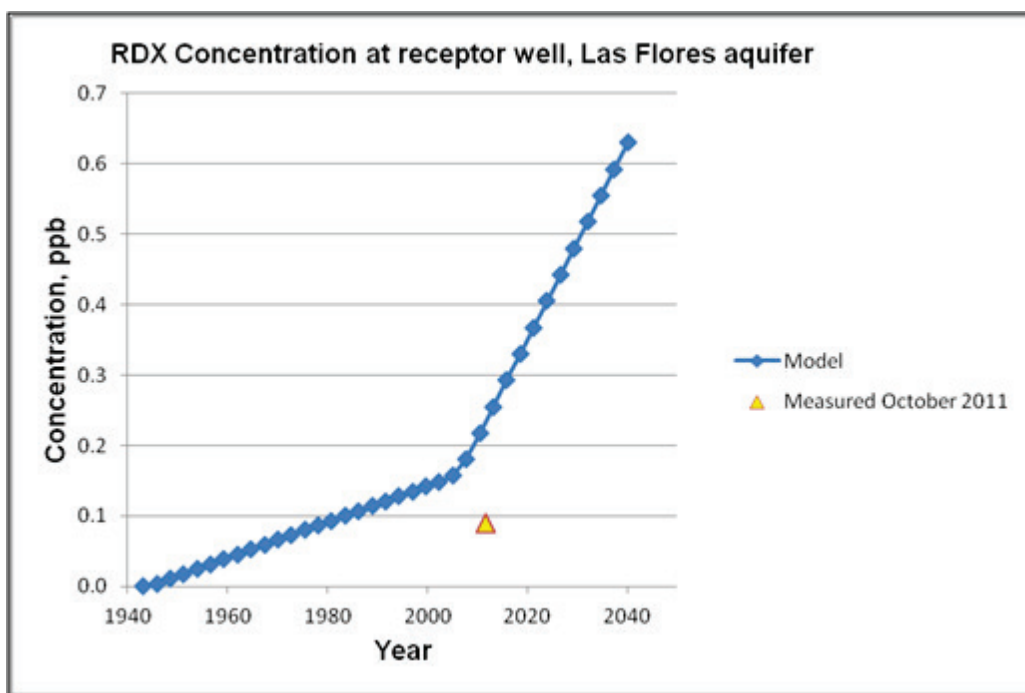


The factor of 0.44 used to scale the portion of Las Flores Creek flow and RDX mass flux that contributes to groundwater recharge is certainly uncertain, and aquifer RDX concentrations are highly sensitive to it. Aquifer concentrations are also sensitive to the width (i.e., the length along the creek flow axis) of the recharge flux plane as well as the Darcy flow velocity. The effects of these input variables will be assessed in the next section on uncertainty analysis. Any or all of these inputs could have been tuned to force model agreement with the one detected observation. However, such agreement is meaningless when four other observations were below detection. It is not stated in the AMP report (2013) where any of the observation wells are actually located, nor is it clear which samples are from what wells. An analysis of annual precipitation rates for the processed Camp Pendleton record revealed that 2010 was an unusually wet year with approximately 27 inches of rainfall for that year, more than double the estimated annual average. It is possible that a recharge pulse greater than the average could have resulted in well concentrations of RDX above detection during 2011.

Thus far, the model does not support the concept that there should not be any RDX above detection at the receptor well for average annual precipita-

tion and stream flow. The fact that four of five samples were below detection suggests that either the observation wells are not located along the RDX plume path resulting from creek recharge, or most of the creek water flow and RDX mass flux travel to the ocean with a much smaller amount diverted to groundwater recharge. Examination via Google™ Earth revealed that there is not a continuously open channel between Las Flores Creek and the ocean, which implies that all, or most, of the creek water does not travel to the ocean and should contribute to groundwater recharge.

Figure 33. Computed and measured concentration of RDX at receptor well, Las Flores aquifer, Camp Pendleton, CA.



As stated above, there was one sample from Las Flores Creek in January 2012 where the RDX concentration was above detection, and its estimated value was 0.28 ppb. The model-computed RDX concentration in the creek was 0.29 ppb in that year. The performance metrics *RR* and *RE* for evaluating model accuracy are 1.04 and 3.6 %, respectively, which is excellent. There was no prior rainfall for the other sampling dates when concentrations were below detection. This result supports the theory that there should be little or no RDX in the creek when there has not been recent significant rainfall.

The performance metrics *RR* and *RE* for evaluating model accuracy for the one detected aquifer concentration of RDX are 2.67 and 167 %, respectively. Although these metrics are fairly poor, it is noted that very close agreement with the observation could have been obtained by adjusting the flux plane width, the Darcy velocity, the proportion of water and RDX mass flux in the stream that diverts to groundwater recharge, or changes in all three of these inputs. The recharge flux plane dimensions and flux rates are poorly known and not easily measured. There is also the poor understanding of the locations of monitoring wells, particularly relative to recharge plume path.

#### **8.4 Uncertainty analysis**

Uncertainty analysis was conducted separately for the soil-stream models and the groundwater models. None of the RDX physicochemical properties are considered highly uncertain, except for degradation rate. Regarding the soil-stream models, all of the site-specific related inputs were fairly well known or estimated, including average annual stream flow rate due to the size and well defined boundaries of the Las Flores watershed. The only input that was particularly uncertain and potentially highly variable was the initial particle size of solid-phase RDX residue. Thus, the initial diameter of RDX particles was treated as uncertain using a normal distribution with a mean of 12,000  $\mu\text{m}$  and upper and lower bounds of 18,000 and 6,000  $\mu\text{m}$ , respectively. The standard deviation of the distribution was set to 2,000  $\mu\text{m}$ . Residue particle size affects solid phase dissolution rates.

The RDX degradation rate is also uncertain, but a sensitivity run with the soil aqueous dissolved half-life set to 10 years revealed essentially no effect on stream concentrations of RDX compared to no degradation. The degradation rate in the stream is of no consequence given the short transit time from AOI to stream terminus. Thus, degradation rates were not treated as uncertain.

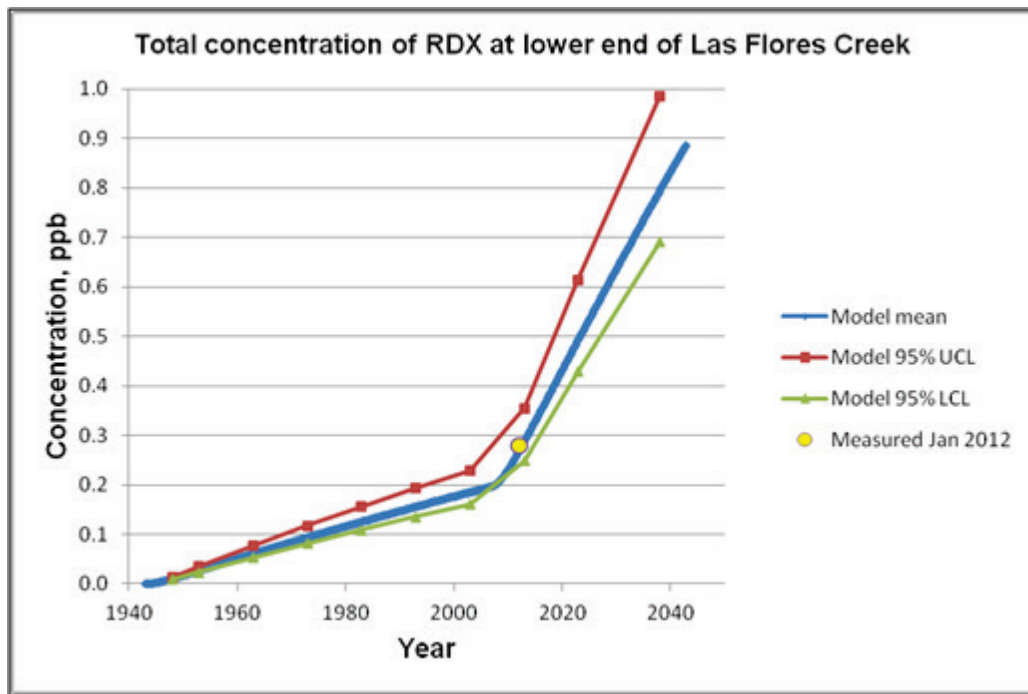
The results of the Monte Carlo simulation with the above uncertainty inputs are plotted in Figure 34 with the 95 % LCL and UCL included. As shown by the plot, the uncertainty of initial RDX residue particle size has a relatively minor influence on resulting stream concentrations of RDX.

The most uncertain and most sensitive of the groundwater model inputs were the water and RDX mass fluxes entering as recharge from Las Flores Creek and the width of the recharge plane (i.e., the length along the creek

flow axis). Additionally, results are relatively sensitive to Darcy velocity. Thus, these three sets of inputs were treated as uncertain. Degradation rates were not treated as uncertain due to the relatively short transit time from recharge zone to receptor well. A sensitivity run with a RDX half-life of 10 years in the vadose zone and aquifer revealed very little change in aquifer concentration of RDX compared with no degradation.

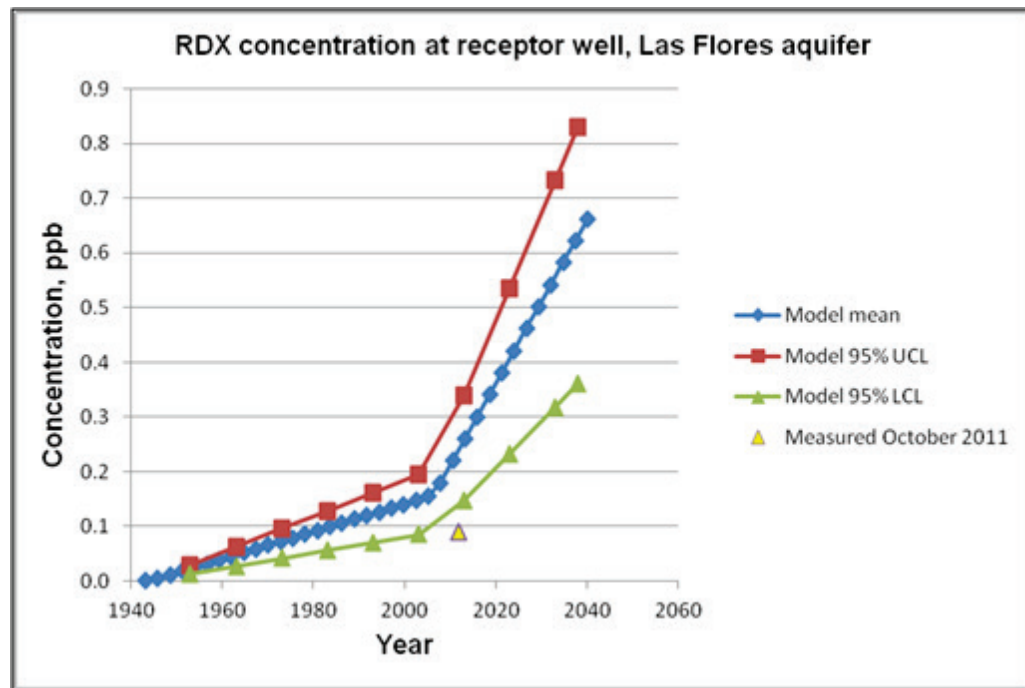
The width of the recharge flux plane was described with a normal distribution with a mean of 3,000 m, upper and lower bounds of 6,000 and 1,500 m, respectively, and standard deviation of 750 m. The Darcy velocity was also described with a normal distribution with a mean of 25.6 cm/day, upper and lower bounds of 35 and 15 cm/day, respectively, and standard deviation of 3.3 cm/day. A normal distribution was used for the recharge water flow rate ( $\text{m}^3/\text{yr}$ ) with a mean of 4.05E6, upper and lower bounds of 8E6 and 2E6, respectively, and standard deviation of 1E6. The RDX mass fluxes of recharge were scaled to the recharge water flow rate so that as recharge flow rate changed randomly during the Monte Carlo simulation, the RDX mass flux of recharge changed accordingly by a scaling factor. The scaling factor increased with time due to the buildup and wash off of RDX in the AOI. Thus, pairs of time in years and scaling factor had to be entered into the uncertainty module's *Equation* option for relating RDX flux to randomly generated water flux. The scaling factor in a given year was constant for each annual recharge flow rate.

Figure 34. Computed and measured concentration of RDX in lower end of Las Flores Creek down-gradient of the ZIA, Camp Pendleton, with 95% UCL and LCL for uncertainty on initial mean particle diameter of RDX residue.



The results of the Monte Carlo simulation for receptor well RDX concentration are plotted in Figure 35 versus year with 95 % UCL and LCL concentrations and measured concentration included. The 95 % confidence bands do not quite capture the measured value. Given the rather liberal extents of the distributions for uncertain variables, these results tend to support the concept that perhaps the receptor wells are not in the direct path of the recharging RDX plume.

Figure 35. Computed and measured concentration of RDX at receptor well in Las Flores aquifer down-gradient of the ZIA, Camp Pendleton, with 95% UCL and LCL for uncertainty on recharge fluxes, flux plain width and Darcy velocity.



## 8.5 Fate of emerging MC (EC) associated with IM

The five ECs DNAN, NTO, NQ, AP, and CL-20 were selected within the TREECS™ validation application of Las Flores watershed, Camp Pendleton, for evaluating their fate relative to that of RDX in the Las Flores aquifer. The inclusion of these five additional constituents in the application required specifying their physicochemical properties, which are not known as well as are those of RDX. As with the previous applications, the EPI Suite component of CTS was used to provide some of the properties information for the five EC, such as HLC and  $K_{oc}$  values. The MC residue loading rate for each EC was set to the same rates as used for RDX. Besides specifying the physicochemical properties and the partitioning distribution coefficients for each EC, the only other additional input that was required was the degradation half-life in each media. All other model inputs were the same as the validation application as shown in Table 17 through Table 20.

### 8.5.1 Initial inputs and results

Inputs were initially set using the best available information within TREECS™-CTS without exerting any additional study or literature review,

thus relying on default methods within the system. The additional soil model inputs that were specified for the five EC are shown in Table 21. Most of the values in this table are the same as those used in the previous applications with the exception of the residue loading rate, solid phase particle diameter, soil volatilization rate, soil  $K_d$ , and aqueous phase half-life. The loading rate and particle diameter were the same as that of RDX for the ZIA validation application. The volatilization rate was different due to different soil properties. Except for CL-20, the soil  $K_d$  values in Table 21 were computed by the soil model UI using  $K_{oc}$  and percentages of sand, silt, clay, and organic matter of 82.25, 11, 6, and 0.75 percent, respectively, which were representative of the loamy sand soil in the ZIA. The degradation half-life in soil was assumed to be the same as that of RDX for comparison purposes, or 1E20 years, or essentially no degradation.

**Table 21. Additional soil model inputs for the five EC for ZIA application, Camp Pendleton.**

Input Description	DNAN	NTO	NQ	AP	CL-20
<b>Site Characteristics</b>					
MC mass residue loading versus time, g/yr, constant for 100 years	9,708 for 1943-2005 60,894 for 2006-2042				
Initial solid phase MC concentration in soil on a soil mass basis at time 0, mg/kg	0	0	0	0	0
Initial total non-solid phase MC concentration in soil on a soil mass basis at time 0, mg/kg	0	0	0	0	0
<b>Fate/Transport Parameters</b>					
Soil-water constituent partition coefficient, $K_d$ , L/kg, computed by soil model UI from $K_{oc}$ , soil texture, and percent organic matter for all except CL-20	0.95	0.76	0.072	0.0001	2.0 <sup>1</sup>
Decay/degradation half-life of aqueous phase constituent, yrs	1.0E20	1.0E20	1.0E20	1.0E20	1.0E20

Input Description	DNAN	NTO	NQ	AP	CL-20
Decay/degradation half-life of adsorbed (particulate) phase constituent, yrs	1.0E20	1.0E20	1.0E20	1.0E20	1.0E20
Initial mean diameter of solid phase constituent residue particles (assume spherical particles), $\mu\text{m}$	12,000	12,000	12,000	NA miscible	12,000
Volatilization rate, m/yr, as computed by soil model UI from molecular diffusivity in air	108.5	166.9	168.1	0 miscible	73.2
Chemical-Specific Properties					
$K_{oc}$ , L/kg (same as the values in Table 6)	158.5	125.9	12	0.016	2.7
Molecular weight (molar mass or averaged molecular mass), g/mol	198	130	104	117.5	438
Aqueous solubility limit, mg/L	276	16,600	3,800	249,000	4.33
Henry's Law constant, atm- $\text{m}^3/\text{g}\cdot\text{mol}$	3.01E-7	4.07E-13	4.49E-12	0	9.39E-25
Solid phase constituent mass density, g/ $\text{cm}^3$	1.34	1.93	1.72	1.95	2.04
Molecular diffusivity in air, $\text{m}^2/\text{day}$	0.56	0.86	0.87	NA Non-volatile	0.37

<sup>1</sup> Mean of range of values reported by Szecsody et al. (2004) for soil

The only additional inputs required for CMS are within the *Constituent Parameters* screen of the CMS UI. Within that screen, all initial EC concentrations and decay rates were set to zero, same as for RDX. Two additional inputs required within that screen for each EC include  $K_{ow}$ , which is used by the model UI to compute  $K_d$  for water column TSS and benthic sediment, and molecular diffusivity in water, which is used by the model UI to compute the mass transfer velocity for diffusion of dissolved constituent between the water column and benthic sediment pore water. The water volatilization rate is also on this input screen with the option selected to compute it by the model UI from HLC, wind speed, and water flow velocity. The values of the two inputs and the computed parameters are shown in Table 22 for each EC. The value of HLC and molecular weight are also displayed on the *Constituent Parameters* screen of the CMS UI, and

these values are supplied by the TREECS™ constituent data base with their values shown in Table 21.

**Table 22. Additional CMS inputs for the five EC for Las Flores Creek application, Camp Pendleton.**

Input Description	DNAN	NTO	NQ	AP	CL-20
$K_{ow}$ , mL/mL	43.6 <sup>1</sup>	2.34 <sup>2</sup>	0.13 <sup>3</sup>	1.45E-6 <sup>4</sup>	1.07 <sup>5</sup>
TSS-water constituent partition coefficient, $K_d$ , L/kg, computed by CMS UI from $K_{ow}$ and $f_{oc}$	.094	0.005	0.0003	3.1E-9	0.002
Benthic sediment-water constituent partition coefficient, $K_d$ , L/kg, computed by CMS UI from $K_{ow}$ and $f_{oc}$	0.094	0.005	0.0003	3.1E-9	0.002
Volatilization rate, m/yr, computed by CMS UI from HLC, wind speed, and water flow velocity	0.006	9.0E-9	1.0E-7	0	1.5E-20
Mass transfer velocity for diffusion of dissolved constituent between water column and sediment pore water, m/day, computed from molecular diffusivity in water and sediment porosity	0.0039	0.0052	0.006	0.0055	0.0023
Molecular diffusivity in water, cm <sup>2</sup> /sec, computed from method by Hayduk and Laudie (1974) except for AP	6.16E-6	8.55E-6	8.45E-6	1.8E-5 <sup>6</sup>	4.18E-6

<sup>1</sup> Measured, Sokkalingam et al. (2008)

<sup>2</sup> Estimated, Sokkalingam et al. (2008)

<sup>3</sup> Measured, Hansch et al. (1995) as cited in EPI Suite

<sup>4</sup> EPA (2008)

<sup>5</sup> Chemspider (<http://www.chemspider.com/>) predicted from ACD/Labs Percepta

Platform - PhysChem module

<sup>6</sup> Hlquily and Clifton (1984)

Only the constituent mass fluxes for recharge to groundwater had to be modified for the User Defined WFF module. The output fluxes from CMS at its terminus for each EC were used to provide these inputs. The only additional inputs required for the vadose zone and aquifer models were the

$K_d$  values for each EC and the degradation half-lives for each EC. All half-lives were set to a large number to represent no degradation, same as for RDX. The  $K_d$  values were computed by the model UIs for each EC using soil composition and  $K_{oc}$ . The UI-computed  $K_d$  values used for each EC are shown in Table 23. The  $K_{oc}$  values were provided by the ARCDDB and are shown in Table 21. The above inputs as well as the other model inputs used in the RDX validation application were used in the EC application for the Las Flores watershed, Camp Pendleton.

**Table 23. EC  $K_d$  values used in vadose and aquifer models for Las Flores basin.**

EC	$K_d$ , L/kg
DNAN	0.23
NTO	0.18
NQ	0.017
AP	2.3E-5
CL-20	0.0038

The results of the EC application are plotted in Figure 36 for stream total concentration versus year. The previous results for RDX are included in the plot for comparison. All results are approaching over time a constant, steady-state stream concentration for each of the two constant loading steps. Only AP and NQ actually reach steady-state for both loading steps, while NTO reaches steady-state for the first loading step. All of the MC results in Figure 36 follow a trend where steady-state is reached faster as solubility increases. However, NQ and NTO depart from this trend somewhat since NTO has a higher solubility than NQ, but NQ reaches steady-state sooner than NTO. This trend departure is due to NTO having a much higher soil  $K_d$  than NQ, resulting in greater retardation. The NTO-to-NQ solubility and soil  $K_d$  ratios are 4.37 and 10.49, respectively; thus,  $K_d$  has a greater effect than solubility for reaching steady-state. The stream EC results are very similar to the results presented for Popolopen Brook at USMA.

The results of the EC application are plotted in Figure 37 for receptor well concentration versus year. Again, the previous results for RDX are included in the plot for comparison. The EC concentrations for the aquifer resemble those of the stream, except they are a little lower due to dilution associated with background Darcy flow. It is emphasized that with no deg-

radiation, all MC would eventually reach the same steady-state concentration if the models were run long enough due to having the same loading rate of residue MC into the AOI.

**Figure 36. Computed water concentrations in Las Flores Creek down-gradient of ZIA, Camp Pendleton, for five EC and RDX.**

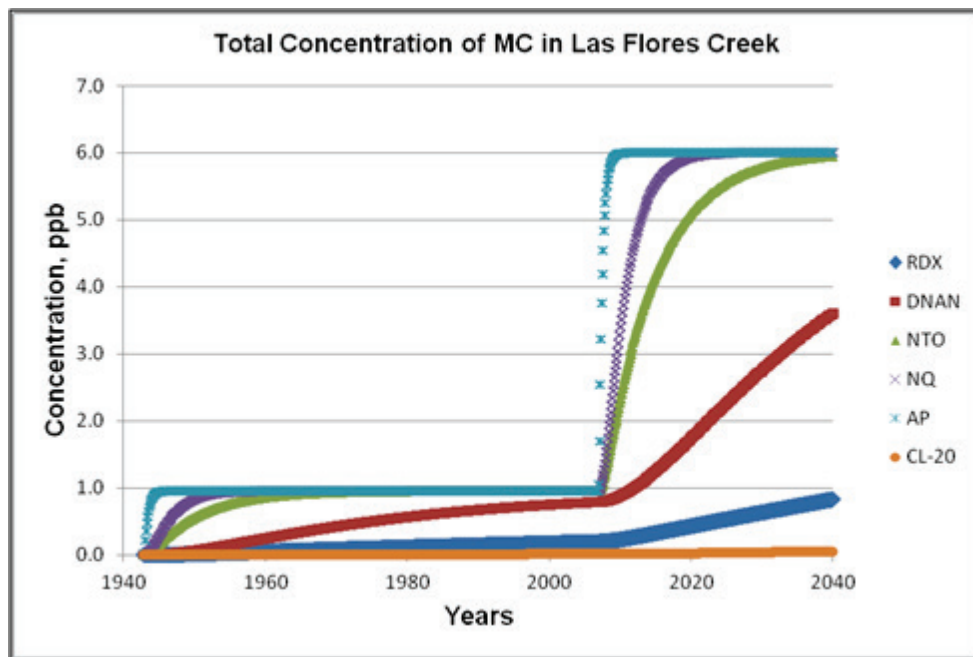
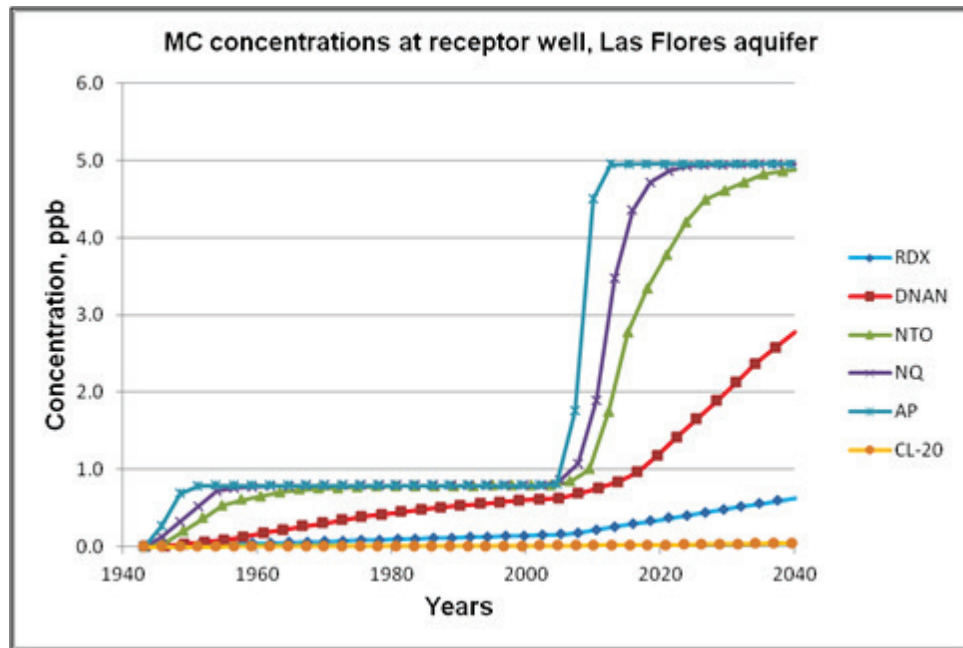


**Figure 37. Computed water concentrations at receptor well of Las Flores aquifer, Camp Pendleton, for five EC and RDX.**



### 8.5.2 Refined inputs and simulation results for DNAN and NTO

As for the previous two study sites, DNAN and NTO were chosen for a more focused study. Of all the chemical-specific inputs, the values for  $K_{oc}$ , which affect the estimates of soil  $K_d$ , and half-life were considered the most uncertain for DNAN and NTO. Thus, refined estimates for soil  $K_d$  and half-life were made for DNAN and NTO and used to examine the effects on their fate.

The characteristics of the 11 soils used in the Dontsova et al. (2014) study were reviewed in an attempt to match as closely as possible the particular soil to the soil texture and pH for the ZIA soils. Matching the soil OC content was considered less important since the measured  $K_d$  values were normalized to OC to provide  $K_{oc}$ . The soils that are the most similar to the surface soils at the ZIA are Camp Guernsey, WY, and Plymouth (MMR, MA). Both soils are loamy sand with texture similar to that of the ZIA. The pH of ZIA soils is 6.1 and the OC content is 0.75 % according to WSS. The characteristics of the two soils studied by Dontsova et al. (2014) and the corresponding measured batch  $K_d$  and OC normalized  $K_{oc}$  values for DNAN and NTO are shown in Table 24 along with the  $R^2$  of the fit for  $K_d$ .

The values of  $K_d$  and  $K_{oc}$  for DNAN of 0.95 and 158.5 L/kg, respectively, in Table 21 agree quite well with the measured values in Table 24 for Camp Guernsey of 0.93 L/kg for  $K_d$  and 121 L/kg for  $K_{oc}$ . This close agreement is probably due to the OC content of Camp Guernsey soil being close to that of the ZIA (0.77 compared with 0.75). Given the close agreement with Camp Guernsey soil, the original  $K_d$  value of 0.95 L/kg for DNAN was retained for the refined simulation.

**Table 24. Soil characteristics and measured batch  $K_d$  and corresponding  $K_{oc}$  values for DNAN and NTO for two soils similar to ZIA soils (from Dontsova et al. 2014).**

Soils	Sand-silt-clay, %	Soil OC, %	Soil pH	DNAN $K_d$ , L/kg	$R^2$ , DNAN $K_d$	DNAN $K_{oc}$ , L/kg	NTO $K_d$ , L/kg	$R^2$ , NTO $K_d$	NTO $K_{oc}$ , L/kg
Camp Guernsey	83-13-4	0.77	8.21	0.93	0.97	121	0.02	0.21	2.6
Plymouth	75-20-5	2.45	4.23	4.38	0.94	179	0.50	0.96	20.41

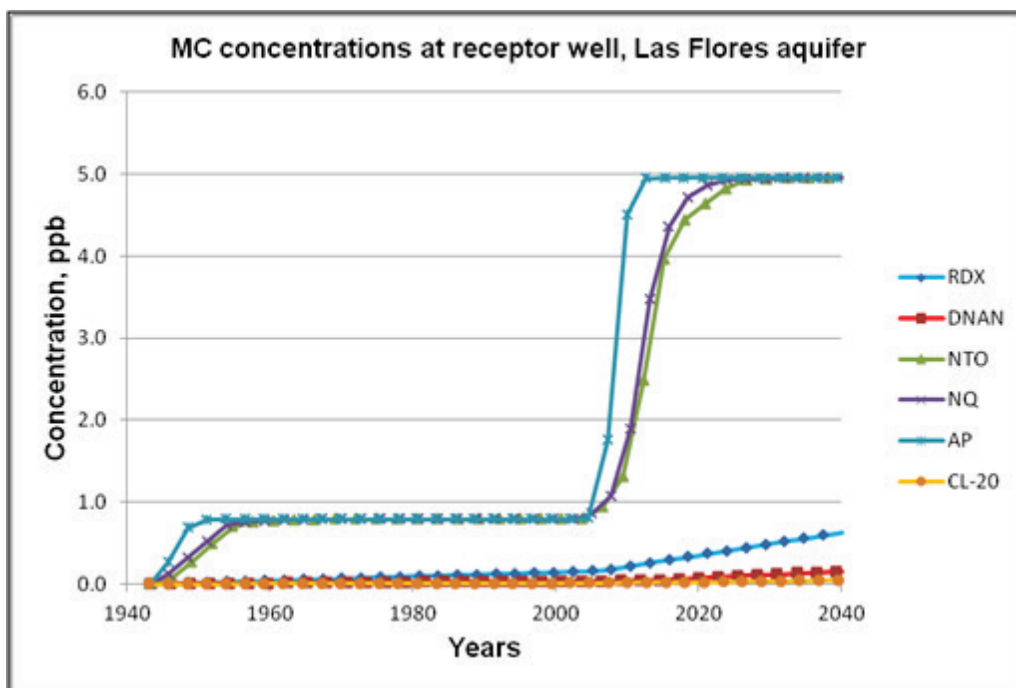
The values of  $K_d$  and  $K_{oc}$  for NTO of 0.76 and 125.9 L/kg, respectively, in Table 21 are higher than the measured values in Table 24, which range

from 0.02 to 0.5 L/kg for  $K_d$  and 2.6 to 20.41 L/kg for  $K_{oc}$ . Also, the relative range in  $K_{oc}$  for NTO is greater than it is for DNAN indicating less correlation of partitioning to OC content for NTO. Partitioning of NTO to soil appears to be more closely associated with soil pH with an inverse relationship (Dontsova et al. 2014). The pH of the ZIA soil falls between the pH values for the two soils in Table 24. A  $K_d$  value for NTO of about 0.26 L/kg, which is the average  $K_d$  for the Camp Guernsey and the Plymouth soils, seems far more appropriate for the ZIA surface soil than the value of 0.76 L/kg that was used originally.

The reasoning used previously for degradation rates (half-lives) of DNAN and NTO at Demo Area 2 and AIA can be applied for the ZIA. Thus, a half-life of 0.6 years for aqueous dissolved DNAN and no degradation of NTO (same as for RDX) were used for the refined simulation of ZIA soils. Additionally, the half-life of DNAN in vadose zone and groundwater was set to 0.6 years, while no degradation was assumed for NTO. Degradation rates for Las Flores Creek were not altered since changes would not affect results due to the very short travel time in the creek. The soil  $K_d$  for DNAN was kept at the original value of 0.95 L/kg, and that of NTO was reduced from 0.76 to 0.26 L/kg for the refined simulation. All other inputs were kept at the same value as for the original EC simulation for the ZIA.

The receptor well results for the above refinements (i.e., improvements in input estimates for DNAN and NTO) are shown in Figure 38 along with the previous result for the other three EC and RDX for comparison. NTO now approaches steady-state sooner, and the concentrations of DNAN are now much lower than originally, even lower than those of RDX. These results clearly indicate the need for better estimates of MC degradation rates in natural environments.

**Figure 38.** Computed water concentrations at receptor well of Las Flores aquifer, Camp Pendleton, for five EC and RDX, with improved inputs for DNAN and NTO.



## 8.6 BMP assessment

The same three types of BMPs that were evaluated for RDX at the AIA study site are assessed for the Las Flores watershed site. These BMPs are:

- BMP 1 – discontinue range use after the year 2015 or after 73 years;
- BMP 2 – amend, repeatedly when necessary, the AOI soil with lime to create alkaline hydrolysis with rapid degradation of RDX; and
- BMP 3 – continuous AOI export treatment of RDX in surface runoff (including soil interflow) through a degradation reactor.

Each BMP was simulated and results compared against base condition results. The base condition was the same as the validated model with the exception of doubling the simulation time from 100 to 200 years so that results could be more fully evaluated. AOI loading of RDX residue is assumed to end after the first 100 years.

BMP 1 had the same inputs as the base condition, except that the RDX loading rate was set to zero in year 2016 and thereafter. BMP 2 had the same inputs as the base condition with the exception that the aqueous dissolved RDX in soil pore water had a degradation half-life of 0.005 years

due to alkaline hydrolysis of the lime soil amendment applied to the AOI soils (see BMP 2a for the MMR application).

BMP 3 involved a porous bed degradation reactor to intercept AOI surface runoff and soil interflow and remove dissolved RDX from the AOI export flux. The validation application revealed that the surface water export flux (including soil interflow flux) of dissolved RDX is about 1000 times greater than that associated with particulate (adsorbed) RDX. A degradation reactor model was developed for TREECS™ as an AOI export treatment BMP option (Dortch and Gerald 2015). This model was applied to the ZIA AOI with the following reactor specifications:

- length: 50 m
- width: 10 m
- depth: 2 m
- flow rate: 16,760 m<sup>3</sup>/day
- bed porosity: 0.5
- bed dry bulk density: 1.32 kg/L
- bed solids – water partitioning distribution coefficient: 0.5 L/kg
- degradation rate: 10.0 day<sup>-1</sup>

The flow rate of 16,760 m<sup>3</sup>/day was calculated from the sum of the average annual water runoff and infiltration rates of 0.103 and 0.03 m/yr, respectively, times the AOI surface area of 6.2E6 m<sup>2</sup> divided by 49.2 days per year, which is the average number of days per year with significant rainfall. A bed solids-to-water partitioning distribution coefficient of 0.5 L/kg was used to represent expected conditions and to be consistent with the value used for the West Point AIA reactor. The same degradation rate used for West Point of 10.0 day<sup>-1</sup> was used for consistency. For the above conditions, the TREECS™ degradation reactor model computed a reactor effluent normalized concentration of 0.5, i.e., the ratio of effluent to influent RDX concentration is 0.5, or 50 % of the RDX concentration is removed. This amount of reduction was used to scale the AOI export fluxes of RDX to surface water, which are needed by the stream model. Otherwise, all other inputs for BMP 3 were the same as those of the base condition.

The results of the three BMP simulations are plotted in Figure 39 as water total concentration of RDX in Las Flores Creek versus years. The results of the base condition and observed concentration are included in the plot for comparison of BMP effectiveness. A similar plot of the BMP effects on groundwater is shown in Figure 40 for the Las Flores aquifer well. Stream

and aquifer results are quite similar. All three BMPs exhibit some effectiveness over the long term, but BMP 2 (amending AOI soil with lime) is by far the most effective.

BMPs 1 and 3 show how RDX residue mass will persist in AOI soils for a long time due to the relatively slow dissolution rate of RDX. The cessation of range use associated with BMP 1 is probably not a viable alternative. BMP 2 is probably a cost effective alternative, but it could be hazardous to work ZIA soils due to unexploded ordnance (UXO) unless range clearance is practiced. Additionally, repeated application of soil amendment may be required over time.

BMP 3 (AOI export treatment with degradation reactor) is not very effective for this site due to the high flow rate associated with such a large AOI watershed area, also making this BMP not very practical. The other comments made for West Point regarding this BMP apply here as well.

**Figure 39.** Computed water concentrations of RDX in Las Flores Creek down-gradient of the ZIA, Camp Pendleton, for three BMPs compared to base condition.

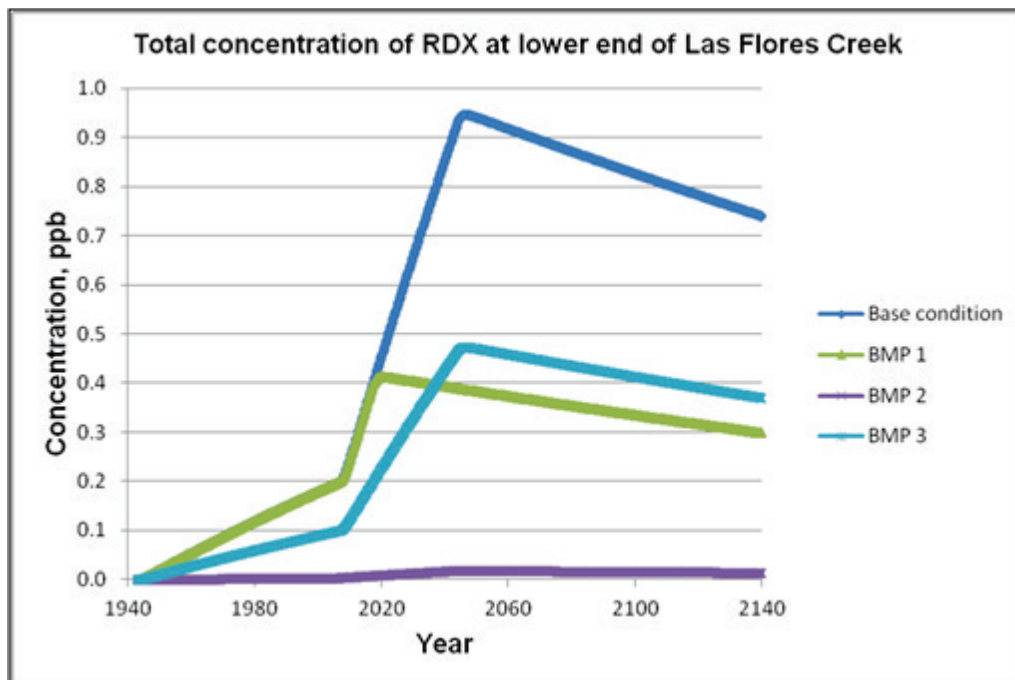
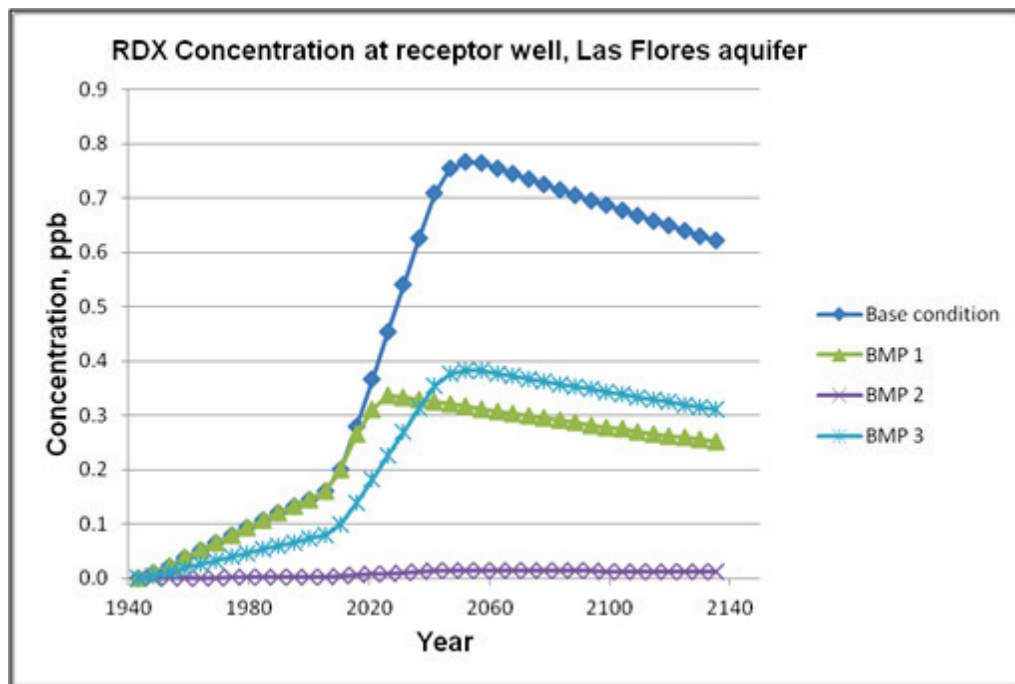


Figure 40. Computed water concentrations of RDX in Las Flores aquifer down-gradient of the ZIA, Camp Pendleton, for three BMPs compared to base condition.



## 9 Performance Assessment

The performance objective ratings are summarized in Table 25 for the application to MMR Demo Area 2, in Table 26 for the application to the AIA of USMA, and in Table 27 for the application to the ZIA of Camp Pendleton. A discussion of each performance objective rating for all three sites follows in the sections below.

**Table 25. Performance objectives success ratings for MMR Demo Area 2 application.**

Performance Objective	Success Rating
TREECS™ accurately simulates long-term fate of MC on ranges	Highly successful: model concentrations were less than a factor of 3 of observed for soil and aquifer
TREECS™-CTS can be used to quantify uncertainty in inputs	Successful: model uncertainty results bracketed observed field MC concentrations at the 95% confidence level
TREECS™-CTS can be quickly set up and run with readily available data	Successful: TREECS™, including CTS use, was set up and validated in 8 labor hours, far less than the criteria of 80 hours
Training requirements are reasonable	Training has not yet occurred.
TREECS™-CTS can be applied to evaluate range management and/or remediation strategies	Successful: TREECS™ was used to evaluate three BMP strategies to reduce RDX concentrations in groundwater
TREECS™-CTS can be applied to evaluate the fate of emerging MC	Successful: TREECS™-CTS was applied to evaluate the fate of DNAN, NTO, NQ, AP, and CL-20 with comparison to results for RDX

**Table 26. Performance objectives success ratings for AIA application.**

Performance Objective	Success Rating
TREECS™ accurately simulates long-term fate of MC on ranges	Highly successful: model concentrations were less than a factor of 3 of observed for Popolopen Brook on three different dates
TREECS™-CTS can be used to quantify uncertainty in inputs	Moderately successful: model uncertainty results bracketed observed field MC concentrations at the 95% confidence level for one of the three observation dates
TREECS™-CTS can be quickly set up and run with readily available data	Successful: TREECS™, including CTS use, was set up and validated in 16 labor hours, far less than the criteria of 80 hours
Training requirements are reasonable	Training has not yet occurred.
TREECS™-CTS can be applied to evaluate range management and/or remediation strategies	Successful: TREECS™ was used to evaluate three BMP strategies to reduce RDX concentrations in surface water

Performance Objective	Success Rating
TREECS™-CTS can be applied to evaluate the fate of emerging MC	Successful: TREECS™-CTS was applied to evaluate the fate of DNAN, NTO, NQ, AP, and CL-20 with comparison to results for RDX

**Table 27. Performance objectives success ratings for ZIA – Las Flores watershed application.**

Performance Objective	Success Rating
TREECS™ accurately simulates long-term fate of MC on ranges	Highly successful: model concentrations were less than a factor of 3 of observed for Las Flores Creek and aquifer for one set of observations above detection
TREECS™-CTS can be used to quantify uncertainty in inputs	Moderately successful: model uncertainty results bracketed observed field MC concentration at the 95% confidence level for Las Flores Creek but did not bracket the observation for Las Flores aquifer
TREECS™-CTS can be quickly set up and run with readily available data	Successful: TREECS™, including CTS use, was set up and validated in 50 labor hours, less than the criteria of 80 hours
Training requirements are reasonable	Training has not yet occurred.
TREECS™-CTS can be applied to evaluate range management and/or remediation strategies	Successful: TREECS™ was used to evaluate three BMP strategies to reduce RDX concentrations in surface water and groundwater
TREECS™-CTS can be applied to evaluate the fate of emerging MC	Successful: TREECS™-CTS was applied to evaluate the fate of DNAN, NTO, NQ, AP, and CL-20 with comparison to results for RDX

## 9.1 Validation accuracy

The validation performance objective at all three study sites is rated highly successful since model-computed media concentrations are within a factor of 3 of observed data in all cases. Very close agreement was obtained for AOI soil and aquifer concentrations at down-gradient of Demo Area 2, MMR. Remarkably close agreement was obtained for surface water downstream of ZIA, Camp Pendleton. Fairly good agreement was obtained for Popolopen Creek downstream of the AIA, USMA. The poorest agreement was for groundwater down-gradient of the ZIA. The primary reason for disagreement in predicted and observed surface water concentrations is related to using annual average rainfall and hydrology rather than daily rainfall and hydrology. Stream concentrations are highly transient depending on recent rainfall to trigger measureable stream values. Lack of

sufficient information regarding monitoring well locations is a contributing factor to the greater disagreement in model and observed for the Las Flores aquifer at Camp Pendleton.

## 9.2 Uncertainty analysis

The objective pertaining to uncertainty analysis was rated successful for Demo Area 2 site and moderately successful for the AIA and ZIA study sites. The latter two sites were less than fully successful due to the fact that not all observed data were captured within the 95% confidence bands of the model analysis. However, it is noted that the expanse of the confidence bands depends on the inputs regarding uncertain parameters, such as their distribution and bounds. In most cases, the bounds were not very well known, so they were assumed, such as halving and doubling the mean, or validation, input value. For this reason and in hind-sight, this performance objective should have been qualitative rather than quantitative since the primary objective was to demonstrate the use of this feature rather than to quantify its utility.

## 9.3 TREECS™-CTS set-up time

This performance objective was rated as fully successful for all three study sites since all times were less than 80 labor hours. Approximately 8 labor hours were required to set up and conduct the validation application for Demo Area 2, MMR. However, this relatively low labor requirement is due to the fact that this site had been previously modeled with TREECS™; therefore, the site information had already been gathered, reviewed and entered into the model. All that was required during the present validation application was to review all inputs, make a few corrections or changes, and plot results.

Approximately 16 labor hours were required to set up and conduct the validation application for AIA, USMA. However, this relatively low labor requirement is due to the fact that other sites at the USMA had been previously modeled with TREECS™ (Dortch 2012), so the site information had already been gathered and analyzed.

Approximately 50 labor hours were required to set up and conduct the validation application for ZIA, Camp Pendleton. This labor included gathering, ,review, and analysis of site information, obtaining and processing various data for soil properties and meteorology, setting up model inputs,

validating the model, and writing-up all sections of this report dealing with input data and model validation. This labor also included assessing model output and making adjustments to better represent the perceived hydrological conditions at this site, which included groundwater recharge from stream flow. This relatively small labor requirement is significant given all of the study components that were performed as listed above. This application validates that these systems can be applied well within 80 labor hours, thus demonstrating the relatively low man-power requirements for TREECS™-CTS.

#### **9.4 Training**

The training objective had not been met at the time this report was written. This training is being planned for 2017.

#### **9.5 BMP assessments**

The performance objective pertaining to evaluating range management and remediation strategies (i.e., BMPs) was rated as successful for all three study sites. At least 3 BMPs were evaluated for RDX at all three sites.

#### **9.6 EC fate**

The performance objective pertaining to evaluating EC fate was rated as successful for all three study sites. Five ECs were modeled, and results were compared with that of RDX at all three sites.

## 10 Cost Assessment

The ESTCP requires that a Cost-Benefit-Analysis (CBA) be conducted for each demonstrated technology. The CBA for this project is accomplished by comparing the costs associated with applying TREECSTM-CTS to the cost of an ORAP Phase II for a study site where monitoring was conducted to assess range environmental impacts. Operational range assessments require periodic evaluation of the potential for an MC source on-range to reach an off-range receptor. If no source-receptor interaction exists, then the range is classified as *unlikely*. If a potential source-receptor interaction is believed to exist, the range is classified as *inconclusive*, and the assessment progresses to the next phase (e.g., ORAP Phase II) in which a more detailed assessment must be conducted, such as field monitoring. The period for range re-evaluations is every five years as a minimum. Periodic site monitoring is currently the approach used to assess MC fate and the environmental risk down-gradient of *inconclusive* at DoD training ranges. Such monitoring is conducted by the Army for ORAP Phase II. The Air Force and Navy also conduct phased studies for assessing off-site migration of contaminants from their training ranges.

### 10.1 Cost model

TREECSTM-CTS can usually be applied to a study site within 80 labor hours. Application includes review of available data, processing inputs, model set-up, model calibration/validation, scenario assessment or assessing PAL exceedance, and preparing written documentation of results. Although all three study site applications reported herein were conducted in less than 80 labor hours, 80 labor hours are used as the cost to apply TREECSTM-CTS. This cost is compared with the average cost to conduct an Army ORAP Phase II study for a single study site. A study site is defined as a single source-receptor interaction. For example, costs associated with assessing the concentrations of a particular MC, such as RDX, in a pond down-gradient of an artillery impact area would constitute a single study site. Under ORAP Phase II, this cost would include sampling, laboratory analysis, and documentation of the impact in the Phase II report.

The cost to apply TREECSTM-CTS is converted from labor hours to dollar costs as follows. A reasonable federal pay grade of GS-12 step 5 (2016 pay scale) is used, which is \$79,554 per year for generic “rest of U.S.” with 2080 hours in a year, or \$38.25 per hour. This hourly rate is multiplied by

a burden factor, (which includes the hourly pay rate, plus benefits, plus organizational overhead). A burden factor of 3.0 is used resulting in a total hourly cost of \$114.74. With a labor requirement of 80 hours, the cost of TREECS™-CTS for a single study site is estimated as \$9,179.

The cost of conducting monitoring as part of ORAP Phase II includes: labor for field sample collection; travel costs to/from and while at the installation being sampled; material required for sample collection; laboratory analysis of samples to determine concentrations; and labor costs for assessment and reporting of results. A reasonable federal pay grade of GS-9 step 5 is used for labor of personnel to collect field samples. This pay grade, which is \$54,855 per year (2016 pay scale) for generic “rest of U.S.” with 2080 hours in a year, requires \$26.37 per hour. This hourly rate is multiplied by a burden factor of 3.0 resulting in total daily cost of \$632.94. Two field personnel are required for three days for travel and field sample collection associated with one AOI and its primary target receiving waters. Thus, the total cost of labor for field sample collection is estimated as \$11,393. Travel cost of two people for three days, including air fare, rental car, lodging, and per diem, is estimated to be \$3,000. Material needed for sample collection, handling, storage, and shipping is roughly \$1,000. Laboratory analysis cost associated with an HE, such as RDX, is about \$50 per sample.\* Assuming sampling of water at three locations, three times (wet, dry, and storm event), with three replicates each, results in 27 samples to be analyzed at a cost of \$1,350. Approximately 20 hours of labor for a GS12 step 5 is required for assessment and reporting of the field sampling results for ORAP. All total, the cost for monitoring a single study site is estimated to be \$19,038. This cost is more than double the cost of applying TREECS™-CTS for the same study site.

## 10.2 Cost drivers

The primary driver in considering whether or not to apply TREECS™-CTS to DoD ranges is access or availability of properly trained personnel for applying models. Such personnel should have some background in modeling and prior experience in applying models. Assuming such personnel are available, there are no other factors that should affect the decision to apply TREECS™-CTS given the relatively low cost. The use of a modeling system such as this will save money in the long-term and provide more valuable

---

\* Personal communication with personnel of the Environmental Chemistry Branch, ERDC

information with additional benefits (such as management alternative assessments) quicker and cheaper than relying solely on field sampling.

Probably the best approach to ensure that qualified personnel are available for conducting the modeling is to utilize environmental contractors that have existing delivery order contracts within the DoD. Many of these contractor firms already have qualified modeling personnel on staff.

A secondary driver for use of TREES™-CTS at a particular site is whether an ORAP Phase II assessment is required. If Phase II is required, then modeling should be performed to reduce costs for Phase II and to provide greater understanding of current and future environmental consequences. Provided that sampling is to be conducted in Phase II, modeling will provide improved insight for sample design, thus, potentially reducing sampling costs while improving sampling quality.

### 10.3 Cost analysis

Currently, ORAP Phase II assessments have been required at approximately 100 installations.\* Assuming three study sites per installation, a cost savings of about \$10,000 per study site (rounding up of the cost savings of \$9,858, which is probably low due to the unexpected costs of field data collection) results in a cost savings of about \$3,000,000 per five-year re-evaluation that is required under ORAP (this figure was computed by multiplying \$10,000 by 3 and then by 100). However, the benefits of using TREECS™-CTS go far beyond the cost savings associated with modeling versus monitoring. Modeling can be used to forecast not only if PALs will be exceeded but when they will be exceeded. Additionally, the modeling system can be used to assess BMP strategies for avoiding future PAL exceedance and to evaluate the carrying capacity of existing and future ranges. Modeling allows the assessment of “what if” scenarios without the risks and costs associated with trial-and-error field implementation. Moreover, TREECS™-CTS usage can and should be an integral part of the successful administration of ORAP and related range sustainment programs which can avoid many millions, if not billions, of dollars being lost if operational ranges are closed due to compliance failure.

---

\* [http://www.ncsi.com/tss11/agenda\\_oacsim.html](http://www.ncsi.com/tss11/agenda_oacsim.html)

## 11 Implementation Issues

There are no major implementation issues associated with applying TREECS™-CTS. Training is helpful and should be conducted for successful use. Installation of TREECS™ on DoD and Army-owned computers requires the System Administrator since it is client based and there are many military security constraints, such as requiring a Certificate of Networthiness (CON) for installed software (TREECS™ has an Army CON). Installation on contractor-owned computers entails much fewer hurdles. CTS is web-based; therefore, it only requires establishing a log-in account for an EPA server.

Presently, there are no DoD or Army directives that require the use of TREECS™, and as a result, TREECS™ has not experienced the use that was originally envisioned during its developmental funding. Thus, the benefits of having a powerful forecast modeling tool such as TREECS™ are not being realized. TREECS™ is a mature, validated modeling tool that is fairly easy to apply relatively quickly. Qualified contract environmental personnel could be readily trained for applying TREECS™-CTS to provide the most expedient and cheapest route to range applications. TREECS™ will not be fully utilized without a requirement for implementation and application. An Army or DoD directive is needed to require such applications, which would provide cost savings, provide much improved site understanding and alternatives assessment, and help ensure range sustainability.

Predicting the fate of ECs associated with IM explosive formulations presents a unique challenge given that less is known regarding the physico-chemical properties of ECs than legacy explosive components. A special effort was made during this project to try to obtain a better understanding of how to properly model ECs. Thus, TREECS™ was applied for laboratory studies of EC fate reported by Dontsova et al. (2014) to expand this understanding. Appendix B provides the results of these modeling studies and lessons learned for predicting the fate of ECs associated with IM.

## References

Air Force Center for Environmental Excellence (AFCEE). 2006. Focused feasibility study for landfill 1, draft report at <http://mmr.org/cleanup/plumes/lf1/ffs/>.

AMEC Earth and Environmental. 2004. *Demo area 2 interim groundwater data summary report*. Final IAGWSP technical team memorandum 04-1. November 24, 2004. Prepared for the U.S. Army Corps of Engineers, Concord, MA, for the U.S. Army/National Guard Bureau, Camp Edwards, MA, by AMEC Earth and Environmental, Westford, MA.

Arcadis – Malcolm Pirnie (AMP). 2013. *Range environmental vulnerability assessment, 5 year review, Marine Corps Air Station and Marine Corps Base Camp Pendleton, Volume I and Volume II (appendices)*. Marine Corps Installations Command, Washington, DC.

Boddu, V. M., K. Abburi, S. W. Maloney, and R. Damavarapu. 2008. Thermophysical properties of an insensitive munitions compound, 2,4-dinitroanisole. *Journal of Chemical and Engineering Data* 53:1120–1125.

Boethling, R. S., and J. Costanza. 2010. Domain of EPI Suite biotransformation models. *SAR and QSAR in Environmental Research*, 21(5–6):415–43.

Boyer, I., J. K. Miller, R.E. Watson, J. DeSesso, II, and C.M. Vogel. 2007. *Comparison of the relative risks of CL-20 and RDX*. Noblis Technical Report. Falls Church, VA: Noblis Center for Science and Technology.

Buck, J. W., G. Whelan, J. G., Droppo, Jr., D. L. Strenge, K. J. Castleton, J. P. McDonald, C. Sato, and G. P. Streile. 1995. *Multimedia Environmental Pollutant Assessment System (MEPAS) application guidance, guidelines for evaluating MEPAS input parameters for version 3.1*. PNL-10395. Pacific Northwest Laboratory, Richland, WA.

Chakka, S., V. M. Boddu, S. W. Maloney, and R. Damavarapu. 2010. Prediction of physicochemical properties of energetic materials via EPI Suite. In *Energetic Materials*, ed. V. Boddu and P. Redner, 77–92. New York, NY: CRC Press.

Dontsova, K., S. Taylor, R. Pesce-Rodriguez, M. Brusseau, J. Arthur, N. Mark, M. Walsh, J. Lever, J. Šimůnek. 2014. *Dissolution of NTO, DNAN, and insensitive munitions formulations and their fates in soils*. Strategic Environmental Research and Development Program (SERDP). ERDC/CRREL TR-14-23. Hanover, NH: U.S. Army Engineer Research and Development Center.

Dortch, M. S., B. E. Johnson, and J. A. Gerald. 2013b. *Modeling firing range best management practices with TREECS™*. ERDC/EL TR-13-6. Vicksburg, MS: U.S. Army Engineer Research and Development Center.

Dortch, M. S. 2012. *Validation of the Training Range Environmental Evaluation and Characterization System (TREECS™)*. ERDC/EL TR-12-3. Vicksburg, MS: U.S. Army Engineer Research and Development Center.

Dortch, M. S. 2013. *Application of TREECS™ to small arms firing ranges, Fort Leonard Wood, MO*. ERDC TN-EQT-13-2. Vicksburg, MS: U.S. Army Engineer Research and Development Center.

Dortch, M. S. 2014. *Evaluation of time-varying hydrology within the Training Range Environmental Evaluation and Characterization System (TREECS™)*. ERDC/EL CR-14-3. Vicksburg, MS: U.S. Army Engineer Research and Development Center.

Dortch, M. S. 2015. *Evaluation of uncertainty of constituent input parameters for modeling the fate of RDX*. ERDC/EL TN-15-2. Vicksburg, MS: U.S. Army Engineer Research and Development Center.

Dortch, M. S. 2016. *Modeling the fate of lead from small arms firing ranges, Fort Jackson, SC*. ERDC/EL CR-16-2. Vicksburg, MS: U.S. Army Engineer Research and Development Center.

Dortch, M. S. and H. M. Smith. 2013. *Modeling RDX reduction in iron bed reactors*. ERDC TN-EQT-13-1. Vicksburg, MS: U.S. Army Engineer Research and Development Center.

Dortch, M. S., and B. E. Johnson. 2012. Overview and validation of the Training Range Environmental Evaluation and Characterization System. *Proceedings from the Fifth International Conference on Environmental Science and Technology*, held on June 25–29, 2012 in Houston, Texas, USA, 463–469.

Dortch, M. S., and J. A. Gerald. 2015. *Modules for modeling firing range best management practices within TREECS™*. ERDC/EL TR-15-7. Vicksburg, MS: U.S. Army Engineer Research and Development Center.

Dortch, M. S., B. E. Johnson, and J. A. Gerald. 2010. *Proof-of-concept application of Tier 1 modeling approach with the Training Range Environmental Evaluation and Characterization System*. ERDC/EL TR-10-19. Vicksburg, MS: U.S. Army Engineer Research and Development Center.

Dortch, M. S., B. E. Johnson, and J. A. Gerald. 2012. *Extension of capabilities for the Tier 1 and Tier 2 approaches within the Training Range Environmental Evaluation and Characterization System (TREECS™)*. ERDC/EL TR-12-11. Vicksburg, MS: U.S. Army Engineer Research and Development Center.

Dortch, M. S., B. E. Johnson, and J. A. Gerald. 2013a. Modeling fate and transport of munitions constituents on firing ranges, *Soil and Sediment Contamination: an International Journal* 22(6):667–688.

Dortch, M. S., B. E. Johnson, J. A. Gerald, Z. Zhang, and A. P. Simmons. 2011b. *Proof-of-concept application of Tier 2 modeling approach within the Training Range Environmental Evaluation and Characterization System*. ERDC/EL TR-11-10. Vicksburg, MS: U.S. Army Engineer Research and Development Center.

Dortch, M. S., B. E. Johnson, Z. Zhang, and J. A. Gerald. 2011a. *Methods for Tier 2 modeling within the Training Range Environmental Evaluation and Characterization System (TREECS™)*. ERDC/EL TR-11-2. Vicksburg, MS: U.S. Army Engineer Research and Development Center.

Dortch, M. S., J. A. Gerald, and B. E. Johnson. 2009. *Methods for Tier 1 modeling with the Training Range Environmental Evaluation and Characterization System*. ERDC/EL TR-09-11. Vicksburg, MS: U.S. Army Engineer Research and Development Center.

Dortch, M. S., S. Fant, and J. A. Gerald. 2007. Modeling fate of RDX at demolition area 2 of the Massachusetts Military Reservation., *Journal of Soil and Sediment Contamination* 16(6): 617–635.

EA Engineering, Science, and Technology, Inc. (EA). 2011. *U.S. Army Garrison West Point, New York, phase II conceptual site model and preliminary technical approach*, Hunt Valley, MD.

Fant, S., and M. S. Dortch. 2007. *Documentation of a one-dimensional, time-varying contaminant fate and transport model for streams*. ERDC/EL TR-07-01. Vicksburg, MS: U.S. Army Engineer Research and Development Center.

Fida, T. T., S. Palamuru, G. Pandey, and J. Spain. 2014. Aerobic biodegradation of 2,4-dinitroanisole by *nocardiooides* sp. strain JS1661. *Applied and Environmental Microbiology* 80(24):7725–7731.

Fuller, E. N., P. D. Schettler, and J. C. Giddings. 1966. A new method for prediction of binary gas-phase diffusion coefficients. *Industrial and Engineering Chemistry* 58:19–27.

Gerald, J. A., B. E. Johnson, and M. S. Dortch. 2012. *User guide for applying the Training Range Environmental Evaluation and Characterization System (TRECS™)*. ERDC/EL TR-12-16. Vicksburg, MS: U.S. Army Engineer Research and Development Center.

Haag, W. R., R. Spanggord, T. Mill, R. T. Podoll, T. W. Chou, D. S. Tse, and J. C. Harper. 1990. Aquatic environmental fate of nitroguanidine. *Environmental Toxicology and Chemistry* 9:1359–1367.

Hansch, C., A. Leo, and D. Hoekman. 1995. In *Exploring QSAR. Hydrophobic, electronic, and steric constants*. American Chemical Society, Washington, DC.

Hawari, J. 2000. Biodegradation of RDX and HMX: From basic research to field application. In *Biodegradation of nitroaromatic compounds and explosives*, ed. J. C. Spain, J. B. Hughes, and H. J. Knackmuss, 277–310. Boca Raton, FL: Lewis Publishers.

Hayduk, W., and H. Laudie. 1974. Prediction of diffusion coefficients for non-electrolysis in dilute aqueous solutions. *American Institute of Chemical Engineers Journal* 20:611–615.

Hilal, S. H. 2003. *Prediction of chemical reactivity parameters and physical properties of organic compounds from molecular structure using SPARC*. EPA/600/R-03/030 (NTIS PB2004-101167).

Hlquily, N., and M. J. Clifton. 1984. Diffusion coefficients of ammonium perchlorate in concentrated aqueous solutions between 20 and 30°C. *Journal of Chemical and Engineering Data* 29:371–373.

Hoffman, D. M. 2003. Voids and density distributions in 2,4,6,8,10,12-hexanitro-2,4,6,8,10,12-hexaazaisowurtzitane (CL-20) prepared under various conditions. *Propellants, Explosives, Pyrotechnics* 28:194–200.

Johnson, B. E., and M. S. Dortch. 2014a. *Hydrology model formulation within the Training Range Environmental Evaluation and Characterization System (TREECS™)*. ERDC/EL TR-14-2. Vicksburg, MS: U.S. Army Engineer Research and Development Center.

Johnson, B. E., and M. S. Dortch. 2014b. Application of TREECS™ modeling system to strontium-90 for Borschi Watershed near Chernobyl, Ukraine. *Journal of Environmental Radioactivity* 131:31–39.

Johnson, J. L., D. R. Felt, W. A. Martin, R. Britto, C. C. Nestler, and S. L. Larson. 2011. *Management of munitions constituents in soil using alkaline hydrolysis*. ERDC/EL TR-11-16. Vicksburg, MS: U.S. Army Engineer Research and Development Center.

Karakaya, P., M. Sidhoum, and C. Christodoulatos. 2003. *Aqueous solubility of CL-20*. Contractor Report ARAET-CR-05005. Stevens Institute of Technology, Hoboken, NJ.

Krzmarzick, M. J., R. Khatiwada, C. I. Olivares, L. Abrell, R. Sierra-Alvarez, J. Chorover, and J. A. Field. 2015. Biodegradation and degradation of the insensitive munitions compound, 3-nitro-1,2,4-triazol-5-one, by soil bacterial communities. *Environmental Science and Technology* 49:5681–5688.

Larson, S. L., J. L. Davis, W. A. Martin, D. R. Felt, C. C. Nestler, G. Fabian, G. O'Connor, G. Zynda, and B. A. Johnson. 2008. *Grenade range management using lime for dual role of metals immobilization and explosives transformation*. ERDC/EL TR-08-24. Vicksburg, MS: U.S. Army Engineer Research and Development Center.

Martin, T. 2016. User's guide for T.E.S.T. (version 4.2) (Toxicity Estimation Software Tool): A program to estimate toxicity from molecular structure. EPA/600/R-16/058, <https://www.epa.gov/chemical-research/toxicity-estimation-software-tool-tes>.

Pennington, J. C., T. F. Jenkins, S. Thiboutot, G. Ampleman, J. Clausen, A. D. Hewitt, J. Lewis, M. R. Walsh, M. E. Walsh, T. A. Ranney, B. Silverblatt, A. Marois, A. Gagnon, P. Brousseau, J. E. Zufelt, K. Poe, M. Bouchard, R. Martel, D. D. Walker, C. A. Ramsey, C. A. Hayes, S. L. Yost, K. L. Bjella, L. Trepanier, T. E. Berry, D. J. Lambert, P. Dubé, and N. M. Perron. 2005. *Distribution and fate of energetics on DoD test and training ranges: Interim report 5*. ERDC/ TR-05-2. Vicksburg, MS: U.S. Army Engineer Research and Development Center.

Perreault, N. N., D. Manno, A. Halasz, S. Thiboutot, G. Ampleman, and J. Hawari. 2012. Aerobic biodegradation of 2,4-dinitroanisole in soil and soil *Bacillus* sp. *Biodegradation* 23:287–295. doi: 10.1007/s10532-011-9508-7.

Richard, T., and J. Weidhaas. 2014. Biodegradation of IMX-101 explosive formulation constituents: 2,4-dinitroanisole (DNAN), 3-nitro-1,2,4-triazol-5-one (NTO), and nitroguanidine. *Journal of Hazardous Materials* 280:372–379.

Ronen, Z., Y. Yanovich, R. Goldin, and E. Adar. 2008. Metabolism of the explosive hexahydro-1,3,5-trinitro-1,3,5-triazine (RDX) in a contaminated vadose zone. *Chemosphere* 1492–1498.

Ruiz, C. E., and T. Gerald. 2001. *RECOVERY version 2.0, a mathematical model to predict the temporal response of surface water to contaminated sediments*. ERDC/EL TR-01-3. Vicksburg, MS: U.S. Army Engineer Research and Development Center.

Sokkalingam, N., J. J. Potoff, V. M. Boddu, and S. W. Maloney. 2008. *Prediction of environmental impact of high-energy materials with atomistic computer simulations*. Wayne State University, Department of Chemical Engineering. Detroit, MI.

Spear, R. J., C. N. Louey, and M. G. Wolfson. 1989. *A preliminary assessment of 3-nitro-1,2,4-triazol-5-one (NTO) as an insensitive high explosive*. Maribyrnong, Australia: Defense Science and Technology Organization Materials Research Laboratory.

Speitel, Jr., G. E., T. L. Engels, D. C. McKinney. 2001. Biodegradation of RDX in unsaturated soil. *Bioremediation Journal*, 5(1): 1-11.

Szecsody, J. E., D. C. Girvin, B. J. Devary and J. A. Campbell. 2004. Sorption and oxic degradation of the explosive CL-20 during transport in subsurface sediments. *Chemosphere* 56:593–610.

Taylor, S. J., E. Park, K. Bullion, and K. Dontsova. 2015. Dissolution of three insensitive munitions formulations. *Chemosphere* 119:342–348.

Taylor, S., J. Lever, M. Walsh, M. E. Walsh, B. Bostick, and B. Packer. 2004. *Underground UXO: Are they a significant source of explosives in soil compared to low- and high-order detonations?* ERDC/CRREL TR-04-23. Hanover, NH: U.S. Army Engineer Research and Development Center.

U.S. Army Aberdeen Test Center (ATC). 2004a. *Final report for the United States Military Academy small arms range environmental screening level assessment*. ATC-8750. Aberdeen Proving Ground, MD.

U.S. Army Aberdeen Test Center (ATC). 2004b. *Addendum 1 Final report for the USMA small arms range environmental screening level assessment*. ATC-8710. Aberdeen Proving Ground, MD.

U.S. Environmental Protection Agency (EPA). 2008. *Fact sheet, emerging contaminant – perchlorate*. EPA 505-F-07-003.

Whelan, G., J. P. McDonald, and C. Sato. 1996. *Multimedia Environmental Pollutant Assessment System (MEPAS): groundwater pathway formulations*. PNNL-10907/UC-630. Pacific Northwest National Laboratory, Richland, WA.

Whelan, G., K. J. Castleton, J. W. Buck, B. L. Hoopes, M. A. Pelton, D. L. Strenge, G. M. Gelston, and R. N. Kickert. 1997. *Concepts of a Framework for Risk Analysis in Multimedia Environmental Systems*. PNNL-11748. Pacific Northwest National Laboratory, Richland, WA.

## Appendix A: Points of Contact

The points of contact during this project are provided below.

POINT OF CONTACT	ORGANIZATION Name/Address	Phone/Fax/E-mail	Project Role
Billy Johnson	ERDC-EL, 3909 Halls Ferry Road, Vicksburg, MS, 39180	Phone: 601-634-3714 Fax: 601-634-3129 Email: billy.e.johnson@usace.army.mil	Project Coordinator, ERDC Demonstration Lead
Mark Dorch	ERDC-EL, 3909 Halls Ferry Road, Vicksburg, MS, 39180	Phone: 601-634-3517 Fax: 601-634-3129 Email: mark.s.dortch@usace.army.mil	Model Setup, Application, Analyses, and Reporting
Eric Weber	Ecosystems Research Division, National Exposure Research Laboratory, U.S. EPA Athens, GA 30605	Phone: (706) 355-8224 E-mail: Weber.Eric@epa.gov	EPA POC for CTS
Andrea Leeson	4800 Mark Center Drive, Suite 17D08, Alexandria, VA 22350-3605	Phone: 571-372-6398 Email: andrea.leeson.civ@mail.mil	Deputy Director & Environmental Restoration Program Manager
Macrina Xavier	11107 Sunset Hills Road, Suite 400 Reston, VA 20190	Email: macrina.xavier@noblis.org	Project reporting
Lisa Miller	11107 Sunset Hills Road, Suite 400 Reston, VA 20190	Email: lisa.miller@noblis.org	Project reporting

## **Appendix B: Predicting the Fate of Insensitive Munitions Explosive Components**

Predicting the fate of emerging constituents (ECs) associated with insensitive munitions (IM) explosive formulations presents a unique challenge given that less is known regarding the physicochemical properties of ECs than legacy explosive components. The work described in this chapter focused on the proper use of TREECS™-CTS to provide useful predictions of the fate of ECs associated with IM.

### **B.1 Modeling laboratory column breakthrough of IMX-101 components**

One of the more comprehensive studies to date involving IM by Dontsova et al. (2014) describes fate processes of the new IM formulations IMX-101, IMX-104, and PAX-21, and their EC components NTO, DNAN, and NQ. Laboratory column breakthrough studies were conducted for IMX-101 as part of that project. TREECS™ was used to model the column studies that involved soils from Camp Swift, TX. This modeling was conducted to evaluate the ability of TREECS™ to predict the dissolution and transport of EC explosive components NTO, DNAN, and NQ that comprise the IMX-101 formulation. The results of this study are described below.

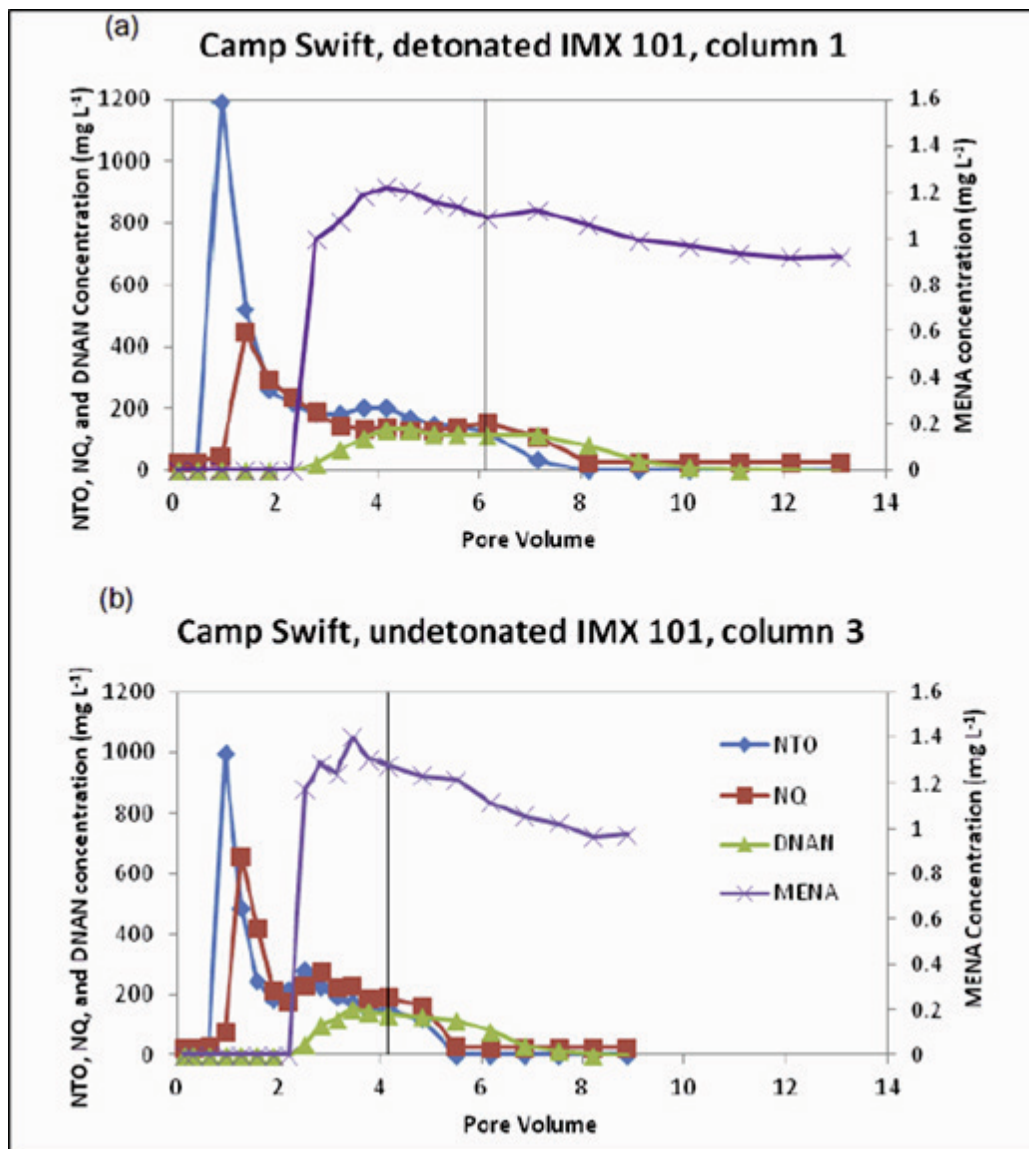
#### **B.1.1 Description of column study**

The results for two column studies with Camp Swift soils were reported by Dontsova et al. (2014). One study involved detonated IMX-101 particles, and the other used undetonated IMX-101 particles. Otherwise, all other study parameters were the same for the two columns.

IMX-101 consists of NTO, DNAN, and NQ. The NTO and NQ are crystalline particles imbedded within a melt-cast DNAN matrix. Other parameters associated with these column studies were obtained from Dontsova et al. (2014) and are described as follows: The columns were 1.18 cm in diameter and 7 cm in length, and each contained 11 to 12 g of soil. The Camp Swift soil consisted of sandy clay loam with 55, 21, 24, and 0.34 percent sand, silt, clay, and organic carbon, respectively. This soil texture results in a porosity of about 0.39 and dry bulk density of about 1.6 g/cm<sup>3</sup>.

A mass of IMX-101 of 0.05 g was added to the soil in each column. A constant water flow rate of 0.01 mL/min was introduced at the top of the column. MC concentrations of the column effluent water were measured over time producing breakthrough curves. Water flow was not interrupted during these column experiments, but the IMX-101 solid particle mass was removed after about 4 to 6 pore volumes of flow to observe the desorption phase breakthrough. The laboratory experimental results of Dontsova et al. (2014) are shown in Figure B41. The DNAN transformation product MENA was also measured as shown in Figure B41, although its concentrations were more than 100 times smaller than that of DNAN.

**Figure B41.** Experimental laboratory column breakthrough curves for IMX-101 EC components from Dontsova et al. (2014); vertical line represents when IMX-101 particles were removed.



The soil mass, bulk density, and surface area of the column were used to compute a soil thickness of 6.3 cm (0.063 m) for the column study. This thickness was needed for setting the soil layer thickness in the model.

### B.1.2 Soil model inputs and results

TREECS™ Tier 2 was applied for a case with an aquifer receptor well, thus, the soil model, the vadose zone model, and the aquifer model were included. The soil model represented the laboratory soil column. The vadose and aquifer models are automatically included for a receptor well, but their set-up and execution were not needed for modeling the column effluent, which represented flux from soil to the vadose zone. These mass fluxes were needed for computing column effluent concentration for comparison with laboratory column results. The inputs for the soil model are presented below.

The laboratory column was represented in the model by a 1.0 m-by-1.0 m surface soil plot of 0.063 m thickness. The use of a unit area and the same thickness as the laboratory column soil allowed preservation of both mass per unit area and soil concentration of IMX-101.

The initial mass of each component was used with the mass of soil (11 g) to compute the initial soil concentration, which resulted in initial concentrations of 895, 1977, and 1673 mg/kg for NTO, DNAN, and NQ, respectively, that were set in the soil model input. There were no constituent loadings, only the initial concentration. The soil properties for sandy clay loam were set in the soil model inputs, and these included dry bulk density of 1.6 g/cm<sup>3</sup>, porosity of 39 %, and volumetric moisture content of 39 %. The moisture content was set equal to the porosity since the soil column was saturated with the continuous influx of water.

The water influx rate of 0.01 mL/min divided by the laboratory column surface area of 1.093 cm<sup>2</sup> for the 1.18 cm diameter column resulted in a water loading rate of 0.009149 cm/min, which is 48.09 m/yr, a quite large rate. Thus, the average annual precipitation and rainfall were both set to 48.1 m/yr. The average annual soil erosion, ET, and runoff were all set to zero. The average annual water infiltration rate was set to 48.1 m/yr. Soil interflow was set to zero.

Dontsova et al. (2014) reported that a Camp Swift soil  $K_d$  for NTO and DNAN of 0.04 and 0.6 L/kg, respectively; thus, these values were used in

the model. The soil  $K_d$  values for NQ was set to 0.13 L/kg. This value was determined with the soil model UI using the soil texture discussed above (55, 21, and 24% for sand, silt, and clay, respectively), an organic matter content of 0.85% (which is consistent with organic carbon of 0.34%), and a  $K_{oc}$  value of 12 L/kg for NQ. No degradation was assumed for all three constituents, thus, the half-lives were set to very large numbers (1E20 years).

The IMX-101 formulation percentages for NTO, DNAN, and NQ were used with their respective solid phase particle densities to compute the IMX-101 particle density. This particle density and initial IMX-101 mass of 0.05 gram was used to compute the particle volume. Assuming spherical particles, the IMX-101 particle diameter was computed to be 3918  $\mu\text{m}$ . As explained previously, IMX-101 consist of a melt-cast DNAN matrix with crystals of NTO and NQ imbedded in the matrix. The NTO and NQ crystals are an order of magnitude smaller than the computed IMX-101 particle size.

Given the much higher solubility of NTO and NQ compared to DNAN as well as their small crystal size (yielding greater specific surface area), NTO and NQ should dissolve much faster than DNAN. However, the NTO and NQ crystals are imbedded within a DNAN matrix that dissolves much slower, thus potentially delaying the exposure of crystals' surface area to water.

The TREECS™ Tier 2 soil model treats each modeled constituent independently. Dissolution of each constituent depends on the constituent's solid phase density, solubility, and initial particle size (Dortch et al. 2011a). The dissolution model presently cannot handle a formulation mixture of constituents. Thus, the particle size of each constituent must be entered into the model. When all three constituents' particle size was set to the IMX-101 particle size of 3918  $\mu\text{m}$ , the peak breakthrough concentrations for each constituent were about two thirds of those measured in the laboratory. Therefore, this particle size was too large and not appropriate for use.

A model run was made with the initial particle sizes of 3918 for DNAN and the crystalline particle sizes for NTO and NQ in an attempt to better match the true size of each constituent particle. This run resulted in an under-

prediction of peak concentration by about half for DNAN and over-prediction of about a factor of 2 and 3 for NTO and NQ. Thus, using the representative individual constituent sizes is not appropriate as expected given the matrix of slower dissolving DNAN.

A third approach was investigated. This approach used the mass-weighted average particle size of 1885  $\mu\text{m}$  for all three constituents. The mass-weighted averaged size was computed using the percent by mass of each constituent in IMX-101 and the representative particle size of each constituent, or the crystalline particle sizes for NTO and NQ and 3918  $\mu\text{m}$  for DNAN. This approach proved to be fairly satisfactory; thus, a particle size of 1885  $\mu\text{m}$  was used for each of the three constituents in the final model inputs.

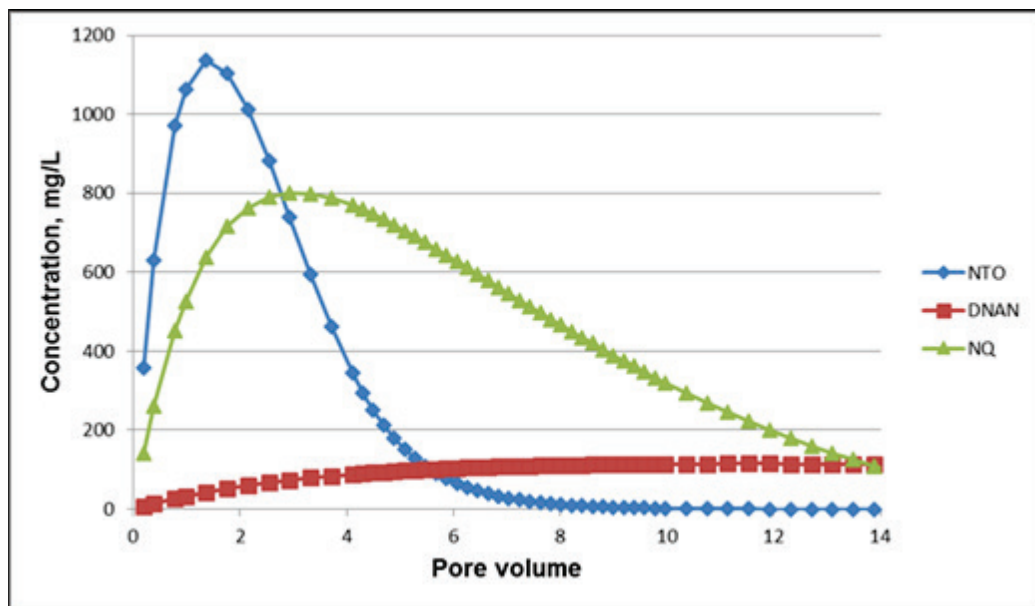
The ARCDDB values for HLC and molecular diffusivity in air (Table 6) were used in the soil model to compute volatilization for each constituent, although volatilization rates for these three EC are minuscule due to their small HLC values. The ARCDDB values for water solubility of 16,642, 276, and 3,800 mg/L for NTO, DNAN, and NQ, respectively, were used in the model. Similarly, ARDC values for molecular weight and solid phase density were used, and these values are shown in Table 6. The soil model was set to run for 0.1 year with a constant time step of 0.0001 year (0.876 hour). The soil model source code had to be modified and recompiled to write to the output file more frequently to capture enough output for these smaller than normal time steps.

Time series of soil model constituent mass flux from soil to the vadose zone were exported to Excel®. These data consisted of pairs of time (years) and constituent mass flux (grams/year). The time values were converted to pore volumes by multiplying time by the inflowing water flow rate of 48.086  $\text{m}^3/\text{yr}$  and dividing by the soil column pore volume of 0.02459  $\text{m}^3$ . The water flow rate is the water loading rate of 48.086  $\text{m}/\text{yr}$  times the soil column area of 1.0  $\text{m}^2$ . The soil column pore volume is soil porosity times the soil volume, which is the product  $1 \times 1 \times 0.063 \text{ m}$ . The mass flux was converted to breakthrough concentration by dividing the mass flux by the water flow rate.

The breakthrough concentration results of the model application of the column study are shown in Figure B42. The model does a reasonably good job of representing the fate of all three ECs when comparing to Figure B41.

The peak breakthrough concentration for NTO agrees very well with the laboratory results as the peak concentration is about mid-way between the laboratory results of peak NTO concentration for detonated and un-detonated IMX-101 particles. The timing of the NTO peak also agrees well with that observed in the laboratory.

**Figure B42. Model results of simulation of the laboratory column breakthrough study for IMX-101 conducted by Dontsova et al. (2014).**



The peak breakthrough concentration for NQ is over-predicted when compared to laboratory results for detonated and un-detonated particles, but it agrees more closely for un-detonated particles with a model peak of about 800 mg/L compared with about 700 mg/L observed. The arrival of the NQ peak is predicted to be slower than observed in the laboratory. A small increase in initial particle size accompanied with a smaller  $K_d$  for NQ produced model results that agree more closely with the measured peak concentration and its timing. A reduction in  $K_d$  can be justified since  $K_{oc}$  is known to be as low as 4 L/kg compared with the value of 12 L/kg that was used to estimate  $K_d$ .

The concentrations for DNAN agree quite well with those measured in the laboratory for both detonated and undetonated particles. The timing of predicted DNAN is similar to that measured as well. Overall, the model results are quite satisfactory, especially considering the complexity of modeling dissolution of the IMX-101 constituent formulation and given the

simplified dissolution model structure that assumes independent constituent dissolution processes. The model did not include the removal of the IMX-101 particles after 4 to 6 pore volumes. Thus, the trailing portions of the model breakthrough curves extend longer with higher concentrations than laboratory results.

There was no model calibration involved in producing the results shown in Figure B42 other than the adjustment of constituent initial particle diameters as discussed above. It was necessary to use particle sizes for NTO and NQ that were greater than their crystalline particle size imbedded with IMX-101. Similarly, it was necessary to use a particle size for DNAN that was smaller than the estimated size of the IMX-101 particle. Thus, the mass-weighted average particle size of representative constituent particles was found to produce reasonably accurate results. The rationale for using the mass-weighted particle size is that the slower dissolving DNAN matrix surrounds the crystalline NTO and NQ particles, thus limiting the crystal surface area exposed to water and slowing their dissolution rate, which is characteristic of a larger particle. However, after some of the fast-dissolving crystals are gone, the exposed DNAN surface area increases, which corresponds to a smaller particle. Particle size affects the specific surface area and its adjustment is the easiest and most logical way to more accurately portray dissolution of melt-cast formulations with the present model.

Particle size adjustments, such as those above, have not been required when modeling the explosive formulation Comp B, which is a melt-cast matrix of TNT with imbedded RDX crystals. It is believed that the reason for this is that TNT is more soluble than RDX, and the matrix is dissolved away more fully exposing the RDX crystals. Thus, Comp B particle size for representing both TNT and RDX is sufficient for modeling the dissolution of both constituents. Additionally, the solubility of these two constituents are much closer than those associated with NTO, NQ, and DNAN.

## B.2 Modeling laboratory column study of NTO transport

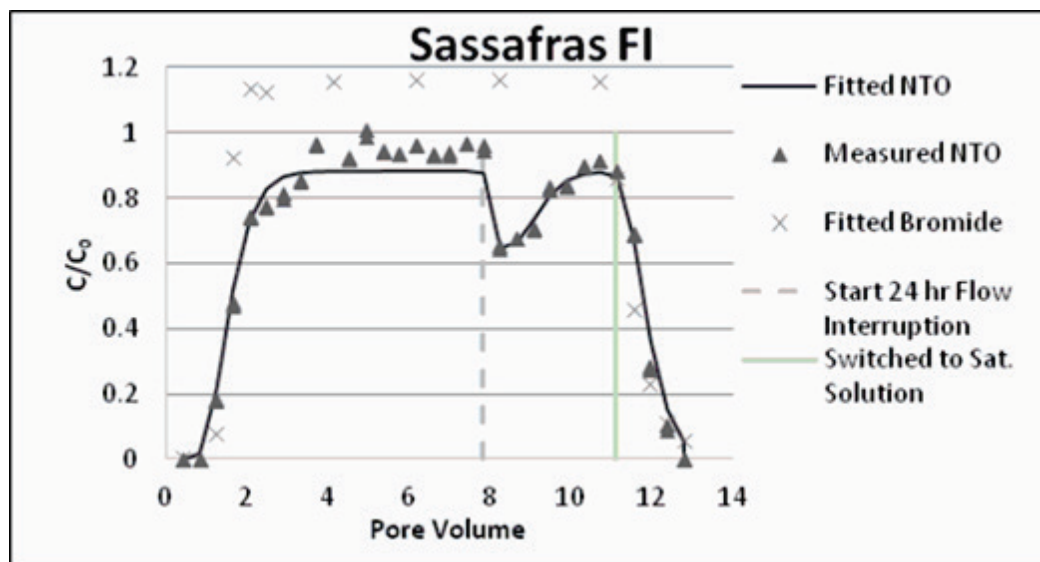
Another laboratory study performed and reported by Dontsova et al. (2014) was the transport of NTO through soil columns for several different soils. One of these studies using Sassafras soils from Aberdeen Proving Ground, MD., was selected for modeling with TREECS™ to evaluate its ability to predict movement of NTO through the vadose zone. The results of this study are described below.

### B.2.1 Description of column study

The set up for this study was very similar to the one described above for the column studies of IMX-101 dissolution and transport with Camp Swift soils as reported by Dontsova et al. (2014). The same size laboratory columns were used. The primary difference in the present study for NTO transport from the previous IMX-101 transport study was that there were no solid particles of NTO in the column, rather a solution of NTO in water was introduced continuously at the top of the water saturated column with a constant flow rate of 0.02 mL/min. Also, the Sassafras soil was selected for modeling rather than the Camp Swift soil because the Sassafras soil provided a greater degradation rate and greater  $K_d$  according to the results of Dontsova et al. (2014). The Sassafras soil is loam which has a porosity of about 0.47 and dry bulk density of about 1.42 g/cm<sup>3</sup>.

The columns were first saturated with a solution of CaCl<sub>2</sub> in water. Flow with the NTO solution was started and run for multiple pore volumes. After about 7.8 pore volumes of Sassafras soil, the flow was turned off for 24 hours. After about 11 pore volumes, the inflow was switched to a solution of CaCl<sub>2</sub> without any NTO. The NTO concentration in the column effluent was monitored over time and normalized to the inflow concentration, and time was converted to pore volumes for analysis of results. The results of this laboratory study for the Sassafras soil are shown in Figure B43.

Figure B43. Experimental laboratory column breakthrough curve for NTO transport resulting from NTO solution introduced in water flow at top of column (Dontsova et al. 2014).



## B.2.2 TREECS™ inputs

The soil column study of NTO transport described above was set up as follows using TREECS™. The Advanced Tier 2 option was used so that the User Defined object could be used to specify the water flow rate and NTO mass flux introduced to the soil column. Thus, there was no need to model the fate of NTO in surface soil since a known flux to soil of NTO mass could be specified. The User Defined WFF Vadose module was selected. This module was linked to the MEPAS vadose model, which represented the soil column. The vadose model was linked to the MEPAS aquifer model so that vadose mass flux through the bottom of the column could be output and converted to column effluent concentration. It was not necessary to set up and run the aquifer model.

The WFF Vadose module was set up for a unit surface of soil of 1 m long by 1 m wide. This module allows the user to specify water flow rate (volume per time) and constituent mass flux (mass per time) versus time as a boundary condition to the next downstream model, which is the vadose zone model. The flow rate of 0.02 mL/min for a 1.093 cm<sup>2</sup> column is equivalent to 96.17 m<sup>3</sup>/yr for a 1 m<sup>2</sup> square column. Thus, the water flow rate was set to a constant 96.17 m<sup>3</sup>/yr in the WFF Vadose module. The flow rate was not stopped and restarted as in the laboratory since the MEPAS vadose zone model only uses a single constant infiltrating flow rate. The model assumes steady-state flow since it was developed for assessing long-term average hydrologic conditions. The NTO influent concentration was assumed to be 1.0 g/m<sup>3</sup>, thus, the NTO influx was set to 96.17 g/yr. Influent concentration is unimportant since the relative concentration (ratio of effluent to influent concentration) is reported. The NTO influx rate was held constant from time zero to 0.0039 years. At year 0.004, the NTO influx was set to zero for the remainder of the simulation, which was continued to 0.005 years. The time for zero NTO influx was estimated based on the plot in Figure B43, which shows that the inflow was switched to the CaCl<sub>2</sub> solution at about 11 pore volumes. Time in years was calculated by multiplying the pore volume by the model soil pore volume of 0.0348 m<sup>3</sup> and dividing by the model flow rate of 96.17 m<sup>3</sup>/yr. The model soil pore volume was determined from the product of the vadose zone thickness of 0.0741 m, the soil surface area of 1 m<sup>2</sup>, and the soil porosity of 0.47. The vadose zone thickness is the same as the soil column length in the laboratory, which was determined by dividing the soil mass of 11.5 g by the product of the soil bulk density of 1.42 g/cm<sup>3</sup> and the column surface area of 1.093 cm<sup>2</sup>.

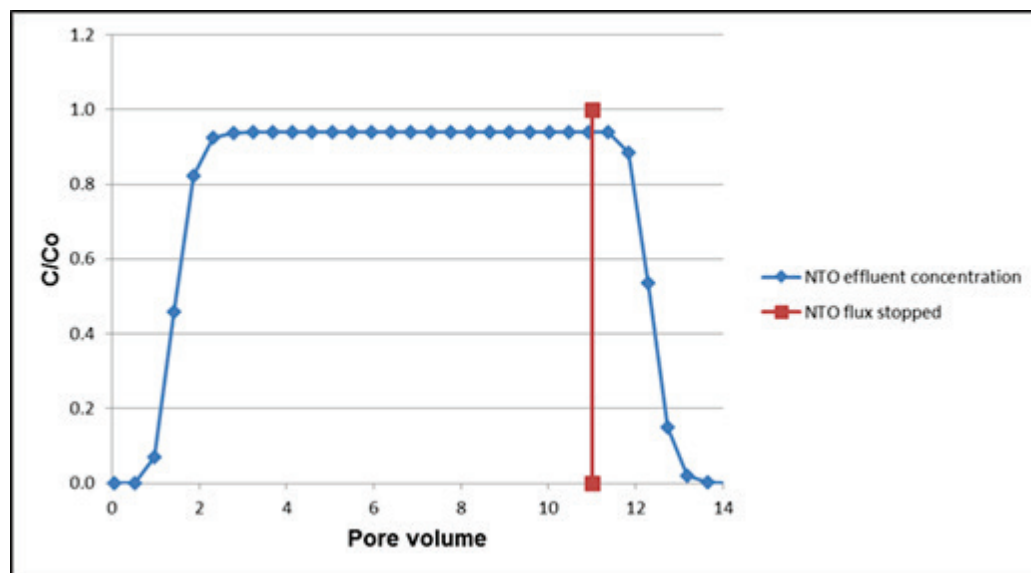
The Sassafras soil composition of sand, silt, clay, and organic matter was set to 41.4, 42.2, 13.15, and 3.25 percent, respectively, in the MEPAS vadose zone model input. The characteristics for loam were chosen in the MEPAS vadose model to set porosity of 46.6%, field capacity of 23.5%, bulk density of 1.42 g/cm<sup>3</sup>, and saturated hydraulic conductivity of 32 cm/day. The vadose zone layer thickness was set to 7.41 cm, and the longitudinal dispersivity was to 0.07 cm. The vadose zone soil  $K_d$  was set to 0.48 L/kg for NTO based on results of a batch soil partitioning study of NTO and Sassafras soil (Dontsova et al. 2014). The vadose zone degradation half-life of NTO was set to 3.61 days based on a first-order degradation rate of 0.008 per hour for NTO in the batch soil study reported by Dontsova et al. (2014).

The model-computed mass flux of NTO (g/yr) versus time (years) through the vadose zone layer was exported to an Excel® spreadsheet and converted to soil column effluent concentration (g/m<sup>3</sup>) by dividing the mass flux by the model infiltration flow rate of 96.17 m<sup>3</sup>/yr. It was not necessary to divide the effluent concentration by the influent concentration to obtain relative concentration since the influent concentration was 1.0 g/m<sup>3</sup>. The model time in years was converted to pore volumes by multiplying by the infiltration flow rate and dividing by the model pore volume of 0.0348 m<sup>3</sup>.

Model column effluent concentration is plotted versus pore volume in Figure B44. Comparison of the results in Figure B44 with those in Figure B43 reveals similar characteristics. The rise and fall of the relative NTO concentration, as well as the peak concentration, for the model correspond well with that observed in the laboratory experiment. Of course, there is no dip in model concentration around 8 pore volumes like there is in the laboratory experiment since it was not possible to stop and restart infiltrating flow in the MEPAS vadose zone model given its assumption of steady-state hydrology as stated previously. Otherwise, the model results closely matched those observed in the laboratory study.

Dontsova et al. (2014) measured NTO transformation (i.e., degradation) rates for 11 different soils that varied between 0.0004 per hour (half-life = 72.2 days) and 0.0221 per hour (half-life = 1.31 days). Dontsova et al. (2014) found a positive relationship of transformation rate to soil OC content.

Figure B44. Model results of simulation of the laboratory column breakthrough study for NTO transport resulting from NTO solution introduced in water flow at top of column as reported by Dontsova et al. (2014).



# REPORT DOCUMENTATION PAGE

1) Form Approved  
2) OMB No. 0704-0188

Public reporting burden for this collection of information is estimated to average 1 hour per response, including the time for reviewing instructions, searching existing data sources, gathering and maintaining the data needed, and completing and reviewing this collection of information. Send comments regarding this burden estimate or any other aspect of this collection of information, including suggestions for reducing this burden to Department of Defense, Washington Headquarters Services, Directorate for Information Operations and Reports (0704-0188), 1215 Jefferson Davis Highway, Suite 1204, Arlington, VA 22202-4302. Respondents should be aware that notwithstanding any other provision of law, no person shall be subject to any penalty for failing to comply with a collection of information if it does not display a currently valid OMB control number. PLEASE DO NOT RETURN YOUR FORM TO THE ABOVE ADDRESS.

1. REPORT DATE (DD-MM-YYYY) April 2017	2. REPORT TYPE Final Technical	3. DATES COVERED (From - To) January 2014 to January 2017		
4. TITLE AND SUBTITLE Field Demonstration and Validation of TREECSTM and CTS for the Risk Assessment of Contaminants on Department of Defense (DoD) Ranges		5a. CONTRACT NUMBER		
		5b. GRANT NUMBER		
		5c. PROGRAM ELEMENT NUMBER ER-201435		
6. AUTHOR(S) Mark S. Dortch, Billy E. Johnson, and Eric J. Weber		5d. PROJECT NUMBER		
		5e. TASK NUMBER		
		5f. WORK UNIT NUMBER		
7. PERFORMING ORGANIZATION NAME(S) AND ADDRESS(ES) Environmental Laboratory U.S. Army Engineer Research and Development Center 3909 Halls Ferry Rd. Vicksburg, MS 39180		8. PERFORMING ORGANIZATION REPORT NUMBER ERDC/EL TR-17-5		
9. SPONSORING / MONITORING AGENCY NAME(S) AND ADDRESS(ES) Environmental Security Technology Certification Program (ESTCP) 4800 Mark Center Dr., Suite 17D08 Alexandria, VA 22350-3605		10. SPONSOR/MONITOR'S ACRONYM(S) ESTCP		
		(1) 11. SPONSOR/MONITOR'S REPORT NUMBER(S) ER-201435		
12. DISTRIBUTION / AVAILABILITY STATEMENT Approved for public release; distribution is unlimited.				
13. SUPPLEMENTARY NOTES				
14. ABSTRACT <p>The Training Range Environmental Evaluation and Characterization System (TREECSTM) was developed to forecast the fate of and risk from munitions constituents (MC), such as high explosives (HE) and metals, within and transported from firing/training ranges to surface water and groundwater. The Chemical Transformation Simulator (CTS) was developed by the U.S. Environmental Protection Agency to provide physicochemical properties of complex organic chemicals. TREECSTM requires such properties for predicting environmental fate of MC. This study validated the capability of TREECSTM and CTS to predict MC (HE RDX) concentrations in receiving waters down-gradient of training/firing ranges for three installations: Demolition Area 2 of Massachusetts Military Reservation, MA.; Artillery Impact Area of the U.S. Military Academy, West Point, NY.; and Zulu Impact Area of Marine Corps Base Camp Pendleton, CA. The study also demonstrated the utility of these modeling system for forecasting the fate of emerging HE NTO, DNAN, and NQ associated with new insensitive munitions and evaluating best management practices for reducing down-gradient receiving water concentrations. The overall benefit of this work is to help transition these tools to the user community for use towards ensuring range compliance and sustainability into the future.</p>				
15. SUBJECT TERMS Hydrogeological modeling, Fate of munitions constituents (MC), Model validation, Physicochemical properties, Emerging constituents (ECs), Best management practices (BMPs), Explosives, Military, Rifle ranges, Bombing and gunnery ranges				
16. SECURITY CLASSIFICATION OF: Unclassified		17. LIMITATION OF ABSTRACT SAR	18. NUMBER OF PAGES 176	19a. NAME OF RESPONSIBLE PERSON
a. REPORT Unclassified	b. ABSTRACT Unclassified	c. THIS PAGE Unclassified		19b. TELEPHONE NUMBER (include area code)